NASA Contractor Report 4126

An Interactive User-Friendly Approach to Surface-Fitting Three-Dimensional Geometries

F. McNeil Cheatwood and Fred R. DeJarnette

COOPERATIVE AGREEMENTS
NCC1-100 and NCC1-22
MARCH 1988

NASA

NASA Contractor Report 4126

An Interactive User-Friendly Approach to Surface-Fitting Three-Dimensional Geometries

F. McNeil Cheatwood and Fred R. DeJarnette
North Carolina State University
Raleigh, North Carolina

Prepared for
Langley Research Center
under Cooperative Agreements
NCC1-100 and NCC1-22

National Aeronautics
and Space Administration

**Scientific and Technical
Information Division**

1988

Summary

Numerical flowfield methods require a geometry subprogram which can calculate body coordinates, slopes, and radii of curvature for typical aircraft and spacecraft configurations. The objective of this research is to develop a surface-fitting technique which addresses two problems with existing geometry packages: computer storage requirements and the time required of the user for the initial setup of the geometry model. Coordinates of cross sections are fit in a least-squares sense using segments of general conic sections. After fitting each cross section, the next step is to blend the cross-sectional curve-fits in the longitudinal direction using general conics to fit specific meridional half-planes. Provisions are made to allow the fitting of fuselages and wings so that entire wing-body combinations may be modeled.

For the initial setup of the geometry model, an interactive, completely menu-driven computer code has been developed to allow the user to make modifications to the initial fit for a given cross section or meridional cut. Graphic displays are provided to assist the user in the visualization of the effect of each modification. This report includes the development of the technique along with a User's Guide for the various menus within the program. Results for the modeling of the Space Shuttle and a proposed Aeroasist Flight Experiment geometry are presented.

Table of Contents

	Page
Nomenclature	iv
Section 1: Introduction	1
Section 2: Fitting the Fuselage Cross Sections	3
Section 3: Modification Features of the Code	11
Section 4: Fitting the Nose Region	18
Section 5: Longitudinal Blending of the Fuselage Cross Sections	24
Section 6: Interactive Graphics Routines	28
Section 7: Wing Section Fitting	32
Section 8: Fitting the Wing Planform	34
Section 9: Spanwise Blending of the Wing Sections	35
Section 10: Viewing the Wing Surface Fit	37
Section 11: Viewing the Wing-Body Combination	38
Section 12: Interpolation Procedure	40
Section 13: Data File Structure and Management	50
Section 14: Results and Discussion	52
Section 15: Concluding Remarks	55
Appendices	
A: Evaluation of Local Conic Equation Coefficients	56
B: Selection of Proper Sign for Global Conic Equation	59
C: Derivation of Conic Fitting Equation for Nose Region	61
D: Ellipsoidal Nose Radius of Curvature Distribution	62
References	64
Tables	66
Figures	95

Nomenclature

a,b,c	Principal axes of an ellipsoid; used in calculating the ellipsoidal distribution for the nose radius of curvature
$\bar{c}$	Length of wing chord at the given spanwise location; used to define spanwise cuts
d_g	Coefficients of equation (4.1), a general 3-dimensional conic equation (g=1,2,3,4,5,6,7,8,9)
k	Index number of a meridional or spanwise cut; used in interpolation process
m_b	Beginning slope of arc "j" (in local coordinates)
m_e	End slope of arc "j" (in local coordinates)
$\bar{r}$	Radius measured from (X=0,Y=0) in a given cross section; calculated value of radius at $\phi = \bar{\phi}$
r,ϕ	Polar coordinates measured from (X=0,Y=0) in a given cross section; used to define meridional cuts
$\hat{r},\phi_0$	Polar coordinates measured with respect to the local origin for a given arc; used to determine the calculated values of the input data points
r',ϕ_r	Polar coordinates measured with respect to an arbitrary reference point in a given cross section; used to determine proper sign to be used in conjunction with the global conic equation
x,y	Local cartesian coordinate system
$\bar{y}$	Chordwise distance from the wing leading edge at a given spanwise station; used to define spanwise cut locations
A_i	Coefficients of global general conic equation (2.1) (i=1,2,3,4,5,6)
A,B,C,D,E	Coefficents of local general conic equation (2.2)
A_k,B_k,C,D_k	Coefficients of nose fit equations (C.2), (4.3), and (4.4) (k=u,l)
AFE	Acronym for Aeroassist Flight Experiment

H_k	Term defined in equation (4.15); used in the nose region fit (k=u,l)
IFI	Refined input data file (binary)
IFO	Refined data file output by the program (binary)
IGUIDE	Input file containing the number of curve-fits which have been completed (binary)
IO	Output file containing a summary of each curve-fit completed thus far by the user
IOUT	IGUIDE file as output during program execution (binary)
IRAW	Raw input data file
ISAVE	Raw data file as saved by the program
IUSE	Data file which contains complete description of geometry model as created by the user (binary)
ND	Total number of data points in a data plane
NDERIV	Input parameter specifying which derivatives are to be calculated in the interpolation process
PHI	Value of ϕ measured from (X=0,Y=0); input parameter for the interpolation process
Q	Term defined in equation (D.5); used in calculating the ellipsoidal distribution for the nose radius of curvature
R	Radius of curvature of the body at the nose
$\bar{R}$	Radius of circular arc for the AFE skirt
RBODY	Value of body radius as calculated in the interpolation process
RZ,RPHI,RZZ, RZPHI,RPHIPHI	Values for r_Z, r_ϕ, r_{ZZ}, $r_{Z\phi}$, and $r_{\phi\phi}$ as calculated in the interpolation process
X,Y,Z	Global cartesian coordinate system
YRATIO	Ratio of the intermediate point y-coordinate to the slope point y-coordinate (for a given arc)

α,β,γ	Coefficients of equation (A.10) which is the local conic equation after it has been rewritten to contain only two unknowns: A and C
$\underline{\delta}$	Rake angle of AFE geometry
ϕ	Angle referenced to (X=0,Y=0); used to find the calculated value corresponding to the coordinate input by the user via the cross-hair
ε,ζ,η	Coefficients defined in equations (B.6), (B.7), and (B.8), respectively; used in determining which sign to use in conjunction with the global conic equation
ε_b	Ellipsoid ellipticity in the YZ-plane; parameter of AFE geometry
θ	Orientation of local coordinate system with respect to the global coordinate system
θ_{YZ}	Elliptical cone half-angle in the symmetry plane of the AFE geometry
μ,ν	Coefficients of the general conic equation (13.6); defined in equations (13.7) and (13.8); used in the interpolation process
ξ	Percent chord location; used in the interpolation process
τ	Angular extent of the circular arc skirt in the upper symmetry plane of the AFE geometry
Δ	Incremental change in the given variable
Θ	Pitch angle of orthographic view
Φ	Roll angle of orthographic view
Ψ	Yaw angle of orthographic view
Ω	Angle used in equation (9.1) to define the constant percent chord spacing
∞	Infinity

Subscripts

beg	Beginning point of a line segment
c	Calculated value
d	Specific data point

end	End point of a line segment
fit	Value obtained from the applicable fitting equation
in	User input value (via the cross-hair)
input	Based on the original input data points
j	Evaluated for arc "j"
k	Curve identification (k=u for upper surface; k=l for lower surface)
l	Lower surface of nose region
nose	Evaluated at the nose of the body
r	Related to an arbitrary reference point
ref	Value based on the cross section or meridional cut nearest the input value of (Z,ϕ); used during the interpolation process
u	Upper surface of nose region
ASTUD	Results using current method; acronym stands for Advanced Surface fitting Technique featuring User-friendly Development
CP	Control point
LE	Leading edge
QUICK	Results using model created from the QUICK geometry package
TE	Trailing edge
XZ	In the XZ-plane
YZ	In the YZ-plane
Z	Partial derivative with respect to Z
^{o}	Related to the local origin of a given arc
^{1}	Evaluated at the first constraining cross section of the nose region fit

$_2$	Evaluated at the second constraining cross section of the nose region fit
$_\phi$	Partial derivative with respect to ϕ

Superscripts

$^{(i)}$	The i-th partial derivative with respect to the argument
$'$	First partial derivative with respect to the argument
$''$	Second partial derivative with respect to the argument
*	Value corresponding to the input (Z,ϕ) request; used during the interpolation process

Section 1: Introduction

Numerical flowfield methods require a geometry subprogram which can calculate body coordinates, slopes, and radii of curvature. The coordinates and slopes are required for such techniques as the HALIS inviscid flowfield code (ref. 1) whose pressure distribution solution may be used to drive a boundary layer code. In addition, the radii of curvature must be supplied for methods which calculate inviscid surface streamlines from the pressure distribution (ref. 2). In this paper a new surface-fitting technique is developed, which addresses two major problems with existing geometry packages: computer storage requirements and the time required of the user for the initial setup of the geometry model.

Previous approaches to the surface-fitting of three-dimensional bodies generally divided the surface into panels. If the panels are represented by flat surfaces (refs. 3,4), then the body slopes are discontinuous at the edges of the panels. Coons' method (ref. 5), which provides for continuous slopes and curvature, involves the specification of 64 parameters for each panel (or patch), many of which are difficult to obtain (most notably the cross derivatives) (ref. 6). In addition, computer storage requirements may be great when a large number of patches are required to describe a geometry. Using spline functions (ref. 7) to generate the surface-fit often yields undesirable wiggles, dimples, or bulges in the resulting model. The QUICK method (ref. 8) is reasonably accurate but the development of a given model requires a large initial setup time.

DeJarnette and Ford (ref. 9) used general conic equations for the cross-sectional curve-fits, and then blended these curve-fits longitudinally using parametric splines. Unfortunately, the use of parametric splines to describe the longitudinal variation of cross sections can yield the same undesirable qualities which plagued the usage of general splines in that capacity. The approach developed in reference 9 for curve-fitting the cross sections is also used in references 10 and 11, while the method for longitudinally blending these cross-sectional fits is altered. In Sliski's approach (ref. 10), the longitudinal variation of cross sections is defined by one of several equations (including general conics and quadratic splines). Sliski's algorithm provides an accurate method for calculating body coordinates and surface derivatives, but it can be difficult to implement. Reference 11 discusses a method which is similar to the current research endeavor in that the longitudinal fit is handled by taking the same approach used to curve-fit the cross sections and applying it to specified meridional cuts. However, the package is cumbersome to use when modeling complex geometries which have drastic changes in longitudinal body curvature. Reference 12 discusses an ongoing investigation into the use of Bezier curves to surface-fit geometries.

It is advantageous to use conic sections rather than cubic or higher order polynomial equations since they eliminate the possibility

of unspecified inflection points in the fit. Therefore, the present technique also uses the cross section curve-fitting technique developed in reference 9. As with the approach described in reference 11, these cross-sectional curve-fits are then blended in the longitudinal direction, again using conic equations applied to specific meridional cuts.

Since the surface-fitting process for an arbitrary geometry is not a straightforward process, provisions should be made to allow the user to modify the current fit with minimal difficulty. Carrying out this procedure interactively eliminates the need for the user to construct lengthy input files which can increase the initial setup time for the model. The creation of such files requires a greater understanding of the code by the user than an interactive, menu-driven code, which allows even a novice to use the code successfully. Graphics routines supplementing these menus help the user to visualize the effects of the specified changes on the surface-fit.

For the initial setup of the geometry model, an interactive, completely menu-driven computer code has been developed to allow the user to make modifications to the initial fit for a given cross section or meridional cut. Graphic displays are provided to assist the user in the visualization of the effect of each modification. This report includes the development of the technique along with a User's Guide for the various menus within the program. Results for the modeling of the Space Shuttle and a proposed Aeroasist Flight Experiment geometry are presented.

Support for this investigation was provided by Cooperative Research Agreements NCC1-22 and NCC1-100 from NASA Langley Research Center.

Section 2: Fitting the Fuselage Cross Sections

To construct a geometry model, a set of data points which is composed of cross-sectional coordinates at various axial locations along the fuselage is necessary. The first step in the surface-fitting process involves curve-fitting each of these fuselage cross sections of coordinates. In many cases, a smooth fit which passes through every data point in a given cross section cannot be realized. In reference 9, a technique is developed which involves dividing a given cross section into **arcs** (Figure 2.1). Each arc is then curve-fit to the coordinates in a least-squares sense with a general 2-D conic equation. This technique is the basis for the present method, so its approach is outlined below.

A portion of a general conic is curve-fit in a least-squares sense through the data points of a given arc. The data points at each end of this arc are referred to as **control points**. The curve for this arc is constrained to pass through these two control points. The slope at each of these control points is constrained to be continuous with each of the two adjacent arcs, unless the slope at a control point has been specified by the user. On the other hand, there is no constraint to make the second derivative continuous at the control points. If no slope specification is made at a given control point, then the value for the slope there is left as part of the solution. A slope specification may be in the form of a discontinuity or continuous slope. In either case, the user must specify the values for the slopes. Alternately, a given arc may be defined to be a **line segment** (Figure 2.2).

That portion of a cross section between a beginning slope specification and an end slope specification is referred to as a **fitting region**. Such a fitting region may contain one or more arcs. The latter case occurs when no slope specifications are made at the control points between adjacent arcs (Figure 2.3). In such a case, the conic equations for each arc in that region are determined simultaneously in order to provide continuous slopes at these intermediate control points. A fitting region may encompass the entire cross section (if only the first and last control points have slopes specified) or as few as three data points (three points with two slopes give five constraints for the five coefficients of the general conic).

> **Note:** Actually, as few as two data points may be contained in a line segment (which is inherently a fitting region). Of course, the equation of the line segment is defined completely by its end points alone.

With the preceding overview in mind, define a cartesian coordinate system whose origin is at the nose of the fuselage, with Z in the axial direction, X in the spanwise direction, and Y perpendicular to the XZ-plane (Figure 2.4). The present method assumes that the fuselage is symmetric about the YZ-plane. For a given cross section of the

fuselage, Z = constant and the **global** (X-Y) general conic equation for one arc is of the form

$$A_1X^2 + A_2XY + A_3Y^2 + A_4X + A_5Y + A_6 = 0 \qquad (2.1)$$

with its global coefficients A_1, A_2, A_3, A_4, A_5, and A_6.

> **Note:** Equation (2.1) may be divided by A_6 (provided $A_6 \neq 0$) to reveal that there are really only five coefficients to be evaluated. This situation is automatically handled within the program.

In the curve-fitting of a given arc, it is convenient to define a **local** coordinate (x-y) system whose origin is the first control point of the arc, and whose x-axis passes through the second control point (Figure 2.5). In this coordinate system, the local general conic equation is

$$A\,x^2 + B\,xy + C\,y^2 + D\,x + E\,y = 0 \qquad (2.2)$$

which inherently passes through the first control point (x = 0, y = 0). The procedure for evaluating A, B, C, D, and E (and determining which sign to use in the quadratic expression for x or y) is outlined in Appendix A (see Reference 9 for the complete development of these relationships).

Once the coefficients A, B, C, D, and E are known, they may be transformed into the global coefficients of equation (2.1) through a rotation of the local coordinate system. Thus,

$$A_1 = A\cos^2\theta + B\sin\theta\cos\theta + C\sin^2\theta \qquad (2.3)$$

$$A_2 = 2(C - A)\sin\theta\cos\theta - B(\sin^2\theta - \cos^2\theta) \qquad (2.4)$$

$$A_3 = A\sin^2\theta - B\sin\theta\cos\theta + C\cos^2\theta \qquad (2.5)$$

$$\begin{aligned} A_4 = {} & 2A(Y_{CP}\sin\theta\cos\theta - X_{CP}\cos^2\theta) \\ & + B[Y_{CP}(\sin^2\theta - \cos^2\theta) - 2X_{CP}\sin\theta\cos\theta] \\ & - 2C(X_{CP}\sin^2\theta + Y_{CP}\sin\theta\cos\theta) \\ & + D\cos\theta + E\sin\theta \end{aligned} \qquad (2.6)$$

$$A_5 = 2A(X_{CP}\sin\theta\cos\theta - Y_{CP}\sin^2\theta)$$

$$+ \; B\left[X_{CP}(\sin^2\theta - \cos^2\theta) + 2\,Y_{CP}\sin\theta\cos\theta\right]$$

$$- \; 2\,C\,(Y_{CP}\cos^2\theta + X_{CP}\sin\theta\cos\theta)$$

$$- \; D\sin\theta + E\cos\theta \qquad (2.7)$$

$$A_6 = A\,(X_{CP}^2\cos^2\theta + Y_{CP}^2\sin^2\theta - 2\,X_{CP}Y_{CP}\sin\theta\cos\theta)$$

$$+ \; B\left[(X_{CP}^2 - Y_{CP}^2)\sin\theta\cos\theta - X_{CP}Y_{CP}(\sin^2\theta - \cos^2\theta)\right]$$

$$+ \; C\,(X_{CP}^2\sin^2\theta + Y_{CP}^2\cos^2\theta + 2\,X_{CP}Y_{CP}\sin\theta\cos\theta)$$

$$+ \; D\,(Y_{CP}\sin\theta - X_{CP}\cos\theta) - E\,(X_{CP}\sin\theta + Y_{CP}\cos\theta) \qquad (2.8)$$

where (X_{CP},Y_{CP}) are the coordinates of the control point at the beginning of the arc.

> **Note:** Recall that if $A_6 \neq 0$, then A_1 through A_5 will be divided by A_6. Therefore, each arc equation for a given cross section will ultimately have either $A_6 = 0$ (required for the curve to pass through the origin) or $A_6 = 1$.

Given one coordinate of a desired location, in using the global conic equation, a quadratic equation is encountered in the solution for the unknown coordinate. Thus, a choice between the "+" or "-" sign is necessary. The criterion for this selection is derived in Appendix B.

The above cross-sectional curve-fitting algorithm is implemented in the following manner. The code initially attempts to read the cross section data from a **refined** data file. This is a file which contains information on previously fitted cross sections: data points, control points, slope and line segment specifications, and their corresponding fitting regions. If this file is not found, or if the end of this file is reached during input, the program automatically attempts to read data from a **raw** data file. This file, as its name implies, contains only the data points -- with no specifications made thus far by the user.

> **Note:** This data retrieval structure allows the user to review any previously fitted cross section as will be discussed later. By allowing raw data to be input, the user need not make any decisions about the fitting of a cross section before it has been viewed on the screen. (Again, this will be discussed in detail later.)

> **Note:** It is important to note that this code expects the data points to be indexed 1 through ND (where ND is the number of

data points in the cross section), moving in a clockwise direction from the top of the cross section. The proper ordering of data points is crucial to the operation of this program!

When raw data points are encountered by the program, a check is performed to insure that the end points of the cross section are in the plane of symmetry. If they are not, they are shifted into the symmetry plane using a quadratic fit through the points nearest the symmetry plane. Next, these first and last data points in the cross section are defined to be control points, and the slope of the arc at these two points is defined to be dY/dX = 0. Therefore, initially an attempt will be made to fit the cross section with just one fitting region and no line segments.

Using these specifications, a solution to this arc is generated, and the resulting fit is drawn on the screen. The data points and control points are also displayed. In general, this initial fit is not satisfactory; however, it is a starting point. The user may at this point modify this fit (by adding control points, slope specifications, etc.) through the modification process (to be discussed in Section 3).

As the code attempts to fit the data according to the current specifications, several conditions will be monitored. If the slopes have been specified at two control points and there are no additional data points between them, then this fitting region will be **redefined** to be a line segment. This is necessary since with only two control points and two slopes (with no intermediate data point), the five conic coefficients are underdetermined. Another check is made on the local slopes of each arc. If they have the same sign, then the fit will yield double roots in the local coordinate system for a portion of the arc (Figure 2.6a). In order to avoid having to choose between two roots, when such a situation arises, a message is issued to the screen, and the user must modify the fit.

Note: Quite often in this case, the user may simply define an additional control point approximately midway through this troublesome arc, refit the cross section, and the double root situation will be avoided (Figure 2.6b).

Using the calculated local coefficients, the values for their corresponding global coefficients are determined via equations (2.3) through (2.8). Then a **defining array**, containing ten-elements per arc, is loaded. Four of the entries in this array are the global (X,Y) coordinates of the beginning and end control points. Two more are the global (X,Y) coordinates of the arc **slope point**. This is the point of intersection of two lines which are tangent to the arc at its control points (Figure 2.7). Also loaded in this array are the global (X,Y) coordinates of the arc **intermediate point**. This is the intersection of the curve-fit with a line which is perpendicular to the x-axis and passes through the slope point (see Figure 2.7).

These eight points contain all the information necessary to regenerate this arc fit from scratch: its end points, an intermediate point, and its end slopes (through the slope point). The last two elements of this array contain the global (X,Y) coordinates for a **local origin** (X_o,Y_o) for the given arc. In a fashion similar to the slope point, it is defined as the intersection of two lines which intersect the arc at its control points, but with a slope **perpendicular** to the tangent of the arc at those points (see Figure 2.7). This point is not necessary to define the arc, but is used to avoid multiple root situations in the global coordinate system.

A pair of global coordinates (X_c,Y_c) corresponding to each input data point is generated from the fitting equation in the following manner. The polar coordinates $(\hat{r},\phi_o)$ of a given input data point are given by

$$\phi_o = \tan^{-1}\left[\frac{Y_d - Y_o}{X_d - X_o}\right] \qquad (2.26)$$

and

$$\hat{r} = \left[(X_d - X_o)^2 + (Y_d - Y_o)^2\right]^{1/2} \qquad (2.27)$$

where (X_d,Y_d) are the global coordinates of the given input data point, and (X_o,Y_o) is the local origin (described in the preceding paragraph). Using this value of ϕ_o, the global equation is solved to find the calculated value of the body radius $(\hat{r}_c)$. Using this radius, the calculated global coordinates (X_c,Y_c) for the data point are

$$X_c = X_o + \hat{r}_c\cos\phi_o \qquad (2.28)$$

and

$$Y_c = Y_o + \hat{r}_c\sin\phi_o \qquad (2.29)$$

A comparison of the value of (X_c,Y_c) with its corresponding input data point value (X_d,Y_d) gives the user a gauge for measuring the accuracy of the current least-squares fit (Figure 2.8).

During the modification process, the user may make certain specifications which will not allow the inherent constraints of this method to be satisfied (for example, no inflection points may exist within an arc). If such a violation occurs, an indicative message will appear on the screen and the user will need to modify the specifications accordingly. When the user specifications for the curve-fit violate no inherent constraints, the user will advance to the **Cross Section / Phi Cut Menu.** At this point, the user has the following options:

1) **Review the Specs for this Fit**
   Allows the user to review both numerically and graphically the current specifications for slopes and line segments, and the resulting fitting regions. Also displayed are the maximum, minimum, and average deviations between the original data and their corresponding calculated values, for each of the arcs, as well as for the entire cross section. After this option is executed, the program returns to the Cross Section / Phi Cut Menu level so that another selection may be made.
2) **Modify this Fit**
   Allows the user to return to the modification level. Therefore, if the current curve-fit is unsatisfactory, then its specifications may be modified.
3) **Locate Break point (Cross Section Only)**

   > **Note:** The inclusion of the wing in a cross section data plane is helpful in developing a fit which adheres well to the data (especially on the lower surface). However, for best results, the actual fitting of a wing or tail surface requires a separate set of data planes aligned normal to the spanwise direction (which is perpendicular to the root chord). As a result, the wing portion of a fuselage cross section should be ignored during the longitudinal blending process of the fuselage.

   Allows the user to eliminate the wing portion of the cross section (after the cross section has been successfully fit) by establishing two **break points** (Figure 2.9). The first break point is located (via the cross-hair) at the control point where the wing upper surface meets the body in the current cross section (this typically occurs at a control point where a discontinuous slope has been specified). The second break point is located on the lower surface of the wing at the point where it intersects the body. If there is also a discontinuity at this juncture, then this second break point is located at that existing control point. If the lower surface of the wing meets the fuselage smoothly, then the second break point is located in the following manner. The arc whose end point is the first break point is extended down to the lower surface of the wing-body. The intersection between this lower surface and the extended arc is defined to be the second break point. This procedure is performed automatically by the code if the user specifies that the second break point is not to be located at an existing control point.
4) **Advance to the Next Cross Section / Phi Cut**
   Allows the user to advance to the next cross section or ϕ-cut when the fit for the current cross section is deemed satisfactory. The fundamental parameters for this fit are saved, and a summary of the fit is written to an output file

(see Table 1 for a sample of this output file), before advancing to the next section. This output file documents the cross section fitting. Included are the data points (with control points and line segment beginnings noted), their corresponding calculated values, the difference between these values, and the conic equations for each of the arcs.

5) **Terminate Session**
Allows the user to terminate the current fitting session. All information about the cross sections (both raw and refined data), including the latest modifications, are saved in restart files.

Note: For example, if the user has previously fit 23 of a total of 40 cross sections, and wishes to modify cross section #11, the following procedure may be used. Choose option (2) of the Review Menu (discussed later in this section), enter "11" when prompted for a cross section index number, and make the desired modifications to this cross section. At this point, the user may enter option (4) to advance to the next section, at which time a prompt for a new index number will be issued. Alternately, the user may enter (5) to terminate this session. In this case the fits for cross sections #1 through #23 (including the modifications to #11) will be saved, along with the raw data for cross sections #24 through #40.

As discussed earlier, the program will first search for data in the refined data file. If this file is not empty, then the user will be prompted with the **Review Menu**. The user's options are described below.

1) **Review All Previous Fittings**
Allows the user to view each of the previously fitted cross sections. If this option is selected, the code will read from the refined data file and display the cross section as currently fitted. At this point the user is at the Cross Section / Phi Cut Menu level, and may exercise any of its options. If option (4) is chosen, the code will advance to the next cross section and repeat the above process. This will continue until the user exercises option (5), or the program reaches the end of the refined data file. In the latter case, the code will automatically begin reading from the raw data file, and the modification process continues. If the end of the raw data file is encountered during reading, the program will issue the message "LAST CROSS SECTION!" to the screen, and automatically advance to the next level: fitting the nose region.

2) **Review Certain Previous Fittings**
Allows the user to review selected cross sections, without having to review all of them. In this case, the user enters the index number of the cross section to be reviewed. This selection is displayed, and the user is placed at the Cross

Section / Phi Cut Menu level and any of its options may be exercised. If option (4) is chosen, the user is prompted for another index number. The information for the cross sections between the last selection and the current selection are read in without displaying each cross section fit on the screen.

3) **Review Only the Last Fitting**
   Allows the user to review only the last cross section that was fit. The information for all the preceding cross sections is read in without displaying each cross section fit on the screen.
4) **Advance to Next Level without Viewing**
   Allows the user to advance to the next fitting level without viewing any if the fits for the current level. This option can only be exercised if all of the cross sections of this level have been successfully fit. If all of the cross sections have been fit, choosing this option will advance the user to the next level: fitting the nose region.

As mentioned above, after all of the cross sections have been successfully fit (the user should encounter the "LAST CROSS SECTION!" message), the next step is to fit the nose region of the fuselage. This process is the topic of Section 4. But first, the next section presents a more detailed look at the modification process involved in the curve-fitting of a cross section.

Section 3: Modification Features of the Code

The **Modification Menu** allows the interactive modification of the curve-fit for the current cross section. This procedure is aided by a graphics package which displays the data points of this section, supplemented by the control points which have been specified and the resulting conic representation of the section. A cross-hair is used to identify data points on this figure which are designated to be control points, to input the coordinates of new data points, and to locate control points where the slope specifications are to be changed. The Modification Menu selections are described below:

1) **Move CP**
   Allows an existing control point to be moved to either an existing data point or to a new data point to be specified by the user.
2) **Add CP**
   Allows the addition of a control point at either an existing data point or at a new data point to be specified by the user.
3) **Del CP**
   Allows the deletion of a current control point. The user has the option to either retain or delete the data point at this location.
4) **Move DP**
   Allows an existing data point to be moved to a new location.
5) **Add DP**
   Allows the addition of a new data point to the existing data field.
6) **Del DP**
   Allows the deletion of a current data point from the existing data field.
7) **Change Specs at a CP**
   Allows the alteration of end slope or beginning slope specifications at a current control point. This process is controlled by the Specifications Menu.
8) **Intermediate Point Changer**
   Allows the variation of the intermediate point for a given arc (and as a result, alter the shape of the arc fit) without affecting its end points or end slopes (Figure 3.1). This yields a different value for the local coefficient C from that calculated in the least-squares solution for the arc. When this option is chosen by the user, the current intermediate points for each of the arcs is displayed on the graph. When the desired intermediate point is identified, the current value of its YRATIO parameter is displayed (a value of YRATIO = 1 causes the Intermediate point to be coincident with the slope point for that arc, while YRATIO = 0 yields a line segment). The user then inputs a value of $0 < \text{YRATIO} < 1$, and the fit for this arc is altered accordingly.

9) **Recalculate Conic Fits**
Selecting options (2) or (7) will automatically activate the least-squares fitter when their modifications have been completed. However, the user must enter (9) to activate this fitter, and in turn reflect the changes in the curve-fit for this section, when any options other than (2) or (7) are exercised.

The **Zoom** feature may be enabled for any of the above options by simply placing a decimal in front of the selection number when entering it. Then using the cross-hair, the user may define a region of the graph to be enlarged. This feature is especially helpful when locating a control point in a region where the data points are clustered, or when choosing the coordinates of a new data point.

When option (4) or (5) is exercised, the **Input Interpretation Menu** is activated. This menu is also activated when (2) is selected to define a control point at a new data point. Through this menu, the user is able to govern how the coordinates of the new data point (which are input from the screen using the cross-hair) are interpreted by the program (Figure 3.2). The selections of this menu are described below:

1) **Xin, Yin**
Allows the user to accept the actual values as entered using the cross-hair to be the coordinates of the new data point.
2) **Xin, Yfit**
Allows the user to accept the X-coordinate as input using the cross-hair, along with the X-coordinate as calculated from the current conic equation at this X-location, to be the coordinates of the new data point.
3) **Xfit, Yin**
Allows the user to accept the Y-coordinate as input using the cross-hair, along with the X-coordinate as calculated from the current conic equation at this Y-location, to be the coordinates of the new data point.
4) **Xfit, Yfit**
Allows the user to select the point generated by the current conic equation, based on the angular location of the value as input by the cross-hair (X_{in}, Y_{in}), to be the coordinates of the new data point. Defining an angle

$$\bar{\phi} = \tan^{-1}\left[\frac{Y_{in}}{X_{in}}\right] \qquad (3.1)$$

a radius $(\bar{r}_{fit})$ based on the current conic equation at this $\bar{\phi}$ is calculated. Thus,

$$X_{fit} = \bar{r}_{fit} \cos\bar{\phi} \qquad (3.2)$$

and

$$Y_{fit} = \bar{r}_{fit} \sin\bar{\phi} \qquad (3.3)$$

5) **Input Coords Using Keypad**
Allows the user to override those coordinates as input via the cross-hair by specifying the desired coordinates of the new data point using the keypad.

When option (2) or (7) of the Modification Menu is executed, the **Specifications Menu** is encountered. This allows the user to define this location to be a Discontinuity or the beginning of a line segment. Alternately, a known value of a continuous slope may be assigned, or the slope at this point may be left arbitrary with no user input for its value. These options are described more fully below:

1) **No Specifications**
Allows the user to leave the slope at this point arbitrary. As a result, in the least-squares fitting for the conic equations of this arc, the only constraint here is that the curve pass exactly through this control point. Since no end slope has been specified, the equation of this arc must be solved simultaneously with those of its adjacent arcs up to the point where an end slope is specified.

> **Note:** As an example, if the beginning slope has been specified at control point #1 (the beginning point of arc #1), and the only other specification is the end slope at control point #4 (the end point of arc #3), then the conic equations for arcs 1, 2, and 3 must be solved simultaneously, since the slopes at control points #2 and #3 have been left arbitrary. If, however, either a continuous or discontinuous slope had been specified at control point #3, then arcs #1 and #2 would be solved simultaneously, while arc #3 would be solved independently. In yet another situation, had arc #2 been defined to be a line segment, then arcs #1 and #3 would be solved independently.

2) **Line Segment**
Allows the definition of this control point to be the beginning point of a line segment. Later menus allow the specification of the end point of this line segment, as well as any discontinuities which might occur at either end of this segment.
3) **Continuous Slope**
Allows the user to assign a value for a continuous slope at this point. As a result, while the equations for the arcs on

either side of this point are solved independently, they will both pass through this point with the same slope.

4) **Discontinuous Slope**
   Allows the user to define this point to be a discontinuity. To do so, the user must assign the end slope of the arc whose end point is this control point, along with the beginning slope of the arc whose beginning point is this control point. As a result, the equations for these arcs are solved independently so that they both pass through the control point, but with different slopes.

If option (2) of tne Specifications Menu is exercised (thereby initiating the line segment creation process), the end point for this line segment must be identified via the **End Point Menu.** The options for this end point are described below:

1) **At an Existing DP**
   Allows the user to define the control point at the end of this line segment to be located at an existing data point. If the desired data point is the one immediately after the control point selected as the beginning point (moving from the top of the graph in a clockwise direction), then the cross-hair need not be moved. Striking any character while the cross-hair is at its current location will instruct the program to define the data point immediately after the beginning point to be the line segment end point.
2) **At an Existing CP**
   Allows the user to define the control point at the end of this line segment to be located at an existing control point. Again, if the desired control point is the one immediately after the control point selected as the beginning point, then the cross-hair need not be moved before striking to select the end point.
3) **At a New DP**
   Allows the user to define the control point at the end of this line segment to be located at a new data point. The coordinates of this data point are located with the cross-hair, subject to the Input Interpretation Menu options described above.

After the end point of the line segment has been defined, the user must next constrain the slopes at each of its ends. These constraints are applied through the **Adjacent Arc Menu** whose options are outlined below:

1) **Slopes Continuous / No User Input**
   Allows the user to constrain the end slope of the arc adjacent to the line segment beginning to be continuous across that common control point, while constraining the beginning slope

of the arc adjacent to the line segment end point to be continuous across their common control point. This is the default condition and therefore requires no additional user input.

2) **Discontinuous Slope at Line Segment Start Pt**
Allows the user to constrain the beginning slope of the arc adjacent to the line segment end to be continuous across that common control point, while defining the end slope of the arc adjacent to the line segment beginning point to be discontinuous across their common control point. The value of the end slope for this arc must be input by the user.

3) **Discontinuous Slope at Line Segment End Pt**
Allows the user to constrain the end slope of the arc adjacent to the line segment beginning to be continuous across that common control point, while defining the beginning slope of the arc adjacent to the line segment end point to be discontinuous across their common control point. The value of the beginning slope for this arc must be input by the user.

4) **Both End Slopes are Discontinuous**
Allows the user to define the end slopes of the arcs adjacent to both ends of the line segment to be discontinuous with the line segment slope. The values of both of these slopes must be input by the user.

Note: If a line segment has been previously defined to begin at the control point chosen to be the beginning of this line segment, then the previously defined end point is retained. That is, the previous definition for this line segment is kept intact. However, the user at this time may choose to change the specifications for the slopes at each end of this segment.

Thus, if the user determines that a particular line segment placement is satisfactory, while the slopes at its ends need to be modified, then the modification may be achieved in the following manner. Apply option (7) of the Modification Menu to the beginning point of the line segment in question. By selecting option (2) of the Specifications Menu, repeat its definition as the beginning of a line segment. Since this has been previously defined to be a line segment, the previously defined end point will be retained by the program, and the user will not encounter the End Point Menu. Instead, the user will advance directly to the Adjacent Arc Menu where the desired alterations in the slopes may be made.

An alternate procedure which would yield the same results as above would again require the execution of option (7) of the Modification Menu, but this time at the end point where the actual change in the slope is to be made. Then by selecting option (4) of the Specifications Menu, the user may vary the slope at that point.

It is seen that the selection of options (2), (3), or (4) above, or options (3) or (4) of the Specifications Menu, requires the input of slope values by the user. The loading of these slopes is made simpler through the use of the "slope-line" (Figure 3.3). The procedure is as follows. When the user selects an option where the slope must be specified, an enlargement of the region around the control point of interest is displayed. Any line segments in this region are also plotted for reference purposes. The "slope-line" is superimposed on the graph. This is a line whose slope is initialized to the value of the slope of a quadratic passing through the control point and the two points nearest it. The user may then rotate this line (pivoted about the control point) in either a clockwise or counterclockwise direction (in one-degree increments) until the desired slope is achieved. As an additional option to the user, the "slope-line" mode of input may be overridden and the slope entered from the keypad.

Note: If the user attempts to define the beginning slope of an arc which has previously been defined to be a line segment, a message will be printed to the screen giving the user the option of retaining the line segment as previously specified, or continuing with the slope specification (in which case the line segment will automatically be deleted by the program). If the loading of an end slope where a line segment ends is mandated by the user's request, the program will skip the end slope input sequence (retaining the previously defined line segment), and advance to the beginning slope specification sequence. These features allow the user to prescribe a discontinuity at either end of an existing line segment (mentioned in the previous Note).

Note: The user may override the default slopes at the first and last control points in a given cross section/longitudinal cut by selecting option (7) in the Modification Menu and then option (3) or (4) in the Specification Menu. The program will recognize that this is either the first or last control point, and thus, rather than prompting for two slope inputs, will simply request the slope which needs to be defined.

Insertion and deletion of data points, control points, line segments, and slopes is made possible by a series of routines which shift the existing entries in the appropriate arrays to allow for insertion of new values. This order-preserving process is necessary since the least-squares fitting routine is structured to march around the cross section in a clockwise direction beginning at its top point (as mentioned earlier).

When a line segment is created, its coefficients and other parameters are calculated separately from the least-squares solver. Then when the least-squares solution for the remainder of the cross section is calculated, the coefficients for this line segment equation are not recalculated. As a result, computational time is reduced since

the specifications for this line segment remain unchanged until the actual line segment is modified.

> **Note:** Changes in the slopes of the adjacent arcs at the line segment end points do not require recalculation of the line segment parameters. Such changes only affect the arc in which they occur, not the line segment adjacent to it.

When line segments are shifted due to the insertion or deletion of fitting regions (other line segments, discontinuities, or continuous slopes), the parameters of those existing line segments are preserved. Again, this eliminates the need to recalculate values which have not changed. This preservation of previous line segment specifications includes the values of the end slopes of the adjacent arcs at the line segment end points. Thus, such information does not have to be repeatedly input by the user.

Now that the modification process has been reviewed, the next topic is the longitudinal blending of the fuselage cross sections. Since the nose region of the fuselage can cause problems, and in many cases is a key region of study, it is handled separately from the remainder of the fuselage. This special treatment is the topic of the next section.

Section 4: Fitting the Nose Region

The **nose region** of the fuselage is treated separately from the remainder of the fuselage. As a first attempt at fitting this region, a general 3-D conic equation was studied:

$$Z^2 + d_1Y^2 + d_2X^2 + d_3YZ + d_4Z + d_5XY + d_6XZ + d_7Y + d_8X + d_9 = 0 \qquad (4.1)$$

To impose symmetry about the Y-Z plane, $d_5 = d_6 = d_8 = 0$. Further constraining it to pass through the origin requires $d_9 = 0$. Also, to have an infinite slope at the origin requires $d_7 = 0$. Thus, an attempt was made to fit the points within the nose region using

$$Z^2 + d_1Y^2 + d_2X^2 + d_3YZ + d_4Z = 0 \qquad (4.2)$$

Since constraining this equation to pass through any four points will define this equation exactly, and there are more than four data points in the nose region, the least squares technique was employed. In applying this approach to the first two cross sections of the fuselage, it was found that the data points were not smooth enough to yield a good nose region representation. Therefore, another approach for the nose region was deemed necessary.

The next approach taken for the nose region was found to yield satisfactory results, so a detailed description is given in the following pages. The approach taken here allows for a unique specification of the nose region based on any two cross sections near the nose of the fuselage.

> **Note:** These two cross sections are not required to have the same number of control points. In fact, there are no constraints on their selection, although it is recommended that they be located axially near the nose of the fuselage.

The selection of the two desired cross sections by the user is accomplished through the **Nose Region Definition Menu.** Here, each of the cross sections of the fuselage are listed according to their index numbers and axial locations. The user then simply enters the index numbers of the two cross sections to be used to define the nose region fit.

Using these specified cross sections, the nose region is fit in the following manner. For a given meridional (ϕ = constant) half-plane, the intersections between this half-plane and the conic fittings for the two cross sections are found (Figure 4.1). These intersection points, along with the nose point (r=0,Z=0), are curve fit in the meridional half-plane (Figure 4.2) using a conic equation which is constrained to pass through the nose point with an infinite value for the derivative r_Z (see Appendix C for details). This equation is

$$r^2 + B_u Z^2 + C Z + D_u r Z = 0. \qquad (4.3)$$

for the upper surface ($\phi = \phi_u$). The equation for the complement of this meridional half-plane ($\phi = \phi_l = \phi_u - \pi$) is

$$r^2 + B_l Z^2 + C Z + D_l r Z = 0. \qquad (4.4)$$

which is on the lower surface. The coefficients for these two equations (henceforth referred to as a meridional **pair**) are evaluated simultaneously for a given value of ϕ_u. Due to symmetry, the curve-fit for $\phi = \phi_l$ is identical to the curve-fit for $\phi = -\phi_u$ (see Figure 4.1). Thus, for a symmetric fuselage, a set of meridional pairs where $0 \leq \phi_u \leq \pi/2$ will encompass the entire fuselage since this gives $-\pi/2 \leq \phi_l \leq 0$.

It can be shown that the radius of curvature at the nose is given by

$$R(\phi) = -\frac{C(\phi)}{2} \qquad (4.5)$$

Since $C(\phi)$ is the same for the upper and lower equations, the radius of curvature is continuous between the upper and lower surface at the nose point.

Equations (4.3) and (4.4) can be cast as the following single equation

$$r^2 + B_k(\phi)\, Z^2 + C(\phi)\, Z + D_k(\phi)\, r\, Z = 0. \qquad (4.6)$$

where: for the upper surface, k = u;
for the lower surface, k = l.

Differentiate (4.6) with respect to ϕ to obtain

$$[2r + D_k Z]\, r_\phi + B_k'(\phi)\, Z^2 + C'(\phi)\, Z + D_k'(\phi)\, r\, Z = 0. \qquad (4.7)$$

Rearrange (4.7) to obtain

$$r_\phi = -\frac{D_k'(\phi)\, r\, Z + B_k'(\phi)\, Z^2 + C'(\phi)\, Z}{2r + D_k Z} \qquad (4.8)$$

Differentiate (4.7) with respect to ϕ to obtain

$$[2r + D_k Z]\, r_{\phi\phi} + 2[r_\phi + D_k'(\phi)\, Z]\, r_\phi + B_k''(\phi)\, Z^2 + C''(\phi)\, Z + D_k''(\phi)\, r\, Z = 0. \qquad (4.9)$$

Rearrange (4.9) to obtain

$$r_{\phi\phi} = - \frac{2[r_\phi + D_k''(\phi)Z]\, r_\phi + D_k''(\phi) r Z + B_k''(\phi) Z^2 + C''(\phi) Z}{2r + D_k Z} \qquad (4.10)$$

Differentiate (4.6) with respect to Z to obtain

$$r_Z = - \frac{(2 B_k Z + C + D_k r)}{2r + D_k Z} \qquad (4.11)$$

Differentiate (4.9) with respect to Z to obtain

$$r_{ZZ} = - \frac{2\{(r_Z + D_k)\, r_Z + B_k\}}{2r + D_k Z} \qquad (4.12)$$

Differentiate (4.9) with respect to ϕ to obtain

$$r_{\phi Z} = - \frac{[2 r_Z + D_k]\, r_\phi + 2 B_k' Z + C' + D_k'[r + Z r_Z]}{2r + D_k Z} \qquad (4.13)$$

The coefficients (B_u, B_l, C, D_u, and D_l) are constant for a given meridional pair, but in general vary with respect to ϕ. These five coefficients must be evaluated for each meridional pair. The four intersection points between the meridional pair and the two cross sections are the only constraints specified thus far. The fifth constraint involves the radius of curvature at the nose point. There is some flexibility here which can be exercised by the user through the **Nose Radius of Curvature Menu.** The options are:

1) **Constant with respect to Phi**
   Allows the user to input a specific value for R which is to be used for all of the meridional cuts ($R = R_{XZ} = R_{YZ}$).
2) **Ellipsoidal Distribution**
   Allows the user to input a value of R_{YZ} at the nose for the YZ (symmetry) plane ($\phi = \pm\pi/2$) and a value of R_{XZ} for the XZ plane ($\phi = 0$). The program then uses the following ellipsoidal distribution (whose derivation is outlined in Appendix

D) of these two values for the meridional cuts where $0 < |\phi| < \pi/2$:

$$R(\phi) = \left[\frac{\sin^2 \phi}{R_{XZ}} + \frac{\cos^2 \phi}{R_{YZ}} \right]^{-1} \qquad (4.14)$$

where

R_{XZ} = radius of curvature in X-Z plane ($\phi = 0$)

R_{YZ} = radius of curvature in Y-Z plane ($\phi = \pm\pi/2$)

3) **Curvature Determined by Program**
Allows the user to leave the radius of curvature as part of the solution. In this case, the program sets $D = D_u = -D_l$ so that the four cross section intersections uniquely determine B_u, B_l, C, and D and no additional constraint is necessary.

Equations (4.6), (4.7), and (4.9) are of the form

$$H_k + B_k^{(i)} Z^2 + C^{(i)} + D_k^{(i)} r Z = 0. \qquad (4.15)$$

where: for (4.6), i = 0 and
$H_k = r_k^2$;

for (4.7), i = 1 and
$H_k = (2 r_k + D_k Z) r_{\phi_k}$; and

for (4.9), i = 2 and
$H_k = (2 r_k + D_k Z) r_{\phi\phi} + 2 [r_k + D_k Z] r_{\phi_k}$.

Applying the constraints to equation (4.15) yields

$$D_k^{(i)} = \frac{H_{k_2} Z_1^2 - H_{k_1} Z_2^2}{Z_1 Z_2 (Z_2 r_{k_1} - Z_1 r_{k_2})} + C^{(i)} \left[\frac{Z_1 - Z_2}{Z_2 r_{k_1} - Z_1 r_{k_2}} \right] \qquad (4.16)$$

If the nose radius of curvature has been specified by the user then the value for $C^{(i)}$ is determined from

$$C^{(i)} = -2 R^{(i)}(\phi) \qquad (4.17)$$

where:

$$R^{(0)}(\phi) = R(\phi) \text{ is defined by equation (4.14)}$$

$$R^{(1)}(\phi) = R'(\phi) = 2\,R^{2}(\phi)\sin\phi\cos\phi\left[\frac{1}{R_{YZ}} - \frac{1}{R_{XZ}}\right] \quad (4.18)$$

$$R^{(2)}(\phi) = R''(\phi) = 2\,R(\phi)\left[\frac{1}{R_{YZ}} - \frac{1}{R_{XZ}}\right] \times \quad (4.19)$$

$$\{R(\phi)\,[\cos^{2}\phi - \sin^{2}\phi] + 2\,R'(\phi)\sin\phi\cos\phi\}$$

Note: If $R_{XZ} = R_{YZ}$, then $R(\phi)$ = constant and $R'(\phi) = R''(\phi) = 0$ so that $C(\phi)$ = constant and $C'(\phi) = C''(\phi) = 0$.

If the radius of curvature is unconstrained by the user, then $C^{(i)}$ is evaluated by equating the expressions for $D_u^{(i)}$ and $-D_l^{(i)}$ given in equation (4.15). Thus,

$$C^{(i)} = \frac{\dfrac{H_{u_2}Z_1^2 - H_{u_1}Z_2^2}{Z_2r_{u_1} - Z_1r_{u_2}} + \dfrac{H_{l_2}Z_1^2 - H_{l_1}Z_2^2}{Z_2r_{l_1} - Z_1r_{l_2}}}{Z_1Z_2(Z_2 - Z_1)\left[(Z_2r_{u_1} - Z\,r_{u_2})^{-1} + (Z\,r_{l_1} - Z\,r_{l_2})^{-1}\right]} \quad (4.20)$$

Finally,

$$B_k^{(i)} = \frac{H_{k_1}r_{k_2}Z_2 - H_{k_2}r_{k_1}Z_1}{Z_1Z_2(Z_2r_{k_1} - Z_1r_{k_2})} + C^{(i)}\left[\frac{r_{k_2} - r_{k_1}}{Z_2r_{k_1} - Z_1r_{k_2}}\right] \quad (4.21)$$

With the coefficients constrained in this fashion, the body radius (r) along with its first and second partial derivatives can be calculated for any (Z,ϕ) location within the nose region using equations (4.6), (4.8), and (4.10) through (4.13).

Once the user has selected the two cross sections which will define the nose region fit, along with the desired radius of curvature option, the program automatically calculates the coefficients for equations spanning (at discrete $\Delta\phi$ increments) the entire Nose Region ($-\pi/2 \leq \phi \leq \pi/2$). The user may then scrutinize this surface-fit aided by the graphics routines accessed through the **Viewer Menu** (Figure 4.3). This plotting package is discussed in detail in Section 6. Should the fit prove to be unsatisfactory, the user may opt to return to the Nose

Region Definition Menu and choose two other "constraining" cross sections, or modify the nose radius of curvature distribution via the Nose Radius of Curvature Menu.

Once a satisfactory fit is realized, the user instructs the program to advance to the next level: longitudinally blending the remainder of the cross sections of the fuselage. This is the topic of the next section.

Section 5: Longitudinal Blending of the Fuselage Cross Sections

When all of the fuselage cross sections and the nose region have been satisfactorily fit, the next step is to **blend** the fuselage cross sections aft of the nose region in the longitudinal direction. This yields a set of equations which describe the entire fuselage surface. As a first attempt for this blending process, the overlapping parabola (or parabolic blending) technique was explored. The process is as follows.

As with the nose region, the longitudinal fitting is handled with equations which hold for a given meridional (ϕ = constant) half-plane. The intersections between this half-plane and the curves of each of the cross section fits are then fit with a series of parabolas. Each of these parabolas is constrained to go through three consecutive intersection points. As a result, the region between any two cross sections is fit by two parabolic expressions. A weighting function is employed to blend these two curves.

This technique yields a body fit which is constrained to pass through each of the cross section fits with a continuous slope. Further, the values for the first and second derivatives can be easily calculated for any point on the fuselage. And perhaps the nicest feature of this approach is the fact that it is completely automatic. That is, once the cross sections and nose region have been fitted, no additional user input is required to generate the fuselage fit -- all of the coefficient evaluations necessary for the blends are performed autonomously by the code.

Unfortunately, some of the very features which make this technique attractive, also make it unacceptable. Since, as mentioned in Section 2, the data points in a given cross section may not be smooth, the resulting curve fit through them may not be smoothly varying between the cross section stations. As a result, forcing the longitudinal blend to pass exactly through each cross-sectional curve-fit yields undesirable "wiggles". In addition, although a continuous slope is desirable in most cases, there are times when the fuselage surface may actually have discontinuities (for example, canopies or pods). With these shortcomings in mind, another approach to the longitudinal blending was taken.

The curve-fitting procedure used for the cross sections is seen as a candidate for the longitudinal blending process since:

1) smoothness of the "data points" (in this case, the radius at each cross section station calculated from the respective cross-sectional curve-fits) is not guaranteed,
2) inflection points not controlled by the user are undesirable, and
3) surface discontinuities and line segments may be allowed.

Thus, equation (2.1) is modified for use in the constant ϕ half-plane:

$$A_1 r^2 + A_2 rZ + A_3 Z^2 + A_4 r + A_5 Z + A_6 = 0 \qquad (5.1)$$

The axial derivatives for a given meridional cut are readily available. Differentiate equation (5.1) with respect to Z to obtain

$$r_Z = - \frac{2 A_3 Z + A_2 r + A_5}{2 A_1 r + A_2 Z + A_4} \tag{5.2}$$

Now differentiate equation (5.2) with respect to Z to obtain

$$r_{ZZ} = -2 \frac{(A_1 r_Z + A_2) r_Z + A_3}{2 A_1 r + A_2 Z + A_4} \tag{5.3}$$

As with the parabolic blending technique, the surface fit here is handled by applying this equation to meridional cuts ($-\pi/2 \leq \phi \leq \pi/2$) of the fuselage cross sections. The intersections between these half-planes and the cross-sectional curve-fits are curve-fit in the longitudinal direction.

> **Note:** The modification plots of a given meridional cut will have the nose of the fuselage at the top, the rear of the fuselage at the bottom, and the body radius measured horizontally due to the above transformations of the equations. The user begins the blending process with the $\phi = \pi/2$ meridional cut, proceeds around the fuselage at prescribed $\Delta\phi$ increments, and finishes the blending session with the $\phi = -\pi/2$ cut. As a result, the upper curve of the symmetry plane is the first meridional cut to be longitudinally fit, while the lower curve of the symmetry plane is the last to be longitudinally fit.

> **Note:** Currently the code divides the fuselage half-space ($-\pi/2 \leq \phi \leq \pi/2$) into 50 equal intervals ($\Delta\phi = 3.6$ degrees). As a result, 51 meridional cuts must be fit to encompass the entire fuselage. This spacing is not sacred, and may be varied by the user.

The approach of the current method differs from that of the method described in reference 11 in the following areas. In the latter, the longitudinal fitting process is applied at every ϕ-location used in the application of the method. For a large number of surface points, this approach can lead to a significant amount of work for the user. In the current approach, the longitudinal fitting process is performed in the initial setup over the entire range of the fuselage ($-\pi/2 \leq \phi \leq \pi/2$) at discrete ϕ-locations. The actual evaluations in the application of this method are accomplished through a set of interpolation routines so that the body radius and its derivatives may be evaluated at any point on the geometry. In contrast, the method of reference 11 also requires that the first and second ϕ-derivatives be longitudinally curve-fit at every ϕ-location where the model is applied, thus requiring even more work of the user.

As with the cross sections, the meridional cuts are broken up into arcs through the specification of control points. The initial specifications place the first control point at the intersection between the meridional half-plane and the cross section specified to be the end of the nose region fit (recall that the nose fit is constrained to pass through this cross-sectional curve-fit). The last control point is located at the intersection between the last cross section of the fuselage and the meridional half-plane. The longitudinal slope at the first control point is obtained from the nose region fit. Therefore, initially the longitudinal fit has a continuous slope across this juncture between the nose region fit and the fuselage afterbody (Figure 5.1).

> **Note:** Initial attempts to use this approach did not treat the nose region separately. That is, the entire fuselage from the nose to the rear was fit as one entity. However, examination of the resulting surface fit revealed that while the wiggles in the Z-direction were eliminated, they did exist in the ϕ-direction. This phenomenon was most prevalent in the nose region and appeared to be largely due to the fact that the meridional cuts were fit independently of each other. Thus, a way to somehow "tie" them together was deemed necessary. A natural choice for this "bridge" between the cuts was to reinstate the nose region fit.

In a manner analogous to the fuselage cross-sectional curve-fitting procedure, the user curve-fits a set of meridional cuts which encompass the entire fuselage beginning in the upper symmetry plane ($\phi = \pi/2$) and rotating around to the lower symmetry plane ($\phi = -\pi/2$). As with each of the fuselage cross-sectional curve-fits, the curve-fit for a given meridional cut is independent of the fits for the other meridional cuts. As a result, the longitudinal locations of the control points may differ from one meridional cut to another. In addition, the longitudinal slope specifications at these control points may also vary from meridional cut to meridional cut.

In general, the fit for a given meridional cut will be similar to those fits adjacent to it (in the ϕ-direction). Therefore, in an attempt to expedite the meridional fitting process, rather than initializing a given cut to the previously mentioned values, the current fit is loaded according to the specifications of the meridional cut which immediately precedes it. Thus, all of the control point, line segment, and slope specifications of the previous fit are retained for the current cut.

> **Note:** While the locations of previous specifications are maintained, they are based on the data coordinates of the current meridional cut. For example, a line segment whose end points in the previous cut were at data points #12 and #14 would again have its end points at these Z-locations in the current cut. However, the r-coordinates of these points

differ between cuts, in general, and these differences are reflected in the coefficients of their respective equations. Similarly, since slopes are also dependent on the coordinates of the data points, the location of all slope specifications are honored, but each is loaded with the value of the slope of a quadratic passing through its specification point and the two points adjacent to it. And finally, the slope at control point #1 is still defined to be the value of the nose region slope at that point.

If these specifications do not yield a satisfactory fit for the current ϕ-cut, the user may modify them in the same manner as the cross sections were modified (discussed in Section 3). When a range of meridional cuts encompassing the entire fuselage has been successfully curve-fit, a plotting array is automatically loaded by the program. This allows the surface-fit of the fuselage (Figure 5.2) to be viewed by the user (see Section 6).

As alluded to at various times thus far in this writing, the process of interactively scrutinizing and modifying a given fitting is aided by the screen graphics capabilities of the program. In addition, the user may also visually analyze the current surface fit of the fuselage through a variety of viewing options. The details of this graphics package are the subject of the next section.

Section 6: Interactive Graphics Routines

An integral part of the user-friendliness of this code revolves around the graphics routines which are accessed during the execution of the program. In fact, it is the user's ability to view the fitting of a given cross section or ϕ-cut that makes the entire interactive modification process work.

In addition, a separate section of the graphics package allows the visual analysis of the fuselage surface fit as generated by the current longitudinal blendings (see Section 5). This section also allows the user to inspect the surface fit of the nose region (see Section 4), and both the wing and wing-body combination (discussed in Sections 9 and 10, respectively).

After a given set of data points (cross section or ϕ-cut) is fit in a least-squares sense according to the specifications made (either by the user or by default), a graphical representation of the cross section is displayed on the terminal screen. The range and domain of this figure have been calculated so that the resulting drawing is an undistorted image of the cross section or ϕ-cut fit. Simply put, the plot of a circular cross section would in fact be a circle.

Included on this figure are the original data points (marked by "+" symbols), those points defined to be control points (the "+" symbol overstruck with a diamond shape), and a plot of the arcs passing through these points (a solid line). The plot is labeled with the index number of the cross section/ϕ-cut being displayed, along with its axial- or ϕ-location on the fuselage.

Several additional graphics devices are employed during the modification process (see Section 3). First of all, a **zoom** option may be activated in conjunction with any of the selections from the Modification Menu in order to make the required selections easier for the user in cluttered areas on the display. A similar close-up of the region of interest is automatically displayed when the slope specification option is exercised by the user. It is within this setting that the rotating slope-line feature is activated.

The user may also vary the intermediate point of an arc. When this option is exercised, the current location of the intermediate point for each arc is displayed (using a "Δ" symbol). When the intermediate point of a given arc is selected, the **defining triangle** for that arc is drawn (Figure 6.1). This is a triangle which passes through the two control points and the slope point of the given arc. A fourth line goes from the vertex at the slope point through the intermediate point to the opposite side of the triangle. This framework serves to guide the user in varying the YRATIO parameter (Figure 6.2).

One final graphics device encountered during the cross section/ϕ-cut fitting process is seen when the specifications review option of the Cross Section/Phi Cut Menu is exercised. Then, along with the tabulated information about the fit, the adjacent illustration of the cut is divided into its fitting regions.

After the cross sections are successfully fit, the nose region is constrained. And then the remaining cross sections are blended longitudinally. Both of these steps (fitting the nose region and the remainder of the fuselage) generate three dimensional surfaces which cannot be handled by the routines mentioned thus far. Viewing them requires a special set of **post-fitting** graphics routines which are accessed through the **Viewer Menu.** Its options are described below.

1) **Orthographic View**
   Allows the user to select an orthographic view of the fuselage which is to be displayed. When this option is chosen, the user must input values for the yaw, roll, and pitch angles (Ψ, Φ, and Θ, respectively) of the desired view.
2) **Top View**
   Allows the user to instruct the program to display the top view of the fuselage ($\Psi = \pi/2$, $\Phi = \pi/2$, and $\Theta = 0$ radians).
3) **Side View**
   Allows the user to instruct the program to display the side view of the fuselage ($\Psi = \pi/2$, $\Phi = 0$, and $\Theta = 0$ radians).
4) **Front View**
   Allows the user to instruct the program to display the front view of the fuselage ($\Psi = \pi$, $\Phi = 0$, and $\Theta = 0$ radians).
5) **Particular Cross Section**
   Allows the user to view a particular cross section of the fuselage. When this option is exercised, the user is prompted for the axial location of the desired cross section. The code takes this input value and compares it with the axial locations of the data planes of the plotting array. [Recall that these stations correspond to the cross sections of input data points which were curve-fit (see Section 2).] The fitted cross section whose axial location is nearest the requested value is the one actually displayed on the screen. First to be drawn on the screen is the cross section as generated from the longitudinal blending of the cross section fits (see Section 4). Then the original cross section fitting (see Section 2) is superimposed on this figure (Figure 6.3). The locations of the input data points and the control points specified in the cross-sectional curve-fitting are also displayed (marked by the same symbols that were used during the modification process). Using this display, the user may easily locate those regions where the longitudinal blend may not be in satisfactory agreement with the original cross section fittings.

   Note: When the Viewing Menu is encountered after the nose region is fit, the axial location input by the user is compared with the "artificial" cross sections which were loaded in the plotting array (see Section 4). The points in the plane nearest this requested location are the ones plotted on the

screen. Since these points are not, in general, located in the plane of an actual cross section of data points, no superimposing of the original fit is performed.

6) **Particular Meridional or Spanwise Pair**
Allows the user to view a particular pair of meridional half-planes as generated by the longitudinal blending of the fuselage cross sections. The user is prompted for the ϕ-location of the desired meridional pair. The program compares this value with those of the meridional pairs which have been fit. The pair whose location is nearest the one requested is displayed (Figure 6.4).

> **Note:** Although the upper and lower surfaces of a given meridional cut are generated by separate longitudinal fits (whose generated points are in different areas of the plotting array), they are displayed as one pair here. As a result, for example, a request to view the ϕ = 90 degree plane will yield the same display as a subsequent request to view the ϕ = -90 degree plane since in both cases the desired meridional pair is formed by the upper and lower surfaces of the symmetry plane.

7) **Refit the Body**
Allows the user to go back and refit the body if, after viewing the surface fit, it is seen that changes are necessary.

> **Note:** The possible approaches to refitting the body require varying degrees of additional input by the user. For example, simply modifying the longitudinal blends at certain meridional cuts requires the least additional input. Redefining the constraints for the nose region fit, however, will require that each of the longitudinal blends be recalculated since such a redefinition may alter the location of the first control point, or the value of the slope at that point, or both, and thus affect the resulting arc equations. Finally, if modifications are made in the cross section fits, then the nose region fit will have to be respecified if there are any modifications to its two defining cross sections. Here also, the longitudinal blends will have to be recalculated to reflect any changes in the surface fit due to these cross section modifications.

8) **Advance to the Next Level**
Allows the user to instruct the program to advance to the next level of the fitting process if the surface fit currently being scrutinized is indeed satisfactory.

Note: The zoom option may be exercised during the execution of options (1) through (6) in order to allow careful examination of key areas (Figures 6.5a and 6.5b).

A **hidden line removal** process is employed during the generation of the plots in options (1) through (4). In addition, although only the $X > 0$ semi-space is contained in the plotting array, its mirror image is also plotted (where visible). The combination of these two features gives the user a realistic view of the body without the clutter caused by drawing those lines which would not be visible if the image was actually a solid object.

The hidden line removal feature mentioned above is based on the **outward normal method**. The mesh formed by the cross section fits and the longitudinal blending fits divides the fuselage surface into a set of four-sided panels. The procedure is as follows. The X-, Y-, and Z-components of the diagonals of a given panel are calculated based on the coordinates of its corner points. Then the cross products of these diagonal components are found. These cross products are the components of the normal to that panel. Now the normal is oriented according to the current values for Ψ, Φ, and Θ. If any component of this resultant vector is pointing toward the screen, then the panel is visible and its boundaries are drawn. Otherwise, the panel is not displayed. This process is repeated for each panel defined by adjacent entries in the plotting array, along with each mirror image, to yield the final product.

Note: Because this technique checks each panel independently, it is not a universal hidden line removal package. That is, there is no check for the possibility of one visible panel (as determined by the outward normal method) actually being behind another visible panel (Figure 6.6). In such a case, all or part of the first panel should be hidden. This deficiency becomes more apparent with the displaying of wing-body combinations (see Section 10).

Section 7: **Wing Section Fitting**

The technique utilized in curve-fitting the fuselage cross sections is again employed here. It was decided that this approach could be most readily applied to the wing by defining a new coordinate system in which the coordinate corresponding to the axial direction of the fuselage would now correspond to the spanwise direction of the wing (Figure 7.1). Further, the wing cross sections (aligned perpendicular to the spanwise direction) assume the role previously played by the fuselage cross sections. In this coordinate system, the Z=0 plane is coplanar with the symmetry plane of the fuselage. Now the equations of Section 2 may be employed without change.

> **Note:** Using the coordinate system described above, in conjunction with the graphics package (see Section 6), yields a plot during the modification session which depicts the wing section to be standing on its end. That is, the leading edge of the wing section will be at the top of the display and its trailing edge will be at the bottom.

Using the fuselage cross section fitting equations, "artificial" data points for wing sections (planes parallel to the X-Y plane) were generated at multiple spanwise locations. However, after several attempts at fitting these artificial wing sections, it was seen that the curve-fits for the fuselage cross sections do not handle the wing portion well enough to generate suitable planes of data for the wing fit. As a result, sets of data points located at several discrete spanwise locations (analogous to the data point sets at discrete axial locations used for surface-fitting the fuselage) were deemed necessary to achieve a good wing surface-fit.

In a process similar to the longitudinal blending of the fuselage cross sections, the upper and lower surface of each wing cross section is fitted separately. The raw data specification process places the first control point at the wing leading edge with a slope of $\partial Y/\partial X = 0$, and a second control point at the trailing edge with a slope whose value matches that of a quadratic passing through the trailing edge and the two points nearest it.

When the upper wing surface at a given spanwise location is successfully fit, the user advances to the fitting of its lower surface. After the lower surface is fit, the entire wing fit for this spanwise location (the upper and lower fits, as constrained by the user's specifications, oriented correctly with respect to each other) is displayed (Figures 7.2a, 7.2b, and 7.2c). Then the user is given these options through the **Wing Section Menu:**

1) **Advance to the Next Wing Section**
   Allows the user to accept the fit for this wing section and advance to the next spanwise station.
2) **Terminate Session**
   Allows the user to terminate the current fitting session. If the current fit for this or any of the other wing sections is unsatisfactory, then the specifications may be modified in the next session.

When the fitting session for the wing sections has been completed, the next phase in the wing surface fitting process is to fit the planform of the wing. This is the topic of the next section.

Section 8: Fitting the Wing Planform

In order to define the leading edge and trailing edge of the wing at any spanwise location, the planform of the wing must be curve-fit. Using the coordinate system shown in Figure 8.1, the equations of Section 2 are again applicable without alteration. The "data points" used in this fitting are the leading and trailing edge chordwise locations (Y-coordinates) for each wing cross section along with their corresponding spanwise positions (X-coordinates).

The raw data specifications place a control point at the leading edge of the root chord with a slope defined by a quadratic passing through it and the two leading edge points nearest it. Similarly, the second control point is placed at the trailing edge of the root chord with a slope defined by a quadratic passing through it and the two trailing edge points nearest it. The modification process is then executed in the usual fashion.

During execution of the program, in sessions following the successful fitting of the wing planform (and the saving of these specifications), the user will encounter the **Planform Review Menu** whose options are outlined below.

1) **Review Planform Fitting**
   Allows the user to review the planform fitting as specified in previous sessions. As usual, the user may modify this fit, review its specifications, or exit this level without making any changes.
2) **Advance to the Next Level Without Reviewing**
   Allows the user to advance to the next level without reviewing the previous fitting of the wing planform.

After successfully developing a satisfactory fit for the wing planform, the next step is to blend the wing section fits in the spanwise direction. This process is the subject of the next section.

Section 9: Spanwise Blending of the Wing Sections

The process of blending the wing cross-sectional curve-fits in the spanwise direction completes the definition of the wing surface. The concept of this procedure is similar to the one employed in the longitudinal blending of the fuselage cross sections. Here, however, **constant percent chord** cuts were found to be better than meridional cuts for the spanwise blending process.

In order to cluster points near the leading and trailing edges, the following transformation from airfoil theory is used

$$\frac{\bar{y}}{\bar{c}} = \frac{1 + \cos\Omega}{2} \qquad (9.1)$$

where

$\bar{y}$ is the chordwise distance from the wing leading edge,

$\bar{c}$ is the chord of the wing at this spanwise location,

$0 \leq \Omega \leq \pi$ for the upper surface,

and

$\pi \leq \Omega \leq 2\pi$ for the lower surface.

Applying equation (9.1) at the leading edge ($\bar{y}/\bar{c} = 0$), $\Omega = \pi$. At the trailing edge ($\bar{y}/\bar{c} = 1$), $\Omega = 0$ for the upper surface, and $\Omega = 2\pi$ for the lower surface. By using expression (9.1) to define the locations of the blending cuts, these spanwise cuts are clustered near the leading and trailing edges of the wing.

Unlike the fuselage, no plane of symmetry is assumed for the wing. The spanwise blending process of the wing cross sections begins at the trailing edge ($\Omega = 0$) and progresses toward the leading edge along the upper surface (at $\Delta\Omega$ = constant intervals). Once the leading edge is reached, the spanwise blending process continues for the lower surface moving from the leading edge back to the trailing edge using the same value for $\Delta\Omega$ that was used for the upper surface. As a result both the upper and lower surfaces of the wing at a given $\bar{y}/\bar{c}$-location will be fit.

During the modification process, each spanwise cut will be displayed on the screen with its wing tip at the top of the figure and its root at the bottom in order to utilize the existing plotting routines (Figure 9.1). The "data points" for each spanwise cut are defined by the wing section fits (these give the X-coordinates of the data points) and their respective spanwise locations (Y-coordinate).

The raw data specifications are analogous to those for the wing planform (see Section 8), so they are not repeated here. And as with the fuselage blending process, the upper and lower surfaces of the wing are fit separately. Also as with the fuselage blending procedure, the current $\bar{y}/\bar{c}$-cut is initialized to the specifications of the fit for the spanwise cut immediately preceding it (see Section 5).

When all of the spanwise cuts have been satisfactorily curve-fit, the program applies the equations at discrete points along the wing span. The values at these locations are stored in a plotting array.

Now the accuracy of the fitting equations may be scrutinized by the user through the set of graphics features analogous to those described in Section 6 (Figure 9.2). Those few differences between scrutinizing the fuselage fit and analyzing the wing fit are detailed in Section 10.

Section 10: Viewing the Wing Surface Fit

The user may examine the wing surface fit graphically using the same options of the Viewing Menu that were accessed for viewing the fuselage (see Section 6). In order to accommodate the differences between the fuselage and wing coordinate systems (see Sections 2 and 7, respectively), a second set of hidden line routines are used. These routines are identical to their fuselage plotting counterparts except for their X-Y-Z orientation. As a result, options (1) through (4) of the Viewing Menu yield the same views for both the fuselage and the wing. Simply put, the front view of the fuselage could be superimposed on the front view of the wing to obtain the front view of the wing-body combination.

If option (5) of the Viewing Menu is activated, the user is prompted for the spanwise location of the desired wing section. Then as with the fuselage viewing, the program compares this value with those locations in the plotting array. The wing section in this array which is closest to the desired location is the one which is displayed on the screen (Figure 10.1).

> **Note:** When the fuselage fit is loaded into the plotting array, its axial locations correspond to those of the input data planes. However, since in general the wing may be defined with fewer data planes, its plotting array contains spanwise stations at locations between the input data planes. As a result, the wing section which is displayed is, in general, not in the same plane as a set of data points. Thus, plotting the original wing section fit and its data points is not applicable here. Recall that an analogous situation exists for viewing the nose region fit.

Exercising option (6) for the wing fit requires the specification of the desired $\bar{y}/\bar{c}$-location rather than the ϕ-location (used with the fuselage). This input value is compared with the cuts that were fit during the spanwise blending process. That cut which is nearest the requested value is the $\bar{y}/\bar{c}$-cut which is displayed. As with the meridional cuts of the fuselage, both the upper and lower surface spanwise blends (a spanwise pair) at this location are displayed simultaneously.

When the fit for the wing surface is found to be satisfactory, the next step is to view the wing-body combination. To do so, the user selects option (8) from the current Viewer Menu. Then a new Viewer Menu will be displayed. The differences between the selections of the previous menu and this current one are discussed in Section 11.

Section 11: Viewing the Wing-Body Combination

The selection of option (8) of the Viewing Menu during the analysis of the wing surface advances the user to another Viewing Menu. At this level, the user may view the wing-body combination as one unit. The selection of options (1) through (4) yields the same views as before. However, since options (5) and (6) have different functions for the fuselage and the wing, the user has an additional choice to make when one of these two options is exercised.

If the user selects option (5), the **Cross/Wing Section Menu** is encountered. Its three options are as follows.

1) **Fuselage Cross Sections**
   Allows the user to view individual cross sections of the fuselage. See Section 6 (specifically, the comments on option (5) in that section) for a more thorough description of this option.
2) **Wing Sections**
   Allows the user to view individual wing sections (see Section 10 for details).
3) **Return to Viewer Menu**
   Allows the user to return to the Viewer Menu.

After one of the first two options is exercised, the user may view as many sections as desired. Exiting this mode returns the user to the Cross/Wing Section Menu where any of these three options may be exercised.

In selecting option (6), the **Longitudinal/Spanwise Menu** is encountered, and the user is again given three options.

1) **Fuselage Meridional Cuts**
   Allows the user to view individual meridional cuts of the fuselage (see Section 6 for a more thorough description).
2) **Wing Spanwise Cuts**
   Allows the user to view individual wing spanwise cuts (see Section 10 for more details).
3) **Return to Viewer Menu**
   Allows the user to return to the Viewer Menu.

As in the previous case, once one of the first two options is exercised, exiting that choice returns the user to the Longitudinal/Spanwise Menu.

At this point, if the user finds the wing-body surface equations to be satisfactory, then the fitting process is complete. The resulting fit may be used to generate body coordinates and derivatives anywhere on the wing-body via a separate set of interpolation routines. These routines take a given (Z,ϕ) value and interpolate the longitudinal blends near that point to evaluate the body radius and partial derivatives there. The user may implement these routines without executing the entire fitting program. As a result, they may be used repeatedly to

define body coordinates and derivatives to form the boundary of various flow field grids without having to model the geometry again each time. Of course, this requires that the "model definition" data files (see Section 13) be kept intact.

Note: Currently, this code does not calculate the actual intersection curve between the wing and body. Future work with this code may involve implementation of such a feature.

Note: Some minor changes in the program logic and array sizes are required to accommodate additional lifting surfaces (vertical and/or horizontal tail, canard, etc.) -- if the user wishes to view the entire configuration simultaneously. Of course, the user may fit each component in separate runs of the code, without having to modify the program's current form.

Section 12: Interpolation Procedure

The model thus far consists of a set of equations which define a number of longitudinal (fuselage) and spanwise (wing) curves at **discrete** ϕ- and $\bar{y}/\bar{c}$-locations, respectively. This provides a skeleton of the model where the cross-sectional curve-fits serve as the bulkheads or ribs, and the meridional curve-fits are the stringers. To apply this model at locations between these defined curves, a set of interpolation routines was developed. For input values of the longitudinal (Z) and circumferential (ϕ) coordinates of the fuselage, this involves calculating the surface radius and derivatives based on the meridional curve-fits in the neighborhood of ϕ.

Initially, a neighborhood of five meridional cuts at the prescribed value of Z was curve-fit in the ϕ-direction with a general conic equation. This curve passes through each of these five points. However, since the meridional cuts were curve-fit independently of each other, a smooth variance in the ϕ-direction is not guaranteed. As a result, this approach generally yielded a hyperbolic equation with imaginary roots (which is undesirable). Increasing this neighborhood to six cuts (and thereby curve-fitting the points in a least-squares sense with the general conic) improved this situation, but some hyperbolic results still persisted. To resolve this problem, each neighborhood was curve-fit in a least-squares sense with an X-parabola, Y-parabola, and line segment, in addition to the general conic. The equation which adhered most closely to the original meridional curve-fits in the neighborhood of ϕ was then used to evaluate the surface radius and derivatives at that (Z,ϕ) location. A more thorough description of this procedure is given below.

For locations along the fuselage, these interpolation routines are accessed by the user through the following call statement:

```
CALL VALUATE(Z,PHI,RBODY,RZ,RPHI,RZZ,RZPHI,RPHIPHI,NDERIV)
```

The definitions of each of these parameters are as follows:

Z,PHI	the (Z,ϕ) location for the desired evaluation;
RBODY	the calculated value for the body radius;
RZ,RPHI,RZZ, RZPHI,RPHIPHI	the calculated values for r_Z, r_ϕ, r_{ZZ}, $r_{Z\phi}$, and $r_{\phi\phi}$, respectively;
NDERIV	an input parameter specifying which derivatives are to be evaluated: = 0: no partial derivatives are calculated, = 1: r_Z and r_ϕ are calculated, or = 2: r_Z, r_ϕ, r_{ZZ}, $r_{Z\phi}$, and $r_{\phi\phi}$ are calculated.

The procedure implemented through this CALL statement for an input value of $Z = Z^*$, $\phi = \phi^*$ is as follows. First, the input value for Z^* is compared with the axial locations of the original fuselage cross sections of data. If this axial location lies within the nose region (Figure 12.1), then the body radius and requested derivatives are determined according to the nose region fit (see Section 4), and their values are returned. However, if this axial location is not within the nose region, then the axial location of the original fuselage cross section of data points which is closest to (but less than) Z^* is defined to be Z_{ref}.

The value of ϕ^* is compared with the locations of the meridional cuts which were fit during the modeling process. The location of the meridional cut which is closest to (but greater than) ϕ^* (Figure 12.2) is called ϕ^*_{ref} (the index number of this cut is k_{ref}, and the value of the body radius at $Z = Z^*$ according to the equation for this cut is r^*_{ref}).

Now the program branches off to one of two divisions. If the value for ϕ^* is within a region defined to be a line segment during the curve-fitting of the fuselage cross section at $Z = Z_{ref}$ (Figure 12.3), then the program advances to Category 1. Otherwise, the code moves to Category 2. The next phase of the interpolation process is carried out according to the guidelines of these two categories.

Category 1:

If ϕ^* lies within a region defined to be a line segment in the fitting of the fuselage cross section at $Z = Z_{ref}$, then during the interpolation process, the neighborhood of ϕ^* is also fit with a line segment. The first step here is to load the angular locations of the beginning and end points of this line segment (ϕ_{beg} and ϕ_{end}, respectively) as defined in the fitting of the fuselage cross section at $Z = Z_{ref}$.

Next, the values for the body radii (r) at $Z = Z^*$ using the meridional cuts between ϕ_{beg} and ϕ_{end} are found (Figure 12.4). Then these (r,ϕ) pairs are fit in a least-squares sense using the following equation for a line segment:

$$(A_4\cos\phi + A_5\sin\phi)\, r + A_6 = 0. \qquad (12.1)$$

which is a subset of the general conic equation (with $A_1 = A_2 = A_3 = 0$)

After the coefficients have been evaluated, this equation is applied at ϕ^* to calculate r^*, the value of r at (Z^*,ϕ^*).

Category 2:

If ϕ^* does not lie within a line segment region of the fit for the fuselage cross section at $Z = Z_{ref}$, then the points in the "neighborhood" of ϕ^* are fit with three non-linear equations. First, the values for the body radii (r) at $Z = Z^*$ using meridional cuts with indices "k_{ref} - 2" through "k_{ref} + 3" are found (see Figure 12.2). These six (r_i,ϕ_i) pairs ($i = k_{ref} - 2, k_{ref} + 3$) are then fit in a least-squares sense using the following equations:

$$(A_1\cos^2\phi + A_2\cos\phi\,\sin\phi + A_3\sin^2\phi)\,r^2 + (A_4\cos\phi + A_5\sin\phi)\,r + A_6 = 0. \qquad (12.2)$$

$$A_1 r^2\cos^2\phi + (A_4\cos\phi + A_5\sin\phi)\,r + A_6 = 0. \qquad (12.3)$$

$$A_3 r^2\sin^2\phi + (A_4\cos\phi + A_5\sin\phi)\,r + A_6 = 0. \qquad (12.4)$$

where

(12.2) is an equation for a general conic,

(12.3) is an equation for an X-parabola ($A_2 = A_3 = 0$),

and

(12.4) is an equation for a Y-parabola ($A_1 = A_2 = 0$).

After their coefficients have been evaluated, each of these equations is applied at ϕ^*_{ref}. The resulting values for r are compared with r^*_{ref} and that set of coefficients which yields the closest agreement with r^*_{ref} is used to evaluate r^*, the value of r at (Z^*,ϕ^*).

Note: For a general conic equation, if

$$A_2^2 - 4A_1A_3 < 0 \qquad (12.5)$$

then the resulting curve is a hyperbola, which should not be used. This expression can only be satisfied by equation (12.2), since for equations (12.3) and (12.4) the left-hand side of this expression is identically zero. Thus, when equation (12.5) is satisfied, the general conic result is not

considered when selecting the best equation for the evaluation r^*.

Categories 1 and 2 are only used to properly determine the coefficients A_1, A_2, A_3, A_4, A_5, and A_6, and then calculate r^*. The interpolation process for the body derivatives is treated with a single approach and does not require a distinction to be made between linear and non-linear regions. First, differentiate equation (12.2) with respect to ϕ to obtain

$$r_\phi = - \frac{\mu'(\phi)\, r^2 + \nu'(\phi)\, r}{2\,\mu(\phi)\, r + \nu(\phi)} \qquad (12.6)$$

where

$$\mu(\phi) = A_1\cos^2\phi + A_2\cos\phi\,\sin\phi + A_3\sin^2\phi \qquad (12.7)$$

$$\nu(\phi) = A_4\cos\phi + A_5\sin\phi \qquad (12.8)$$

$$\mu'(\phi) = 2\,(A_3 - A_1)\cos\phi\,\sin\phi + A_2(\cos^2\phi - \sin^2\phi) \qquad (12.9)$$

$$\nu'(\phi) = A_5\cos\phi - A_4\sin\phi \qquad (12.10)$$

Now differentiate equation (12.6) with respect to ϕ to obtain

$$r_{\phi\phi} = - \frac{2\mu\, r_\phi^2 + [4r\,\mu' + 2\nu']\, r_\phi + \mu''(\phi)\, r^2 + \nu''(\phi)\, r}{2\mu\, r + \nu} \qquad (12.11)$$

where

$$\mu''(\phi) = 2(A_3 - A_1)(\cos^2\phi - \sin^2\phi) - 4A_2\cos\phi\,\sin\phi \qquad (12.12)$$

$$\nu''(\phi) = -A_4\cos\phi - A_5\sin\phi \qquad (12.13)$$

Equations (12.6) and (12.11) are evaluated at $Z = Z^*$, $r = r^*$ to obtain values for r_ϕ^* and $r_{\phi\phi}^*$. [Note that the same values for A_1 through A_6 that were used to calculate r^* are used again here.]

In a procedure analogous to the evaluation of r^* in Category 2, the approach for determining r_Z^* is as follows. The values for r_Z at $Z = Z^*$ using meridional cuts "k_{ref} + 3" through "k_{ref} - 2" are calculated (see Section 5 for the equation of r_Z for a given meridional cut). These

(r_Z,ϕ) pairs are then fit in a least-squares sense using the following equations:

$$(A_1\cos^2\phi + A_2\cos\phi\sin\phi + A_3\sin^2\phi)\, r_Z^2 + (A_4\cos\phi + A_5\sin\phi)\, r_Z + A_6 = 0. \qquad (12.14)$$

$$A_1 r_Z^2\cos^2\phi + (A_4\cos\phi + A_5\sin\phi)\, r_Z + A_6 = 0. \qquad (12.15)$$

$$A_3 r_Z^2\sin^2\phi + (A_4\cos\phi + A_5\sin\phi)\, r_Z + A_6 = 0. \qquad (12.16)$$

After their coefficients have been evaluated, each of these equations is applied at ϕ^*_{ref}. That equation which yields the closest agreement with $r^*_{Z,ref}$ (the value of r_Z for $Z = Z^*$, $\phi = \phi^*_{ref}$) is used to evaluate r^*_Z. As before, if equation (12.5) is satisfied by the coefficients of (12.14), then only the parabolic fittings, (12.15) and (12.16), are considered when selecting the equation for the evaluation r^*_Z.

Now differentiate (12.14) with respect to ϕ to obtain

$$r_{Z\phi} = -\frac{\mu'(\phi)\, r_Z^2 + \nu'(\phi)\, r_Z}{2\,\mu(\phi)\, r_Z + \nu(\phi)} \qquad (12.17)$$

where $\mu(\phi)$, $\nu(\phi)$, $\mu'(\phi)$, and $\nu'(\phi)$ are given by (12.7), (12.8), (12.9), and (12.10), respectively. Using the same set of coefficients used to calculate r^*_Z, equation (12.17) is evaluated at $\phi = \phi^*$, $r_Z = r^*_Z$ to obtain the value for $r^*_{Z\phi}$.

Finally, the approach for determining r^*_{ZZ} is as follows. The values for r_{ZZ} at $Z = Z^*$ using meridional cuts "k_{ref}+ 3" through "k_{ref}- 2" are calculated (see Section 5 for the equation of r_{ZZ} for a given meridional cut). These (r_{ZZ},ϕ) pairs are then fit in a least-squares sense using the following equations:

$$(A_1\cos^2\phi + A_2\cos\phi\sin\phi + A_3\sin^2\phi)\, r_{ZZ}^2$$

$$+ (A_4\cos\phi + A_5\sin\phi)\, r_{ZZ} + A_6 = 0. \qquad (12.18)$$

$$A_1 r_{ZZ}^2 \cos^2\phi + (A_4\cos\phi + A_5\sin\phi)\, r_{ZZ} + A_6 = 0. \qquad (12.19)$$

$$A_3 r_{ZZ}^2 \sin^2\phi + (A_4\cos\phi + A_5\sin\phi)\, r_{ZZ} + A_6 = 0. \qquad (12.20)$$

After their coefficients have been evaluated, each of these equations is applied at ϕ^*_{ref}. That equation which yields the closest agreement with $r^*_{Z,ref}$ (the value of r_{ZZ} for $Z = Z^*$, $\phi = \phi^*_{ref}$) is used to evaluate r^*_{ZZ}. Again, if equation (12.5) is satisfied, only the parabolic fittings are considered when selecting the best equation for the evaluation r^*_{ZZ}.

In the special case of the upper and lower symmetry plane ($\phi = \pm\pi/2$), the values for r, r_Z, and r_{ZZ} may be obtained directly from the first and last meridional cuts, respectively, which lie in the symmetry plane. In addition, it is seen that for symmetry, r_ϕ and $r_{Z\phi}$ should be identically zero.

For $\phi = \pm\pi/2$ radians, equations (12.7) through (12.10) become

$$\mu(\phi) = A_3 \qquad (12.21)$$

$$\nu(\phi) = A_5\sin\phi = \pm A_5 \qquad (12.22)$$

$$\mu'(\phi) = -A_2 \qquad (12.23)$$

$$\nu'(\phi) = -A_4\sin\phi = -(\pm A_4) \qquad (12.24)$$

so that (12.6) becomes

$$r_\phi = \frac{A_2 r^2 \pm A_4 r}{2A_3 r \pm A_5} \qquad (12.25)$$

For $r_\phi = 0$, equation (12.25) requires that $A_2 = A_4 = 0$. Therefore, those meridional cuts in the neighborhood of the symmetry plane are fit using

$$(A_1\cos^2\phi + A_3\sin^2\phi)\, r^2 + A_5 r \sin\phi + A_6 = 0. \qquad (12.26)$$

For $\phi = \pm\pi/2$ radians, equations (12.12) and (12.12) become

$$\mu''(\phi) = -2\,(A_3 - A_1) \qquad (12.27)$$

$$\nu''(\phi) = -A_5\sin\phi = -(\pm A_5) \qquad (12.28)$$

so that (12.11) becomes

$$r_{\phi\phi} = \frac{2\,(A_3 - A_1)\, r^2 + A_5 r \sin\phi}{2\,A_3 r + A_5\sin\phi} \qquad (12.28)$$

which can be written as

$$r_{\phi\phi} = r - \frac{2\,A_1 r^2}{2\,A_3 r + A_5\sin\phi} \qquad (12.29)$$

It should be noted that during the development of this approach, the equation selections were monitored and it was found that the type of equation which yielded the best fit over the range of (Z,ϕ) locations varied. Therefore, it was determined that a selection process between the four types of conic equations was necessary to insure the best possible surface-fit.

The interpolation process for the wing is somewhat similar to that of the fuselage. In fact, rather than the wing global coordinate system, the fuselage coordinate system is used here also. These interpolation routines are accessed by the user through the following call statement:

```
CALL WINGUSE(Z,X,RBODY,RZ,RPHI,RZZ,RZPHI,RPHIPHI,NDERIV)
```

where X is the spanwise location of the desired evaluation. The definitions of the remaining parameters are identical to those of the subroutine VALUATE mentioned earlier, so they are not repeated here.

The procedure implemented through this CALL statement for an input value of $Z = Z^*$, $X = X^*$ is as follows. First, the input value for X^* is compared with the spanwise locations of the original wing cross sections of data. The spanwise location of the original wing cross section of data points which is closest to (but less than) X^* is defined to be X_{ref}. Next, the axial location of the leading and trailing edges of the wing (Z_{LE} and Z_{TE}, respectively) are found at the spanwise location X =

X^*. Using these values, the percent chord location (Figure 12.5) of any axial position at this spanwise station is calculated from:

$$\xi = \frac{Z - Z_{LE}}{Z_{TE} - Z_{LE}} \tag{12.30}$$

Evaluating equation (12.30) at $Z = Z^*$ gives $\xi = \xi^*$. This value of ξ^* is compared with the locations of the spanwise cuts which were fit during the modeling process. The location of the spanwise cut which is closest to (but greater than) ξ^* is called ξ^*_{ref} (the index number of this cut is k_{ref}, and the distance to the wing surface from the XZ-plane at $X = X^*$ according to the equation for this cut is Y^*_{ref}).

Now the program branches off to one of two divisions. If the value for ξ^* is within a region defined to be a line segment during the curve-fitting of the wing cross section at $X = X_{ref}$, then the program advances to Category 1. Otherwise, the code moves to Category 2. The next phase of the interpolation process is carried out according to the guidelines of these two categories.

Category 1:

If ξ^* lies within a region defined to be a line segment in the fitting of the cross section at $X = X_{ref}$, then during the interpolation process, the neighborhood of ξ^* is also fit with a line segment. The first step here is to load the percent-chord locations of the beginning and end points of this line segment (ξ_{beg} and ξ_{end}, respectively) as defined in the fitting of the wing cross section at $X = X_{ref}$.

Next, the distance from the XZ-plane to the wing surface (Y) at $X = X^*$ is found using the spanwise cuts between ξ_{beg} and ξ_{end}. Then these (Y,ξ) pairs are fit in a least-squares sense using the following equation (where ξ has been converted to Z) for a line segment:

$$A_4Y + A_5Z + A_6 = 0. \tag{12.31}$$

which is a subset of the general conic equation (with $A_1 = A_2 = A_3 = 0$)

After the coefficients have been evaluated, this equation is applied at ξ^* to calculate Y^*, the value of Y at (X^*,Z^*).

Category 2:

If ξ^* does not lie within a line segment region of the fit for the wing cross section at $X = X_{ref}$, then the points in the "neighborhood" of ξ^* are fit with three non-linear equations. First, the distances from the XZ-plane to the surface of the wing (Y) at $X = X^*$ are found using the spanwise cuts with indices "k_{ref} - 2" through "k_{ref} + 3". These six (Y_i, ξ_i) pairs ($i = k_{ref} - 2, k_{ref} + 3$) are then fit in a least-squares sense using the following equations (where ξ has been converted to Z):

$$A_1 Y^2 + A_2 YZ + A_3 Z^2 + A_4 Y + A_5 Z + A_6 = 0. \qquad (12.32)$$

$$A_1 Y^2 + A_4 Y + A_5 Z + A_6 = 0. \qquad (12.33)$$

$$A_3 Z^2 + A_4 Y + A_5 Z + A_6 = 0. \qquad (12.34)$$

where

(12.32) is an equation for a general conic,
(12.33) is an equation for a Y-parabola ($A_2 = A_3 = 0$),

and

(12.34) is an equation for a Z-parabola ($A_1 = A_2 = 0$).

After their coefficients have been evaluated, each of these equations is applied at ξ^*_{ref}. The resulting values for Y are compared with Y^*_{ref} and that set of coefficients which yields the closest agreement with Y^*_{ref} is used to evaluate Y^*, the value of Y at (X^*, ξ^*). As with the fuselage, if equation (12.5) is satisfied, the general conic result is not considered when selecting the best equation for the evaluation Y^*.

As with the fuselage, Categories 1 and 2 are only used to properly determine the coefficients A_1, A_2, A_3, A_4, A_5, and A_6, and then calculate Y^*. The corresponding value of r^* is found by evaluating the following equation at (X^*, Y^*):

$$r = | X^2 + Y^2 |^{1/2} \qquad (12.35)$$

As with the fuselage, the interpolation process for the wing derivatives is treated with a single approach and does not require a distinction to

be made between linear and non-linear regions. First, differentiate (12.32) with respect to Z to obtain

$$Y_Z = - \frac{2 A_3 Z + A_2 Y + A_5}{2 A_1 Y + A_2 Z + A_4} \qquad (12.36)$$

To convert this value of Y_Z to r_Z, differentiate equation (12.35) with respect to Z to get

$$r_Z = Y Y_Z \left| X^2 + Y^2 \right|^{-1/2} = Y Y_Z / r \qquad (12.37)$$

Now differentiate (12.36) with respect to Z to obtain

$$Y_{ZZ} = -2 \frac{(A_1 Y_Z + A_2) Y_Z + A_3}{2 A_1 Y + A_2 Z + A_4} \qquad (12.38)$$

To convert this value of Y_{ZZ} to r_{ZZ}, differentiate equation (12.37) with respect to Z to get

$$r_{ZZ} = \frac{Y Y_{ZZ} + Y_Z^2 - r_Z^2}{r} \qquad (12.39)$$

Equations (12.36) and (12.38) are evaluated at $X = X^*$, $Y = Y^*$, to obtain values for Y_Z^* and Y_{ZZ}^*. Then these values are substituted into equations (12.37) and (12.39) to evaluate r_Z^* and r_{ZZ}^*.

The evaluation of the ϕ-derivatives for the wing is left as an area of future work. Additional future work might involve allowing the user to specify a value of (Z,ϕ), with the value of r and its derivatives returned whether that location is on the wing or the fuselage. This structure would be in lieu of the present framework which requires (Z,X) to be input for the wing evaluation. Such a capability would involve logistics to handle the possibility that a given ϕ-cut might intersect the fuselage and both the upper and lower surfaces of the wing (Figure 12.6).

Section 13: File Structure and Manipulation

To execute this code, the user must first create a raw data file. This file should contain the global (X,Y) coordinates of the input data points grouped according to cross sections at several axial (Z) locations. The format for each cross section is as follows:

line 1: ND (number of data points in this cross section); FORMAT (I5)
line 2: Z (axial location of this cross section); FORMAT (G13.6)
line 3: (X_i,Y_i) coordinates for i=1,ND; FORMAT (10G13.6)

This is referred to as the IRAW file.

Note: Currently the (X,Y) coordinates must be ordered starting from the upper symmetry plane (data point #1) and rotating around the cross section to the lower symmetry plane (point #ND). Future work might allow these coordinates to be input in a random fashion. The program would then take these points and place them in the order necessary for the proper implementation of this code's algorithm.

In order to model a wing-body configuration, an additional set of wing section coordinates grouped according to wing sections at several spanwise locations must be appended to this file. These coordinates are measured according to the wing coordinate system (see Section 7) so that the format for each wing section is as follows:

line 1: ND (number of data points in this wing section); FORMAT (I5)
line 2: Z (spanwise location of this wing section); FORMAT (G13.6)
line 3: (X_i,Y_i) coordinates for i=1,ND; FORMAT (10G13.6)

The fuselage data and this wing data should be separated by one blank line.

During the execution of the program, as each cross section or blending fit is completed by the user, several of its defining parameters are stored in a refined data file (referred to as the IFO file). These defining parameters include control point locations and the global coefficients for each arc equation. In future fitting sessions, this file will be used to reload the user-prescribed fittings for each of the sections which were previously fitted.

As mentioned in Section 2, the user may terminate the current fitting session before the model is completed, and the fittings which were made during that session are saved. In order to have this capability, additional data files must be created. The portion of the raw data file which has not yet been accessed by the user is saved in

the ISAVE file, and the number of sections which have been fit thus far is saved in the IGUIDE file.

> **Note:** To utilize these restart files, the user must reload their information from the IFO, ISAVE, and IOUT files to the IFI, IRAW, and IGUIDE files, respectively. This feature allows the user to end an interactive modification session at any time without losing the changes made in that session. If the user prefers not to keep those changes made during the most recent modification session, then this reloading process should not be performed. Future work in this area might include the automation of the file reloading operation mentioned above. In such a scenerio, when the current modification was ended, the user would be given the option to save or disgard those changes made during that session.

The spacings for the meridional cuts and spanwise blends, along with the parameters which describe the nose region fit, are saved in the IUSE file. This file also replicates the information which is stored in the IFO and IGUIDE files. Thus, all of the information necessary to reproduce the constructed geometry model is contained in the IUSE file. This file is accessed by the interpolation routines when the constructed model is being used to evaluate the body radius and its partial derivatives at a given (Z,ϕ) location.

> **Note:** To reduce storage requirements, the following files are stored in binary form: IFI, IFO, IGUIDE, and IUSE. Since these are binary files, the user should not attempt to edit them, type them to the screen, or print them!

> **Note:** Addresses for these files are assigned in PROGRAM MAIN of the code.

Section 14: Results and Discussion

The accuracy of a model for a given geometry can have a significant effect on the results obtained from flowfield calculations. As an example, consider two models of the Space Shuttle. The first is simply a hyperboloid, which is axisymmetric by definition. This shape matches the windward plane of symmetry of the Shuttle geometry well, but the cross sections, wing, and canopy are not modeled. The second representation is the HALIS QUICK model (see reference 1). This model was used in the HALIS inviscid flowfield code, and it provides a good model of the windward surface of the Shuttle, including the wing.

Some results from a viscous-shock-layer (ref. 13) code using these two models are shown in Figure 14.1. This heat transfer comparison is for the windward symmetry plane of the Shuttle. It can be seen that the results using the QUICK model are in better agreement with the flight data than those obtained using the hyperboloid model. This difference can be attributed to the fact that the QUICK model allows the flowfield calculations to take into account the effect of spanwise flow along the wing. In addition, the QUICK model properly accounts for the expansion region at the rear of the fuselage, whereas the hyperboloid does not.

A geometry model for the Shuttle was created using the current method from a set of data points grouped according to fuselage cross sections. The complexities of this geometry provided an excellent test for the many features of this code. As the cross-section curve-fitting process advanced along the fuselage away from the nose, the cross sections became increasingly more challenging, bringing with them the necessity to make the program more powerful.

For this Space Shuttle model, the nose radius of curvature was left as part of the solution (option 3 of the Nose Radius of Curvature Menu), and the nose fit was constrained to pass through the curve-fits of the second and third cross sections of input coordinates. Wing cross section data was also available, so the wing-body combination was modeled. Using the interpolation routines, the agreement between this model, the original input data points, and the HALIS QUICK model was examined. Since the QUICK model used here does not attempt to model a large portion of the upper part of the fuselage, comparisons between the two models and the original data are restricted, for the most part, to the windward surface of the fuselage and wing. The results of this comparison are presented in Table 2 (the nose region), Table 3 (the fuselage aft of the nose region), and Table 4 (the wing). It can be seen that both models are in good agreement with the original input coordinates for the majority of the compared portions of the geometry (Figures 14.2 through 14.15).

A geometry (ref. 14) for the proposed Aeroassist Flight Experiment (AFE) was chosen as a second test case for the current geometry package. This configuration is a raked elliptic cone with an ellipsoidal nose and

circular arc skirt (Figure 14.16). As shown in reference 14, this body surface and its partial derivatives can be completely defined analytically. For this case the following values were used in conjunction with the cylindrical afterbody option:

$\tau = \theta_{YZ} = 60$ degrees $\quad \delta = 73$ degrees $\quad \bar{R} = .1 \quad \varepsilon_b = 1.$

Next, eleven cross sections of 37 data points each (positioned at $\Delta\phi = 5$ degree increments) were generated. The spacing for the cross sections and their data points was chosen arbitrarily, although the number of cross sections was kept small intentionally in order to tax the code's ability to model a geometry based on a minimal amount of input. This point is of interest since the number of cross sections used to generate the model dictates the time required for the user to surface-fit a particular geometry.

Using these data planes, the AFE geometry was successfully surface-fit by a user who was unfamiliar with the code and its operation. This modeling process was performed during several sessions, and the total time expended by the user (starting from raw data, periodically modifying given curve-fits, until the model was completed) was approximately three hours.

For this geometry, the nose region is constrained to pass through the first and second cross-sectional curve-fits. Since the analytic equation for the nose region of this geometry is an ellipsoid, the nose radii of curvature in the XZ- and YZ-planes are given by equations (D.10) and (D.11), respectively. Based on the specified input parameters (and the resulting values for a, b, and c in ref. 14) for this case, these relations yield

$$R_{XZ} \approx .6836643 \qquad R_{YZ} \approx .4499019.$$

The computed distribution of the nose radii of curvature, based on these values for the principle radii of curvature, is presented in Table 5. Also presented in Table 5 is the distribution obtained when the nose radius of curvature is not specified by the user. The two distributions are found to be virtually identical. This is to be expected as shown in the following argument. The two cross sections chosen to model the nose region are indeed within the ellipsoidal nose region of the AFE geometry. Therefore, they are symmetric about the XZ-plane (Figure 14.17). As a result, the coefficients for the upper and lower portions of a given meridional pair should be identical. Thus, when the nose radius of curvature is determined as part of the solution, not only is $D_l = -D_u$ as assigned by the program, but the symmetry causes $B_l \approx B_u$. On the other hand, when the nose radius of curvature is specified, the symmetry causes $B_l \approx B_u$ and $D_l \approx -D_u$. Thus, the distributions of the nose radii of curvature should be nearly identical for the two nose region definitions.

In order to validate this AFE surface-fit, the body radii and partial derivatives as calculated from the model are compared with their corresponding analytic values in Tables 6 and 7. As a further test, the

locations of these comparisons are chosen so as not to coincide with the cross sections and meridional cuts which were actually curve-fit to generate the model. The results of this comparison, in general, show excellent agreement for the body radii, very good agreement for the first partial derivatives, and for the most part, inconsistent agreement for the second partial derivatives (see Tables 6 and 7). So in its current form, a model developed using this geometry package should meet the needs of a flowfield code which requires the geometry subroutine to calculate the surface coordinates and even first partial derivatives. However, the constructed model may not serve satisfactorily when the second partial derivatives must also be provided by the geometry subroutine.

The proper spacing and density of the input data can be crucial to the development of acceptable cross-sectional curve-fits. In each cross section, data points should be placed in the upper and lower planes of symmetry, at each discontinuity and inflection point, and at the beginning and end points of any line segments. These special data point locations will ultimately be defined to be control points (Figure 14.18) in the cross-sectional curve-fitting process. (Recall that each pair of control points define the end points of the arc which connects them.) In addition, at least one intermediate data point (Figure 14.19) should be located between each of these data points (except for between those data points which define the ends of a line segment) in order to provide the fifth constraint for the conic equation (two end points, two end slopes, and an intermediate point). Including two or more such intermediate points requires a least-squares solution to the given arc. In general, a minimal number of intermediate points is recommended since overspecification can actually hamper the curve-fitting process, and the resulting fit may actually be inferior to a fit obtained from using fewer data points.

The guidelines of the above paragraph are directly applicable to the wing cross sections as well. And since the same least-squares curve-fitting technique is used in blending the fuselage and wing cross sections in the longitudinal and spanwise directions, respectively, these guidelines may also be applied to these cases, recognizing that the data points are now actually intersections between the meridional (or spanwise) cuts and the fuselage (or wing) cross sections. Thus, for an optimal fuselage surface blending, the cross sections of data should be located at each longitudinal discontinuity and inflection point, and at the beginning and end points of any longitudinal line segments. As with the cross sections, at least one intermediate point should be located between each of these points. In addition, several cross sections should be clustered near the nose in order to provide a good nose region definition.

These criteria provide that, in general, only a few wing cross sections are necessary for a good wing surface-fit. In fact, a simple wing (for example, a wing with linearly varying twist and taper, and no breaks in the planform) may be accurately surface-fit using only two wing sections--one at the wing root and one at the wing tip.

Section 15: Concluding Remarks

An interactive, user-friendly, completely menu-driven code for surface-fitting arbitrary geometries has been developed. Provisions have been made to handle bodies, wings, and wing-body combinations. The present method calculates first and second partial derivatives, in addition to the body radius, for any point on the configuration. Geometry comparisons for the Space Shuttle and a proposed Aeroassist Flight Experiment (AFE) geometry show good agreement between the values calculated from the models and those of the input coordinates (Space Shuttle) and actual geometry (AFE). Numerical results show that the accuracy of the geometry model can have a significant effect on the flowfield calculations.

Appendix A: Evaluation of the Local Conic Equation Coefficients

Repeating equation (2.2), the general conic equation in local coordinates is

$$A x^2 + B xy + C y^2 + D x + E y = 0 \qquad (A.1)$$

which inherently passes through the first control point ($x = 0$, $y = 0$). Let $x = x_{CP}$ be the location of the second control point (which recall also lies on the x-axis). The constraint that the curve pass through this point $(x_{CP},0)$ yields

$$D = - A x_{CP} \qquad (A.2)$$

To find the slope in this local system, differentiate equation (A.1) with respect to x:

$$\frac{dy}{dx} = \frac{A x_{CP} - 2 A x - B y}{B x + 2 C y + E} \qquad (A.3)$$

Apply equation (A.3) at the first control point, and define it to be the beginning slope, m_b. This yields

$$m_b = \left.\frac{dy}{dx}\right|_{0,0} = \frac{A x_{CP}}{E} \qquad (A.4)$$

so that

$$E = \frac{A x_{CP}}{m_b} \qquad (A.5)$$

Similarly, apply equation (A.3) at the second control point, and define it to be the end slope, m_e. This yields

$$m_e = \left.\frac{dy}{dx}\right|_{x_{CP},0} = \frac{-A x_{CP}}{B x_{CP} + E} \qquad (A.6)$$

so that

$$B = - A \left[\frac{1}{m_b} + \frac{1}{m_e} \right] \qquad (A.7)$$

From these relations, it is seen that the end slopes of an arc do not affect the coefficient C, and vice versa.

As mentioned earlier, the slope at a given control point may be left arbitrary by the user, in which case the global slope for the resulting arc equations will be continuous with adjacent segments across this control point. Reference 9 establishes the following relations at control point "j" (denoted by the subscript "j") to insure these conditions:

$$\frac{A_j}{m_{e_j}} = \frac{A_j \cos\Delta\theta_{j+1} - A_{j+1}}{\sin\Delta\theta_{j+1}} \qquad (A.8)$$

and

$$\frac{A_j}{m_{b_j}} = \frac{A_{j-1} - A_j \cos\Delta\theta_j}{\sin\Delta\theta_j} \qquad (A.9)$$

where $\Delta\theta$ is the difference in the orientation of the two adjacent local coordinate systems (Figure A.1).

Substitute equations (A.2), (A.5), (A.7), (A.8), and (A.9) into equation (A.1) to obtain

$$\alpha_j A_{j-1} + \beta_j A_j + \gamma_j A_{j+1} + C_j y^2 = 0 \qquad (A.10)$$

where

$$\alpha_j = \frac{x_{CP} y - xy}{\sin\Delta\theta_j} \qquad (A.11)$$

$$\beta_j = x^2 + xy\,(\cot\Delta\theta_j - \cot\Delta\theta_{j+1}) - x_{CP} y \cot\Delta\theta_j - x_{CP} x \qquad (A.12)$$

$$\gamma_j = \frac{x\,y}{\sin\Delta\theta_{j+1}} \qquad (A.13)$$

Note: The above relations are for arcs where both end slopes have been left arbitrary. The values of these parameters for the arcs where either one or both end slopes is specified are given in Reference 9.

There are two unknowns (A_j, C_j) for each arc where both end slopes have been left arbitrary (but forced to be continuous across the control point, recall). Therefore, one intermediate data point for each arc, along with the continuous slope requirement, will constrain the conic equation (if, in fact, these conditions may be satisfied by a conic). Since in general there will be more than one data point between two

control points, these curves are overdetermined, and a least-squares solution of equation (A.10) is sought (Reference 9).

The equation for each arc as determined from the above procedure must be checked for complex roots. It is shown in reference 9 that no complex roots occur within the arc if

$$A_j C_j \geq (A_j/m_{b_j})(A_j/m_{e_j}) \qquad (A.14)$$

This inequality is checked within the program. If it is not satisfied, then C_j is replaced by a value which satisfies

$$A_j C_j = (A_j/m_{b_j})(A_j/m_{e_j}) \qquad (A.15)$$

Note: Since as mentioned before, the value of C_j does not affect the end slopes of its arc, this substitution does not affect the fitting equations of the arcs adjacent to the arc where this change is made.

With the values of A_j and C_j for each arc defined, the values of D_j, E_j, and B_j are found from equations (A.2), (A.5), and (A.7), respectively.

Given one coordinate of a desired location, in using equation (A.1), a quadratic equation is encountered in the solution for the unknown coordinate. A choice between the "+" or "-" sign must be made beforehand. Reference 9 establishes that the proper sign to use here is

the "+" sign if $A_j/m_{b_j} > 0$ and $A_j/m_{e_j} < 0$ (A.16)

and

the "-" sign if $A_j/m_{b_j} < 0$ and $A_j/m_{e_j} > 0$ (A.17)

Appendix B: Proper Sign Selection in Using the Global Conic Equation

Define

$$r = \{ (X - X_r)^2 + (Y - Y_r)^2 \}^{1/2} \qquad (B.1)$$

and

$$\phi_r = \tan^{-1} \left[\frac{Y - Y_r}{X - X_r} \right], \quad 0 \leq \phi_r \leq 2\pi \qquad (B.2)$$

where (X_r, Y_r) may be any reference point, so that

$$X = X_r + r \cos\phi_r \qquad (B.3)$$

and

$$Y = Y_r + r \sin\phi_r \qquad (B.4)$$

Now substitute equations (B.3) and (B.4) into equation (2.1) to get

$$\varepsilon r^2 + \zeta r + \eta = 0 \qquad (B.5)$$

where

$$\varepsilon = A_1 \cos^2\phi_r + A_2 \sin\phi_r \cos\phi_r + A_3 \sin^2\phi_r \qquad (B.6)$$

$$\zeta = (2 A_1 X_r + A_4 + A_2 Y_r) \cos\phi_r + (2 A_3 Y_r + A_5 + A_2 X_r) \sin\phi_r \qquad (B.7)$$

and

$$\eta = A_1 X_r^2 + A_2 X_r Y_r + A_3 Y_r^2 + A_4 X_r + A_5 Y_r + A_6 \qquad (B.8)$$

Note that η is constant for a given arc (provided the reference point is fixed).

Given one coordinate of a desired location, in using equation (B.5), a quadratic equation is encountered in the solution for the unknown coordinate. A choice between the "+" or "-" sign must be made beforehand. An outline of the development of the criteria for this selection is shown below.

Apply equation (B.5) at the control point at the end of arc "j-1" to obtain

$$\eta = - [\varepsilon_j r_j^2 + \zeta_j r_j] \qquad (B.9)$$

Substitute equation (B.9) back into equation (B.5) to obtain

$$\varepsilon r^2 + \zeta r - [\varepsilon_j r_j^2 + \zeta_j r_j] = 0 \qquad (B.10)$$

Solve for $\bar{r}$ to get

$$\bar{r} = \frac{-\zeta \pm \{ \zeta^2 + 4\varepsilon [\varepsilon_j \bar{r}_j^2 + \zeta_j \bar{r}_j] \}^{1/2}}{2\varepsilon} \qquad \text{(B.11)}$$

Evaluate equation (B.11) at the control point at the end of the current arc to obtain

$$\bar{r}_j = \frac{-\zeta_j \pm \{ \zeta_j^2 + 4\varepsilon_j \zeta_j \bar{r}_j + 4\varepsilon_j^2 \bar{r}_j^2 \}^{1/2}}{2\varepsilon_j} \qquad \text{(B.12)}$$

which can be written as

$$\bar{r}_j = \frac{-\zeta_j \pm \{ (2\varepsilon_j \bar{r}_j + \zeta_j)^2 \}^{1/2}}{2\varepsilon_j} \qquad \text{(B.13)}$$

In accordance with equation (B.13), use

the "+" sign when $2\varepsilon_j \bar{r}_j + \zeta_j > 0$ (B.14)

and

the "-" sign when $2\varepsilon_j \bar{r}_j + \zeta_j < 0$ (B.15)

Appendix C: Derivation of Conic Fitting Equation for Nose Region

The general conic equation in a meridional half-plane can be written

$$A_1 r^2 + A_2 r Z + A_3 Z^2 + A_4 r + A_5 Z + A_6 = 0. \qquad (C.1)$$

In order for this equation to pass through the origin, $A_6 = 0$. Now rewrite equation (C.1) as

$$r^2 + B_k Z^2 + C Z + D_k r Z + A_k r = 0. \qquad (C.2)$$

where

$$B_k = \frac{A_3}{A_1}, \quad C = \frac{A_5}{A_1}, \quad D_k = \frac{A_2}{A_1}, \text{ and } \quad A_k = \frac{A_4}{A_1}.$$

Differentiate equation (C.2) with respect to Z to obtain

$$\frac{dr}{dZ} = - \frac{D_k r + 2 B_k Z + C}{2 r + D_k Z + A_k} \qquad (C.3)$$

At the nose (r=0, Z=0) this gives

$$\left.\frac{dr}{dZ}\right|_{nose} = - \frac{C}{A_k} \qquad (C.4)$$

For a blunt body, $r_Z \to \infty$ at the nose. This condition is satisfied if $A_k = 0$ and $C \neq 0$. Thus, for a blunt body, the nose fit equation is

$$r^2 + B_k Z^2 + C Z + D_k r Z = 0. \qquad (C.5)$$

Appendix D: Ellipsoidal Nose Radius of Curvature Distribution

The equation for an ellipsoid with its center at $(0,0,\frac{c}{2})$ is

$$\left[\frac{Z-c}{c}\right]^2 + \left[\frac{X}{a}\right]^2 + \left[\frac{Y}{b}\right]^2 = 1 \qquad (D.1)$$

Use the polar transformation

$$X = r\cos\phi \quad \text{and} \quad Y = r\sin\phi \qquad (D.2)$$

to obtain

$$\left[\frac{Z-c}{c}\right]^2 + \frac{r^2\cos^2\phi}{a^2} + \frac{r^2\sin^2\phi}{b^2} = 1 \qquad (D.3)$$

Rearrange equation (D.3) to obtain

$$r^2 = Q\left\{1 - [Z/c - 1]^2\right\} \qquad (D.4)$$

where

$$Q = \left[\frac{\cos^2\phi}{a^2} + \frac{\sin^2\phi}{b^2}\right]^{-1} \qquad (D.5)$$

Differentiate equation (D.4) with respect to Z to obtain

$$r\,r_Z = -\frac{Q}{c}\left[\frac{Z}{c} - 1\right] \qquad (D.6)$$

Differentiate equation (D.6) with respect to Z to obtain

$$r\,r_{ZZ} + (r_Z)^2 = -\frac{Q}{c^2} \qquad (D.7)$$

The definition of the radius of curvature is

$$\frac{1}{R} = \frac{|r_{ZZ}|}{\left[1 + (r_Z)^2\right]^{3/2}} = \frac{|r^3 r_{ZZ}|}{\left[r^2 + (r\,r_Z)^2\right]^{3/2}} \qquad (D.8)$$

By using the above values for r_Z and r_{ZZ}, the radius of curvature at the nose (where $r \to 0$ as $Z \to 0$) is found to be

$$R^{-1} = \frac{c}{Q} = c\left[\frac{\cos^2\phi}{a^2} + \frac{\sin^2\phi}{b^2}\right] \qquad (D.9)$$

In the XZ-plane ($\phi = 0$) this gives

$$R_{XZ}^{-1} = \frac{c}{a^2} \qquad (D.10)$$

and in the YZ-plane ($\phi = \pm\pi/2$) this gives

$$R_{YZ}^{-1} = \frac{c}{b^2} \qquad (D.11)$$

Substitute equations (D.10) and (D.11) into equation (D.9) to get

$$R^{-1} = \frac{\cos^2\phi}{R_{XZ}} + \frac{\sin^2\phi}{R_{YZ}} \qquad (D.12)$$

When option (2) of the Nose Radius of Curvature Menu is chosen, the user must specify values for R_{XZ} and R_{YZ}. Then for a given meridional (ϕ = constant) cut, the value for $R(\phi)$ is defined by equation (D.12). If option (1) of this menu is exercised, then equation (D.12) gives $R = R_{XZ} = R_{YZ}$ where this value must be supplied by the user.

References

1. Weilmuenster, K.J. and Hamilton, H.H. II, "Calculations of Inviscid Flow Over Shuttle-Like Vehicles at High Angles of Attack and Comparisons with Experimental Data," NASA TP-2103, May 1983.

2. DeJarnette, F.R. and Hamilton, H.H., II, "Inviscid Surface Streamlines and Heat Transfer on Shuttle-Type Configurations," Journal of Spacecraft and Rockets, Volume 10, May 1973, pp. 314-321.

3. Margason, R.J. and Lamar, J.E., "Vortex-Lattice Fortran Program for Estimating Subsonic Aerodynamic Characteristics of Complex Planforms," NASA TN D-6142, February 1971.

4. Woodward, F.A., "Analysis and Design of Wing-Body Combinations at Subsonic and Supersonic Speeds," Journal of Aircraft, Volume 5, Number 6, November-December 1968, pp. 528-534.

5. Coons, S.A., "Surfaces for Computer-Aided Design of Space Forms," Massachusetts Institute of Technology, MAC-TR-41, (Contract No. AF-33(600)-42859), June 1967.

6. Bezier, P., Numerical Control Mathematics and Applications, John Wiley and Sons, New York, 1972.

7. DeJarnette, F.R., "Calculation of Inviscid Surface Streamlines and Heat Transfer on Shuttle Type Configurations." Part I.-Description of Basic Method, NASA CR-111921, August 1971.

8. Vachris, A.F. and Yeager, L., "QUICK-GEOMETRY, A Rapid Response Method for Mathematically Modeling Configuration Geometry." Applications of Computer Graphics in Engineering, NASA SP-390, October 1975, pp. 49-73.

9. DeJarnette, F.R. and Ford, C.P., "Surface Fitting Three-Dimensional Bodies." Applications of Computer Graphics in Engineering, NASA SP-390, October 1975, pp. 447-474.

10. Sliski, N.J., "A Numerical Technique for Describing Three-Dimensional Surfaces," AFWAL-TR-83-3038, September 1983.

11. Perkins, J.N., "An Interactive Method for Surface Fitting Three-Dimensional Bodies," AIAA-83-0220, January 1983.

12. Crisp, V.K., Rehder, J.J., and Schwing, J.L., "Intersection of Three-Dimensional Geometric Surfaces," NASA TP-2454, July 1985.

13. Thompson, R.A., "Three-Dimensional Viscous-Shock-Layer Applications for the Space Shuttle Orbiter," AIAA-85-0246, January 1985.

14. Cheatwood, F.M., DeJarnette, F.R., and Hamilton, H.H. II, "Geometrical Description for a Proposed Aeroassist Flight Experiment Vehicle," NASA TM-87714, July 1986.

Table 1: Sample Output for Cross-Sectional Curve-Fit

C R O S S S E C T I O N 27: Z = 562.

D A T A P O I N T S

PT	INPUT VALUE	CALCULATED VALUE	DEVIATION	RELATIVE DEVIATION
1	(0.00000E+00, 162.88)			CP
2	(11.258 , 162.65)	(11.200 , 162.36)	.2900	.1779E-02
3	(25.008 , 161.06)	(24.752 , 160.51)	.6046	.3709E-02
4	(36.067 , 158.19)	(35.976 , 158.06)	.1571	.9680E-03
5	(46.229 , 154.89)	(46.388 , 155.05)	.2274	.1407E-02
6	(56.828 , 151.14)	(56.954 , 151.24)	.1593	.9868E-03
7	(65.649 , 147.42)	(65.671 , 147.44)	.2550E-01	.1580E-03
8	(74.454 , 142.82)	(74.521 , 142.85)	.7361E-01	.4570E-03
9	(82.370 , 138.23)	(82.138 , 138.14)	.2473	.1537E-02
10	(89.381 , 132.76)	(89.356 , 132.76)	.2635E-01	.1647E-03
11	(95.059 , 127.32)	(95.188 , 127.35)	.1318	.8293E-03
12	(98.968 , 122.36)	(99.348 , 122.42)	.3847	.2445E-02
13	(102.43 , 116.97)	(102.65 , 116.99)	.2309	.1485E-02
14	(104.12 , 112.49)	(104.32 , 112.50)	.2039	.1330E-02
15	(104.93 , 108.03)			LS
16	(105.53 ,-3.9900)			CP
17	(124.94 ,-12.348)	(124.02 ,-12.169)	.9339	.7439E-02
18	(136.81 ,-19.233)	(136.02 ,-18.969)	.8335	.6033E-02
19	(141.63 ,-22.878)	(141.92 ,-22.989)	.3065	.2136E-02
20	(145.57 ,-26.062)	(145.99 ,-26.242)	.4568	.3089E-02
21	(148.62 ,-29.674)	(150.08 ,-30.374)	1.620	.1069E-01
22	(151.23 ,-32.833)	(151.89 ,-33.178)	.7484	.4836E-02
23	(152.04 ,-36.849)			CP
24	(150.20 ,-40.370)	(149.53 ,-39.954)	.7846	.5044E-02
25	(136.28 ,-48.115)	(136.35 ,-48.166)	.8508E-01	.5887E-03
26	(118.83 ,-54.461)	(118.83 ,-54.461)	.6474E-04	.4953E-06
27	(100.52 ,-59.013)	(100.54 ,-59.038)	.3339E-01	.2865E-03
28	(71.087 ,-64.250)	(70.994 ,-64.095)	.1807	.1886E-02
29	(35.920 ,-67.158)	(36.036 ,-67.546)	.4051	.5319E-02
30	(0.00000E+00,-68.735)			CP

ARC 1 EQN: 0.16699E-04XX * 0.27738E-04XY * 0.60919E-04YY + -.45180E-02X + -.16062E-01Y * 1 = 0.

ARC 2 EQN: (LINE SEGMENT) -.94777E-02X + -.51187E-04Y * 1 = 0.

ARC 3 EQN: 0.15567E-03XX + 0.50637E-03XY * 0.61447E-03YY + -.25252E-01X + -.33741E-01Y + 1 = 0.

ARC 4 EQN: 0.79956E-04XX + -.12781E-03XY * 0.14406E-02YY + -.87848E-02X * 0.11357 Y * 1 = 0.

Table 2: Comparison for the Nose Region of the Shuttle

X	Y	ϕ(deg)	r_{input}	r_{ASTUD}	r_{QUICK}	Q/A*
			Z = 2.0000			
0.0000	12.843	90.000	12.843	9.7835	9.7980	Q
2.2730	12.454	79.657	12.660	9.8060	9.7980	A
4.9490	11.636	66.959	12.645	9.8530	9.7980	A
7.1930	10.364	55.238	12.616	9.8748	9.7980	A
9.0060	8.6390	43.808	12.480	9.8705	9.7980	A
10.852	5.5870	27.241	12.206	9.7845	9.7980	Q
11.781	3.8400	18.053	12.391	9.7048	9.7980	Q
12.311	.31300	1.4564	12.315	9.7082	9.7980	Q
12.355	-1.4560	-6.7211	12.440	9.8046	9.7980	A
12.410	-3.6680	-16.466	12.941	10.022	9.7980	A
12.023	-5.8900	-26.100	13.388	10.351	9.7980	A
10.762	-8.5770	-38.554	13.762	10.588	9.7980	A
9.4790	-10.379	-47.595	14.056	10.561	9.7980	A
6.8590	-11.772	-59.773	13.624	10.369	9.7980	A
5.1000	-12.258	-67.410	13.277	10.223	9.7980	A
2.0160	-12.777	-81.034	12.935	10.019	9.7980	A
0.0000	-12.833	-90.000	12.833	9.9728	9.7980	A
			Z = 12.000			
0.0000	23.456	90.000	23.456	23.456	23.117	A
4.7280	23.130	78.447	23.608	23.559	23.104	A
9.1830	21.908	67.258	23.755	23.738	23.075	A
12.763	20.223	57.743	23.914	23.824	23.053	A
16.375	17.212	46.428	23.757	23.753	23.057	A
19.576	12.863	33.308	23.424	23.474	23.143	A
21.914	7.6080	19.146	23.197	23.191	23.385	A
22.904	3.2060	7.9682	23.127	23.197	23.712	A
23.452	-1.2060	-2.9438	23.483	23.539	24.161	A
23.588	-6.9560	-16.431	24.592	24.592	24.622	A
21.946	-12.306	-29.281	25.161	25.569	24.689	A
20.271	-16.328	-38.851	26.029	25.627	24.964	A
15.912	-19.087	-50.184	24.850	25.084	24.608	A
12.416	-20.941	-59.336	24.345	24.427	23.820	A
8.0240	-22.373	-70.270	23.768	23.686	22.977	A
3.6120	-22.920	-81.044	23.203	23.197	22.466	A
0.0000	-23.059	-90.000	23.059	23.059	22.331	A

* This is a "quick-reference" column. An entry of "A" indicates the ASTUD results are closer to the input data point, while a "Q" indicates the QUICK results are closer.

Table 2 (continued)

X	Y	ϕ(deg)	r_{input}	r_{ASTUD}	r_{QUICK}	Q/A
			Z = 22.000			
0.0000	31.413	90.000	31.413	31.413	31.275	A
5.4990	31.106	79.975	31.588	31.606	31.209	A
11.711	30.362	68.908	32.542	32.091	31.006	A
17.531	27.397	57.385	32.526	32.503	30.718	A
22.044	23.517	46.852	32.233	32.458	30.469	A
26.156	17.857	34.322	31.670	31.864	30.298	A
29.413	10.851	20.250	31.351	31.093	30.390	A
30.428	5.1210	9.5533	30.856	30.874	30.726	A
31.011	-1.0610	-1.9595	31.029	31.260	31.385	A
31.624	-8.5700	-15.163	32.765	32.765	32.313	A
30.006	-15.244	-26.932	33.656	33.710	32.374	A
26.568	-19.748	-36.623	33.104	33.235	32.512	A
21.783	-23.397	-47.046	31.967	32.084	32.064	Q
16.093	-26.181	-58.422	30.732	30.703	30.915	A
10.384	-28.081	-69.706	29.939	29.594	29.883	Q
4.6440	-28.654	-80.794	29.028	28.932	29.255	A
0.0000	-28.754	-90.000	28.754	28.754	29.088	A

Table 3: Shuttle Comparison Aft of the Nose Region

X	Y	ϕ(deg)	r_{input}	r_{ASTUD}	r_{QUICK}	Q/A*
			Z = 32.000			
0.0000	38.049	90.000	38.049	38.002	37.933	A
8.0950	37.350	77.771	38.217	37.933	37.750	A
16.095	35.753	65.764	39.209	38.496	37.282	A
22.825	31.473	54.049	38.878	38.796	36.707	A
29.161	24.972	40.575	38.392	38.395	36.133	A
32.382	19.289	30.781	37.692	37.748	35.899	A
35.188	12.270	19.224	37.266	37.169	35.923	A
36.649	6.1060	9.4590	37.154	36.712	36.253	A
37.225	-.07700	-.11852	37.225	36.909	36.886	A
37.436	-9.8070	-14.680	38.699	39.054	38.342	A
35.406	-18.259	-27.280	39.837	40.310	38.667	A
31.540	-23.653	-36.868	39.424	39.431	38.729	A
25.876	-27.758	-47.010	37.948	38.326	37.872	Q
19.741	-30.545	-57.126	36.369	37.361	36.497	Q
12.703	-32.468	-68.632	34.865	35.977	35.119	Q
5.6350	-33.063	-80.328	33.540	34.921	34.254	Q
0.0000	-33.187	-90.000	33.187	34.593	34.026	Q
			Z = 42.000			
0.0000	43.809	90.000	43.809	43.981	43.807	Q
7.4690	43.147	80.179	43.789	44.144	43.630	Q
14.582	42.017	70.861	44.475	43.819	43.176	A
20.859	39.093	61.917	44.310	44.073	42.571	A
26.276	35.260	53.306	43.974	44.094	41.940	A
33.991	28.393	39.872	44.289	43.749	41.087	A
38.671	19.229	26.439	43.188	43.243	40.646	A
40.698	9.9910	13.793	41.906	41.925	40.785	A
42.320	-.58500	-.79196	42.324	41.825	41.756	A
42.578	-9.8720	-13.054	43.707	43.801	43.297	A
40.170	-18.791	-25.070	44.348	45.088	44.115	Q
35.920	-25.105	-34.950	43.824	44.773	44.168	Q
30.306	-30.129	-44.832	42.734	43.221	43.155	Q
23.303	-32.979	-54.755	40.381	41.897	41.426	Q
15.392	-34.969	-66.243	38.207	39.887	39.615	Q
7.4570	-36.075	-78.321	36.838	38.853	38.387	Q
0.0000	-36.741	-90.000	36.741	38.307	37.988	Q

* This is a "quick-reference" column. An entry of "A" indicates the ASTUD results are closer to the input data point, while a "Q" indicates the QUICK results are closer.

Table 3 (continued)

X	Y	ϕ(deg)	r_{input}	r_{ASTUD}	r_{QUICK}	Q/A
			Z = 52.000			
0.0000	49.110	90.000	49.110	49.332	49.189	Q
8.3950	48.408	80.162	49.131	49.341	48.952	Q
17.296	45.935	69.367	49.083	48.957	48.226	A
25.339	42.118	58.968	49.153	49.206	47.261	A
33.879	35.655	46.463	49.184	48.962	46.085	A
40.235	27.821	34.662	48.917	48.456	45.247	A
44.424	17.729	21.756	47.831	47.546	44.873	A
46.393	8.0340	9.8246	47.083	46.163	45.175	A
47.450	-.35200	-.42503	47.451	46.139	46.004	A
47.650	-10.082	-11.947	48.705	48.176	47.626	A
46.062	-18.965	-22.378	49.813	49.506	48.866	A
41.360	-27.027	-33.163	49.408	49.616	49.086	A
33.977	-33.816	-44.864	47.937	47.365	47.516	Q
26.512	-36.624	-54.099	45.213	45.444	45.479	A
18.586	-38.556	-64.264	42.802	43.189	43.478	A
8.4310	-39.650	-77.996	40.536	41.826	41.729	Q
0.0000	-40.264	-90.000	40.264	41.194	41.237	A
			Z = 62.000			
51.150	-11.501	-12.672	52.427	52.431	51.848	A
50.335	-16.402	-18.049	52.940	53.212	52.750	Q
48.187	-21.324	-23.871	52.694	53.737	53.410	Q
46.039	-26.245	-29.686	52.994	53.754	53.665	Q
42.989	-30.291	-35.169	52.589	53.351	53.413	A
38.599	-33.913	-41.302	51.381	52.023	52.268	A
34.195	-36.646	-46.982	50.122	50.544	50.792	A
30.660	-38.033	-51.126	48.852	49.272	49.662	A
26.244	-39.877	-56.650	47.738	47.722	48.226	A
22.258	-40.826	-61.401	46.499	46.579	47.117	A
17.377	-41.344	-67.203	44.847	45.467	45.969	A
13.391	-42.293	-72.431	44.362	45.041	45.149	A
9.3920	-42.354	-77.497	43.383	44.332	44.555	A
4.0660	-42.878	-84.583	43.070	43.731	44.060	A
0.0000	-42.946	-90.000	42.946	43.593	43.946	A
			Z = 87.000			
60.328	-14.659	-13.658	62.083	64.632	61.169	Q
59.469	-20.885	-19.351	63.030	62.749	62.437	A
57.272	-26.228	-24.606	62.992	63.366	63.342	Q
53.741	-31.578	-30.438	62.332	62.695	63.703	A
50.205	-35.594	-35.336	61.542	62.189	62.845	A

Table 3 (continued)

X	Y	ϕ(deg)	r_{input}	r_{ASTUD}	r_{QUICK}	Q/A
		Z = 87.000 (continued)				
46.224	-39.612	-40.595	60.875	60.681	60.983	Q
40.459	-42.306	-46.278	58.538	57.989	58.659	Q
36.025	-44.548	-51.038	57.292	55.796	56.750	Q
30.699	-45.907	-56.229	55.226	53.920	54.847	Q
24.926	-46.822	-61.971	53.043	52.106	53.036	Q
19.595	-47.292	-67.494	51.191	50.732	51.615	Q
15.598	-47.755	-71.912	50.238	50.102	50.708	A
10.267	-48.224	-77.981	49.305	49.098	49.793	A
5.3780	-48.247	-83.640	48.546	48.529	49.276	A
0.0000	-48.718	-90.000	48.718	48.302	49.075	Q
		Z = 112.00				
67.243	-12.631	-10.639	68.419	69.479	68.375	Q
67.215	-17.963	-14.962	69.574	70.502	69.555	Q
65.851	-23.733	-19.819	69.997	71.165	70.672	Q
64.045	-29.057	-24.404	70.328	71.831	71.343	Q
60.906	-34.373	-29.439	69.936	70.927	71.412	A
55.994	-38.791	-34.713	68.118	68.316	70.132	A
50.640	-42.763	-40.179	66.280	66.013	67.507	A
44.847	-45.843	-45.629	64.131	63.836	64.596	A
39.949	-47.595	-49.991	62.139	61.659	62.361	Q
33.273	-49.337	-56.004	59.508	58.965	59.608	Q
27.936	-50.198	-60.903	57.448	57.088	57.704	Q
22.156	-50.611	-66.358	55.248	55.243	55.958	A
16.821	-51.028	-71.756	53.729	53.918	54.609	A
11.044	-50.997	-77.781	52.179	52.775	53.532	A
4.8230	-50.964	-84.594	51.192	52.031	52.837	A
0.0000	-51.835	-90.000	51.835	51.850	52.669	A
		Z = 137.00				
75.104	-17.164	-12.873	77.040	79.232	76.406	Q
74.216	-22.496	-16.863	77.551	78.264	77.532	Q
72.882	-27.829	-20.899	78.014	78.560	78.195	Q
71.105	-33.162	-25.003	78.458	78.625	78.317	Q
68.883	-35.829	-27.481	77.644	77.959	78.083	A
66.661	-38.495	-30.005	76.978	77.081	77.569	A
64.439	-40.717	-32.288	76.225	75.084	76.828	Q
61.328	-43.383	-35.275	75.121	73.510	75.406	Q
54.217	-47.383	-41.152	72.004	70.473	71.766	Q
47.551	-49.605	-46.211	68.715	68.136	68.527	Q
40.441	-50.938	-51.553	65.040	65.309	65.390	A

Table 3 (continued)

X	Y	ϕ(deg)	r_{input}	r_{ASTUD}	r_{QUICK}	Q/A
		Z = 137.00 (continued)				
34.219	-52.272	-56.790	62.476	62.704	62.723	A
27.998	-53.160	-62.225	60.082	60.417	60.415	Q
21.776	-53.605	-67.891	57.859	58.140	58.496	A
11.999	-54.938	-77.680	56.233	55.666	56.279	Q
6.2220	-54.938	-83.538	55.289	54.920	55.574	Q
0.0000	-54.938	-90.000	54.938	54.631	55.308	A
		Z = 162.00				
81.326	-18.052	-12.515	83.305	83.191	83.292	Q
80.882	-22.941	-15.835	84.073	84.335	84.346	A
79.548	-29.162	-20.133	84.725	84.825	84.964	A
77.326	-34.051	-23.767	84.491	84.195	84.789	A
74.216	-38.495	-27.415	83.606	83.171	83.967	Q
70.660	-41.606	-30.490	81.999	82.227	82.764	A
66.216	-45.161	-34.295	80.150	79.725	80.606	A
59.106	-48.716	-39.496	76.595	76.164	76.800	Q
49.773	-51.383	-45.912	71.537	72.047	72.028	Q
43.552	-52.716	-50.438	68.379	69.599	68.992	Q
37.774	-54.049	-55.051	65.941	66.953	66.274	Q
27.109	-55.382	-63.919	61.661	62.610	62.150	Q
19.998	-55.827	-70.292	59.301	59.914	60.024	A
13.332	-56.271	-76.671	57.829	58.145	58.536	A
7.1100	-56.716	-82.855	57.160	57.220	57.661	A
0.0000	-56.893	-90.000	56.893	56.837	57.313	A
		Z = 182.00				
85.398	-20.614	-13.571	87.851	87.410	88.844	A
83.585	-29.495	-19.437	88.636	88.848	89.978	A
79.553	-37.479	-25.226	87.939	88.096	88.991	A
74.196	-43.679	-30.485	86.098	85.585	86.489	Q
66.179	-48.091	-36.005	81.807	82.390	82.442	A
58.611	-51.172	-41.124	77.806	78.167	78.103	Q
50.603	-53.362	-46.520	73.540	74.192	73.770	Q
43.041	-55.110	-52.010	69.926	70.979	69.915	Q
34.592	-56.409	-58.482	66.171	67.166	66.172	Q
25.255	-57.705	-66.363	62.990	63.392	62.731	Q
17.256	-57.673	-73.343	60.199	60.423	60.607	A
9.2560	-57.641	-80.877	58.379	58.905	59.188	A
0.0000	-58.051	-90.000	58.051	58.263	58.592	A

Table 3 (continued)

X	Y	ϕ(deg)	r_{input}	r_{ASTUD}	r_{QUICK}	Q/A
			Z = 187.00			
86.361	-20.060	-13.077	88.660	88.209	89.876	A
86.316	-25.837	-16.664	90.100	89.776	90.938	A
84.049	-31.597	-20.603	89.792	89.820	91.093	A
80.445	-37.790	-25.162	88.879	89.088	90.045	A
73.731	-43.960	-30.804	85.841	86.317	87.141	A
64.353	-49.664	-37.659	81.289	81.871	81.700	Q
57.670	-51.834	-41.949	77.541	78.136	77.975	Q
49.650	-54.438	-47.634	73.679	74.103	73.413	Q
42.526	-56.160	-52.866	70.444	70.931	69.786	A
34.965	-56.989	-58.469	66.860	67.600	66.550	Q
25.625	-57.805	-66.092	63.230	63.912	63.160	Q
17.179	-58.184	-73.551	60.667	60.707	60.860	A
0.0000	-58.937	-90.000	58.937	58.578	58.875	Q
			Z = 202.00			
89.251	-19.040	-12.042	91.259	91.137	92.906	A
89.270	-23.928	-15.005	92.421	92.558	93.943	A
88.400	-28.820	-18.057	92.979	93.101	94.388	A
86.638	-32.826	-20.751	92.648	92.884	94.212	A
82.664	-39.508	-25.545	91.620	92.169	92.704	A
77.352	-44.861	-30.112	89.419	88.999	90.014	A
69.371	-49.781	-35.663	85.384	85.917	85.383	Q
61.383	-52.478	-40.528	80.758	81.219	80.829	Q
53.835	-54.285	-45.238	76.453	77.118	76.667	Q
44.953	-56.097	-51.293	71.886	73.197	72.006	Q
40.070	-57.449	-55.105	70.043	70.723	69.507	Q
36.071	-57.465	-57.883	67.848	69.016	67.891	Q
27.186	-58.388	-65.033	64.407	65.528	64.484	Q
18.301	-59.311	-72.852	62.070	61.818	61.875	Q
0.0000	-59.382	-90.000	59.382	59.430	59.652	A
			Z = 222.00			
94.214	-18.052	-10.847	95.928	94.927	96.343	Q
94.658	-20.719	-12.346	96.899	96.297	96.895	Q
94.214	-23.385	-13.940	97.073	96.449	97.486	Q
94.214	-26.052	-15.457	97.750	97.539	97.875	Q
93.325	-29.162	-17.353	97.775	97.294	98.094	Q
91.547	-33.607	-20.158	97.521	96.943	97.902	Q
87.548	-40.273	-24.703	96.367	95.985	96.386	Q
81.771	-45.605	-29.149	93.629	93.844	93.618	Q
69.327	-51.383	-36.545	86.293	87.130	86.760	Q

Table 3 (continued)

X	Y	ϕ(deg)	r_{input}	r_{ASTUD}	r_{QUICK}	Q/A
		Z = 222.00 (continued)				
52.884	-56.716	-47.002	77.546	77.137	76.757	A
27.553	-58.938	-64.944	65.060	66.748	65.574	Q
0.0000	-60.272	-90.000	60.272	60.364	60.542	A
		Z = 242.00				
96.880	-18.052	-10.555	98.547	99.478	99.635	A
97.325	-19.830	-11.516	99.325	99.402	99.992	A
97.769	-21.608	-12.463	100.13	99.640	100.36	Q
97.769	-24.274	-13.943	100.74	100.06	100.92	Q
97.325	-27.829	-15.957	101.23	100.89	101.38	Q
95.103	-33.607	-19.462	100.87	100.91	101.28	A
92.881	-37.606	-22.042	100.21	100.26	100.54	A
89.770	-42.050	-25.099	99.130	99.250	99.013	Q
82.215	-47.828	-30.188	95.115	95.180	95.115	Q
73.771	-52.272	-35.320	90.413	89.668	89.834	Q
53.329	-58.049	-47.427	78.827	77.911	77.613	A
28.442	-60.715	-64.899	67.047	67.451	66.465	A
15.110	-61.604	-76.219	63.430	62.704	62.796	Q
0.0000	-61.160	-90.000	61.160	61.082	61.293	A
		Z = 262.00				
99.835	-17.301	-9.8315	101.32	103.47	102.77	Q
100.74	-19.961	-11.207	102.70	102.67	103.28	A
101.20	-21.291	-11.881	103.41	102.87	103.54	Q
100.76	-22.627	-12.656	103.27	103.11	103.86	A
100.80	-27.516	-15.268	104.49	104.45	104.68	A
99.059	-32.417	-18.121	104.23	104.97	104.70	Q
96.871	-36.878	-20.841	103.65	104.00	103.94	Q
93.790	-40.901	-23.562	102.32	102.74	102.53	Q
88.935	-45.381	-27.034	99.844	100.71	99.932	Q
80.084	-50.337	-32.152	94.590	94.871	94.860	Q
62.796	-56.244	-41.850	84.301	83.942	83.968	Q
37.937	-59.986	-57.689	70.976	71.114	70.954	Q
17.502	-61.029	-73.998	63.489	63.824	64.003	A
0.0000	-61.601	-90.000	61.601	61.601	61.932	A
		Z = 282.00				
103.55	-17.608	-9.6508	105.03	106.38	106.08	Q
104.88	-19.830	-10.707	106.74	104.83	106.48	Q
105.77	-21.608	-11.546	107.95	105.40	106.82	Q

Table 3 (continued)

X	Y	ϕ(deg)	r_{input}	r_{ASTUD}	r_{QUICK}	Q/A
		Z = 282.00 (continued)				
105.77	-24.718	-13.154	108.62	106.01	107.50	Q
104.88	-28.274	-15.087	108.62	107.40	108.06	Q
103.55	-31.829	-17.087	108.33	108.25	108.09	A
101.32	-36.273	-19.697	107.62	107.80	107.40	A
97.769	-41.161	-22.831	106.08	105.84	105.63	A
92.881	-45.161	-25.930	103.28	103.08	103.09	Q
85.326	-49.161	-29.949	98.475	99.384	98.961	Q
69.327	-55.827	-38.843	89.011	87.891	88.373	Q
47.551	-59.382	-51.313	76.074	76.123	76.148	A
24.442	-61.604	-68.359	66.276	66.527	66.398	Q
0.0000	-62.048	-90.000	62.048	62.022	62.479	A
		Z = 302.00				
108.40	-22.566	-11.759	110.73	107.16	110.31	Q
108.40	-26.106	-13.540	111.50	107.94	111.09	Q
107.52	-30.088	-15.634	111.65	109.81	111.50	Q
106.19	-33.185	-17.354	111.26	110.58	111.32	Q
104.42	-36.283	-19.161	110.55	112.14	110.68	Q
99.996	-40.707	-22.151	107.96	108.98	108.78	Q
89.377	-47.787	-28.132	101.35	102.54	102.81	A
73.448	-54.424	-36.538	91.414	91.462	92.282	A
61.944	-57.078	-42.659	84.232	84.707	85.050	A
49.556	-58.848	-49.899	76.934	77.857	78.011	A
26.548	-61.060	-66.501	66.582	67.903	67.632	Q
0.0000	-62.388	-90.000	62.388	62.444	62.903	A
		Z = 322.00				
112.04	-23.309	-11.752	114.44	107.96	113.72	Q
112.48	-25.088	-12.574	115.24	108.31	114.09	Q
111.58	-29.529	-14.824	115.42	109.92	114.84	Q
109.78	-33.968	-17.192	114.92	111.47	114.60	Q
107.55	-36.627	-18.806	113.62	111.10	113.90	Q
102.20	-42.386	-22.525	110.64	110.55	111.03	A
95.965	-46.810	-26.002	106.77	106.32	107.24	A
88.395	-51.229	-30.094	102.17	101.73	102.06	Q
79.497	-54.311	-34.340	96.278	95.566	96.353	Q
68.822	-56.942	-39.604	89.324	88.804	89.524	Q
54.594	-59.117	-47.278	80.469	80.868	81.119	A
31.475	-62.152	-63.141	69.667	69.331	69.697	Q
0.0000	-62.939	-90.000	62.939	62.865	63.326	A

Table 3 (continued)

X	Y	ϕ(deg)	r_{input}	r_{ASTUD}	r_{QUICK}	Q/A
			Z = 342.00			
115.15	-24.261	-11.897	117.68	108.22	117.19	Q
115.59	-26.484	-12.905	118.59	108.64	117.66	Q
115.14	-29.594	-14.415	118.88	109.48	118.20	Q
112.90	-33.585	-16.567	117.79	110.41	118.07	Q
109.77	-38.017	-19.103	116.17	111.61	116.76	Q
105.31	-42.445	-21.952	113.54	112.77	114.19	Q
99.072	-46.865	-25.316	109.60	108.75	110.18	Q
91.502	-50.837	-29.056	104.68	104.20	105.08	Q
84.380	-53.921	-32.580	100.14	99.481	100.05	Q
75.929	-55.667	-36.247	94.149	93.806	94.870	A
58.140	-59.156	-45.496	82.944	83.298	83.625	A
32.796	-62.616	-62.356	70.685	70.287	70.611	Q
0.0000	-62.939	-90.000	62.939	63.287	63.749	A
			Z = 362.00			
105.27	-43.678	-22.534	113.97	114.10	116.14	A
100.35	-46.733	-24.972	110.70	110.98	112.85	A
90.084	-50.618	-29.332	103.33	105.26	106.29	A
77.596	-54.478	-35.072	94.810	96.496	97.520	A
57.989	-59.146	-45.566	82.831	83.935	84.203	A
39.744	-61.163	-56.984	72.942	74.181	74.355	A
19.727	-62.716	-72.539	65.745	66.480	66.817	A
0.0000	-63.835	-90.000	63.835	63.708	64.172	A
			Z = 402.00			
91.339	-53.592	-30.402	105.90	106.23	107.35	A
82.864	-55.692	-33.905	99.840	100.43	101.36	A
63.248	-59.853	-43.420	87.079	87.694	87.941	A
45.873	-62.713	-53.815	77.700	77.697	77.738	A
31.641	-63.397	-63.477	70.854	71.077	71.460	A
31.647	-62.952	-63.311	70.459	71.174	71.546	A
0.0000	-64.719	-90.000	64.719	64.551	65.018	A
			Z = 432.00			
99.845	-51.656	-27.355	112.42	113.49	115.25	A
85.124	-56.373	-33.514	102.10	102.64	103.55	A
68.635	-60.182	-41.246	91.283	91.490	91.718	A
37.033	-64.258	-60.044	74.166	73.862	74.129	Q
0.0000	-65.612	-90.000	65.612	65.183	65.652	Q

Table 3 (continued)

X	Y	ϕ(deg)	r_{input}	r_{ASTUD}	r_{QUICK}	Q/A
			Z = 462.00			
101.71	-53.532	-27.758	114.94	115.39	116.69	A
83.921	-58.355	-34.813	102.22	102.06	102.74	A
67.020	-61.849	-42.702	91.197	90.872	90.863	A
46.125	-63.995	-54.217	78.885	79.082	79.014	Q
23.453	-66.134	-70.474	70.169	69.550	69.748	Q
0.0000	-66.880	-90.000	66.880	65.815	66.286	Q
			Z = 512.00			
101.03	-57.074	-29.464	116.03	115.22	116.15	Q
69.383	-62.323	-41.932	93.264	93.831	93.596	Q
35.990	-65.765	-61.310	74.969	75.155	75.302	A
0.0000	-66.496	-90.000	66.496	66.869	67.344	A
			Z = 562.00			
100.52	-59.013	-30.416	116.56	116.09	116.77	Q
71.087	-64.250	-42.108	95.820	95.576	95.054	A
35.920	-67.158	-61.860	76.161	76.016	76.172	Q
0.0000	-68.735	-90.000	68.735	67.923	68.401	Q
			Z = 612.00			
100.16	-61.084	-31.378	117.32	115.53	117.09	Q
68.093	-66.460	-44.305	95.150	94.451	93.669	A
35.621	-68.719	-62.600	77.403	76.741	76.921	Q
0.0000	-69.619	-90.000	69.619	68.976	69.458	Q
			Z = 662.00			
100.46	-62.947	-32.070	118.55	117.23	118.69	Q
71.922	-68.218	-43.486	99.129	97.465	97.251	A
38.105	-70.285	-61.536	79.950	78.662	79.068	Q
0.0000	-70.503	-90.000	70.503	70.030	70.515	Q
			Z = 712.00			
78.561	-67.141	-40.518	103.34	104.17	104.31	A
37.605	-70.343	-61.871	79.764	79.687	80.235	A
0.0000	-71.392	-90.000	71.392	71.084	71.573	Q

Table 3 (continued)

X	Y	ϕ(deg)	r_{input}	r_{ASTUD}	r_{QUICK}	Q/A
			Z = 762.00			
100.41	-66.476	-33.507	120.42	120.49	121.33	A
63.004	-70.266	-48.119	94.376	94.625	94.916	A
33.646	-71.530	-64.809	79.048	79.338	79.669	A
0.0000	-72.288	-90.000	72.288	72.137	72.630	A
			Z = 812.00			
100.88	-68.048	-34.001	121.69	122.69	122.63	Q
58.607	-71.398	-50.619	92.371	93.586	93.333	Q
29.690	-73.175	-67.916	78.969	78.679	79.115	Q
0.0000	-73.168	-90.000	73.168	73.191	73.687	A
			Z = 862.00			
101.61	-69.859	-34.510	123.31	123.06	123.34	Q
68.213	-72.748	-46.843	99.726	99.363	99.597	Q
38.400	-74.376	-62.693	83.704	82.826	83.393	Q
0.0000	-75.131	-90.000	75.131	74.245	74.744	Q
			Z = 912.00			
75.205	-73.898	-44.498	105.44	104.36	104.70	Q
41.850	-76.237	-61.236	86.968	85.069	85.648	Q
0.0000	-76.721	-90.000	76.721	75.298	75.801	Q
			Z = 962.00			
100.46	-72.067	-35.656	123.63	123.52	124.33	A
73.753	-74.074	-45.124	104.53	104.77	105.24	A
41.744	-75.062	-60.920	85.889	86.548	87.119	A
0.0000	-76.697	-90.000	76.697	76.352	76.859	Q
			Z = 1012.0			
99.476	-72.690	-36.157	123.20	123.93	124.73	A
69.722	-74.910	-47.054	102.34	103.20	103.65	A
37.748	-76.687	-63.792	85.474	85.708	86.198	A
0.0000	-78.463	-90.000	78.463	77.406	77.915	Q

Table 3 (continued)

X	Y	ϕ(deg)	r_{input}	r_{ASTUD}	r_{QUICK}	Q/A
			Z = 1062.0			
100.29	-74.183	-36.490	124.74	124.74	125.02	A
73.163	-76.445	-46.257	105.81	105.80	105.49	A
45.162	-77.806	-59.867	89.963	89.918	89.401	A
22.954	-77.920	-73.586	81.231	81.619	81.093	Q
0.0000	-78.459	-90.000	78.459	78.459	77.949	A
			Z = 1073.0			
106.97	-73.492	-34.490	129.78	129.71	130.28	A
60.199	-77.951	-52.322	98.490	98.559	96.923	A
35.289	-79.027	-65.937	86.548	85.679	84.755	A
0.0000	-79.590	-90.000	79.590	78.639	77.722	A
			Z = 1082.0			
107.36	-73.137	-34.265	129.90	130.22	130.91	A
58.439	-76.770	-52.721	96.482	98.068	96.253	Q
48.656	-77.496	-57.877	91.504	91.948	90.777	A
34.425	-78.593	-66.346	85.802	85.475	84.272	A
18.433	-78.773	-76.830	80.901	80.683	79.490	A
0.0000	-78.845	-90.000	78.845	78.700	77.481	A
			Z = 1112.0			
69.522	-75.792	-47.471	102.85	103.79	102.39	Q
36.671	-77.782	-64.758	85.993	85.980	84.178	A
36.668	-77.338	-64.633	85.590	86.063	84.262	A
0.0000	-77.571	-90.000	77.571	78.226	76.369	A
			Z = 1162.0			
120.06	-69.813	-30.177	138.88	126.20	140.35	Q
100.95	-71.855	-35.444	123.91	123.79	124.46	A
60.955	-74.147	-50.577	95.986	95.733	94.865	A
0.0000	-74.917	-90.000	74.917	75.171	73.701	A
			Z = 1212.0			
125.68	-66.473	-27.875	142.17	142.95	139.64	A
100.36	-68.249	-34.216	121.37	119.20	119.92	Q
79.048	-69.137	-41.174	105.02	103.61	104.34	Q
59.508	-69.581	-49.462	91.557	91.170	91.441	Q
0.0000	-70.469	-90.000	70.469	72.688	70.469	Q

Table 4: Shuttle Wing Comparison (in Fuselage Coordinate System)

Spanwise Location: X = 103.46

Y	Z	ϕ(deg)	r_{input}	r_{ASTUD}	r_{QUICK}
-28.307	283.52	-15.301	107.27	107.27	108.35
-31.457	287.34	-16.911	108.14	108.12	109.00
-34.450	302.87	-18.416	109.05	109.26	111.13
-37.580	328.96	-19.962	110.08	110.16	114.18
-41.374	365.15	-21.796	111.43	111.29	117.46
-45.250	411.13	-23.622	112.93	112.76	120.31
-49.553	466.33	-25.591	114.72	114.77	121.78
-53.965	530.16	-27.546	116.69	116.99	121.97
-58.105	601.96	-29.318	118.66	118.94	121.78
-61.629	680.94	-30.780	120.43	120.15	123.06
-63.115	766.26	-31.384	121.20	121.12	126.88
-64.397	856.92	-31.898	121.87	122.04	130.11
-66.414	951.90	-32.696	122.95	123.09	131.86
-66.571	1050.2	-32.758	123.03	122.95	134.84
-62.079	1150.5	-30.964	120.66	120.69	138.76

Spanwise Location: X = 159.29

Y	Z	ϕ(deg)	r_{input}	r_{ASTUD}	r_{QUICK}
-31.793	626.16	-11.287	162.43	163.29	165.21
-34.276	626.76	-12.144	162.94	163.30	165.89
-37.163	634.68	-13.132	163.57	163.55	167.94
-40.030	649.71	-14.107	164.24	164.35	171.21
-43.209	671.14	-15.177	165.05	165.08	174.28
-46.098	699.08	-16.140	165.83	165.72	176.91
-48.711	733.11	-17.004	166.57	166.50	179.04
-50.828	773.00	-17.697	167.20	167.29	182.20
-52.924	818.36	-18.379	167.85	167.94	185.67
-54.842	868.82	-18.998	168.47	168.43	188.64
-55.935	924.11	-19.349	168.83	168.81	190.81
-56.950	983.06	-19.673	169.17	169.19	191.93
-58.033	1044.9	-20.018	169.53	169.60	192.44
-58.137	1109.2	-20.051	169.57	169.48	193.10
-53.746	1175.0	-18.645	168.11	168.18	198.62

Table 4 (continued)

Spanwise Location: X = 256.02

Y	Z	ϕ(deg)	r_{input}	r_{ASTUD}	r_{QUICK}
-32.252	845.62	-7.1798	258.05	258.09	246.41
-34.302	846.35	-7.6310	258.31	258.40	247.54
-38.160	851.18	-8.4775	258.85	258.81	253.15
-41.111	861.06	-9.1224	259.30	259.31	263.69
-43.167	875.16	-9.5704	259.64	259.68	275.66
-44.555	893.15	-9.8722	259.87	259.89	286.34
-45.354	914.77	-10.046	260.01	259.96	293.49
-45.910	939.78	-10.166	260.11	260.04	294.58
-46.452	967.87	-10.284	260.20	260.14	295.15
-47.031	998.75	-10.409	260.31	260.26	295.71
-47.693	1032.1	-10.552	260.43	260.39	295.79
-48.466	1067.5	-10.719	260.57	260.53	294.84
-49.057	1104.6	-10.847	260.68	260.70	294.42
-48.019	1142.9	-10.623	260.49	260.56	298.54
-45.284	1182.1	-10.030	260.00	259.85	303.94

Spanwise Location: X = 312.57

Y	Z	ϕ(deg)	r_{input}	r_{ASTUD}	r_{QUICK}
-29.429	903.23	-5.3786	313.96	314.17	303.57
-31.116	903.80	-5.6849	314.12	314.23	304.44
-34.321	907.61	-6.2661	314.45	314.46	308.81
-36.871	915.65	-6.7275	314.74	314.74	317.34
-38.184	927.32	-6.9647	314.90	314.91	329.01
-39.354	942.13	-7.1759	315.04	314.98	340.68
-40.174	959.94	-7.3238	315.15	315.07	350.44
-40.762	980.53	-7.4298	315.22	315.18	356.53
-41.279	1003.7	-7.5231	315.29	315.30	357.85
-41.869	1029.1	-7.6292	315.37	315.41	357.54
-42.536	1056.6	-7.7494	315.45	315.51	356.61
-43.196	1085.7	-7.8682	315.54	315.58	355.71
-43.799	1116.3	-7.9766	315.63	315.57	355.17
-42.621	1147.9	-7.7647	315.47	315.45	361.59
-40.106	1180.1	-7.3115	315.14	315.10	369.89

Table 4 (continued)

Spanwise Location: X = 455.76

Y	Z	ϕ(deg)	r_{input}	r_{ASTUD}	r_{QUICK}
-26.175	1047.5	-3.2870	456.52	456.61	439.20
-26.936	1047.7	-3.3823	456.56	456.62	439.39
-28.342	1049.2	-3.5584	456.64	456.65	440.42
-29.200	1052.9	-3.6659	456.70	456.70	442.58
-29.640	1058.2	-3.7209	456.73	456.72	445.39
-30.129	1064.9	-3.7821	456.76	456.75	448.66
-30.571	1073.0	-3.8374	456.79	456.78	452.18
-31.025	1082.4	-3.8943	456.82	456.82	455.75
-31.495	1092.9	-3.9531	456.85	456.85	459.21
-31.918	1104.5	-4.0060	456.88	456.88	462.23
-32.136	1117.0	-4.0333	456.90	456.90	464.74
-32.175	1130.3	-4.0381	456.90	456.91	466.76
-32.100	1144.2	-4.0287	456.89	456.90	468.23
-31.860	1158.6	-3.9988	456.88	456.86	469.08
-30.696	1173.2	-3.8531	456.80	456.79	469.40
-28.578	1187.9	-3.5879	456.66	456.66	469.23

Table 5: Comparison of Nose Radius of Curvature Distribution for AFE Geometry

ϕ (degrees)	Nose Radius of Curvature Distribution	
	Case* 1	Case 2
90.00	0.4499019	0.4498996
86.40	0.4505093	0.4505070
82.80	0.4523314	0.4523291
79.20	0.4553689	0.4553667
75.60	0.4596215	0.4596193
72.00	0.4650875	0.4650855
68.40	0.4717616	0.4717597
64.80	0.4796330	0.4796311
61.20	0.4886820	0.4886803
57.60	0.4988769	0.4988754
54.00	0.5101695	0.5101683
50.40	0.5224903	0.5224892
46.80	0.5357429	0.5357424
43.20	0.5497993	0.5497990
39.60	0.5644929	0.5644931
36.00	0.5796162	0.5796168
32.40	0.5949159	0.5949169
28.80	0.6100940	0.6100952
25.20	0.6248106	0.6248125
21.60	0.6386928	0.6386951
18.00	0.6513472	0.6513498
14.40	0.6623791	0.6623823
10.80	0.6714153	0.6714188
7.20	0.6781296	0.6781335
3.60	0.6822667	0.6822707
0.00	0.6836643	0.6836684

* For Case 2, the nose radius of curvature was left as part of the solution. For Case 1, these values were specified:

R_{XZ} = 0.6836643 & R_{YZ} = 0.4499019.

For both options here, the nose region was constrained by the user to pass through these two cross sections:

Number	Axial Location
1	0.1697E-01
2	0.6028E-01

Table 6: Comparison for Nose Region of AFE Geometry*

Z = 0.84871E-02

ϕ(deg)	r	r_Z	r_ϕ	r_{ZZ}	$r_{Z\phi}$	$r_{\phi\phi}$
90.0	0.86975E-01	5.0752	0.12999E-08	-307.65	0.75854E-07	0.29739E-01
	0.86975E-01	5.0752	0.10551E-08	-307.65	0.10450E-06	0.29739E-01
67.5	0.89238E-01	5.2072	-.11357E-01	-315.65	-.66268	0.27049E-01
	0.89238E-01	5.2072	-.92174E-02	-315.65	-.91295	0.19385E-01
45.0	0.95523E-01	5.5740	-.19699E-01	-337.88	-1.1495	0.12187E-01
	0.95523E-01	5.5740	-.15988E-01	-337.88	-1.5836	0.56503E-03
22.5	0.10336	6.0310	-.17644E-01	-365.59	-1.0296	-.26252E-01
	0.10336	6.0310	-.14321E-01	-365.59	-1.4184	-.37336E-01
0.0	0.10722	6.2563	0.0000	-379.24	0.0000	-.55708E-01
	0.10722	6.2563	0.0000	-379.24	0.0000	-.55709E-01
-22.5	0.10336	6.0310	0.17644E-01	-365.59	1.0296	-.26252E-01
	0.10336	6.0310	0.14321E-01	-365.59	1.4184	-.86943E-02
-45.0	0.95523E-01	5.5740	0.19699E-01	-337.88	1.1495	0.12187E-01
	0.95523E-01	5.5740	0.15988E-01	-337.88	1.5836	0.32541E-01
-67.5	0.89238E-01	5.2072	0.11357E-01	-315.65	0.66268	0.27049E-01
	0.89238E-01	5.2072	0.92174E-02	-315.65	0.91295	0.37820E-01
-90.0	0.86975E-01	5.0752	-.12999E-08	-307.65	-.75854E-07	0.29739E-01
	0.86975E-01	5.0752	-.10551E-08	-307.65	-.10450E-06	0.29739E-01

* For a given value of ϕ, the first line contains the analytic results, and the second line contains the ASTUD results.

Table 6 (continued)

Z = 0.34381E-01

ϕ(deg)	r	r_Z	r_ϕ	r_{ZZ}	$r_{Z\phi}$	$r_{\phi\phi}$
90.0	0.17249	2.4089	0.25781E-08	-39.438	0.36003E-07	0.58980E-01
	0.17249	2.4089	0.28670E-08	-39.437	0.41704E-07	0.58981E-01
67.5	0.17698	2.4716	-.22523E-01	-40.464	-.31454	0.53645E-01
	0.17698	2.4716	-.25047E-01	-40.464	-.36434	0.38960E-01
45.0	0.18945	2.6456	-.39067E-01	-43.314	-.54558	0.24169E-01
	0.18945	2.6456	-.43445E-01	-43.314	-.63197	0.98480E-02
22.5	0.20498	2.8626	-.34993E-01	-46.865	-.48867	-.52064E-01
	0.20498	2.8626	-.38914E-01	-46.865	-.56605	-.69384E-01
0.0	0.21264	2.9695	0.0000	-48.615	0.0000	-.11048
	0.21264	2.9695	0.0000	-48.616	0.0000	-.11048
-22.5	0.20498	2.8626	0.34993E-01	-46.865	0.48867	-.52064E-01
	0.20498	2.8626	0.38914E-01	-46.865	0.56605	0.84437E-02
-45.0	0.18945	2.6456	0.39067E-01	-43.314	0.54558	0.24169E-01
	0.18945	2.6456	0.43445E-01	-43.314	0.63197	0.96739E-01
-67.5	0.17698	2.4716	0.22523E-01	-40.464	0.31454	0.53645E-01
	0.17698	2.4716	0.25047E-01	-40.464	0.36434	0.89054E-01
-90.0	0.17249	2.4089	-.25781E-08	-39.438	-.36003E-07	0.58980E-01
	0.17249	2.4089	-.28670E-08	-39.437	-.41704E-07	0.58981E-01

Table 7: AFE Geometry Comparison Aft of Nose Region

Z = 0.68979E-01

ϕ(deg)	r	r_Z	r_ϕ	r_{ZZ}	$r_{Z\phi}$	$r_{\phi\phi}$
90.0	0.23765	1.2423	0.41540E-08	-40.562	0.65588E-07	0.95033E-01
	0.23766	1.2423	0.0000	-40.562	0.0000	0.84623E-01
67.5	0.24488	1.3729	-.36117E-01	-48.999	-.75219	0.83610E-01
	0.24418	1.3357	-.32760E-01	-38.869	-.51184	0.76937E-01
45.0	0.26362	1.9023	-.54363E-01	0.0000	-.39228	0.33632E-01
	0.25852	1.3173	-.60151E-01	0.0000	-1.1398	0.48285E-01
22.5	0.28523	2.0583	-.48692E-01	0.0000	-.35137	-.72447E-01
	0.28387	1.9014	-.61068E-01	0.0000	-1.7366	-.84682E-01
0.0	0.29588	2.1351	0.0000	0.0000	0.0000	-.15374
	0.29582	2.1348	0.36836E-02	0.0000	-.83418E-01	-.20199
-22.5	0.28523	2.0583	0.48692E-01	0.0000	0.35137	-.72447E-01
	0.28523	2.0566	0.49535E-01	0.0000	0.33478	-.77776E-01
-45.0	0.26362	1.9023	0.54363E-01	0.0000	0.39228	0.33632E-01
	0.26359	1.8997	0.55577E-01	0.0000	0.39493	0.44674E-01
-67.5	0.24627	1.7771	0.31341E-01	0.0000	0.22616	0.74647E-01
	0.24628	1.7772	0.31271E-01	0.0000	0.23270	0.64727E-01
-90.0	0.24003	1.7321	-.35874E-08	0.0000	-.25887E-07	0.82071E-01
	0.24003	1.7321	0.0000	0.0000	0.0000	0.82039E-01

* For a given value of ϕ, the first line contains the analytic results, and the second line contains the ASTUD results.

Table 7 (continued)

Z = 0.10793

ϕ(deg)	r	r_Z	r_ϕ	r_{ZZ}	$r_{Z\phi}$	$r_{\phi\phi}$
90.0	0.26705	0.42289	0.54790E-08	-12.799	0.20696E-07	0.12535
	0.26705	0.42289	0.0000	-12.799	0.0000	0.12337
67.5	0.27681	0.46121	-.50112E-01	-13.355	-.20501	0.13165
	0.27684	0.48316	-.50582E-01	-14.226	-.31237	0.13399
45.0	0.30681	0.60476	-.10259	-15.961	-.58275	0.12859
	0.30907	0.96977	-.10212	-76.145	-.20764	0.12214
22.5	0.35468	1.0531	-.12927	-30.627	-2.2247	-.74964E-01
	0.35632	1.2695	-.12653	-89.256	-1.5738	-.10158
0.0	0.37905	2.1351	0.0000	0.0000	0.0000	-.19695
	0.37862	2.0995	0.19219E-01	2.0455	-.89428E-01	-.45404
-22.5	0.36540	2.0583	0.62378E-01	0.0000	0.35137	-.92810E-01
	0.36526	2.0566	0.59181E-01	0.0000	0.33478	-.20884E-01
-45.0	0.33771	1.9023	0.69642E-01	0.0000	0.39228	0.43084E-01
	0.33759	1.8997	0.71207E-01	0.0000	0.39493	0.77506E-01
-67.5	0.31549	1.7771	0.40150E-01	0.0000	0.22616	0.95628E-01
	0.31555	1.7772	0.39728E-01	0.0000	0.23270	0.26208E-01
-90.0	0.30749	1.7321	-.45957E-08	0.0000	-.25887E-07	0.10514
	0.30749	1.7321	0.0000	0.0000	0.0000	0.10511

Table 7 (continued)

Z = 0.14905

ϕ(deg)	r	r_Z	r_ϕ	r_{ZZ}	$r_{Z\phi}$	$r_{\phi\phi}$
90.0	0.27495	0.0000	0.61629E-08	0.0000	0.0000	0.30672
	0.27495	0.19664E-06	0.0000	0.0000	0.0000	0.14072
67.5	0.28600	0.75623E-02	-.57076E-01	-10.001	-.15352	0.15216
	0.28595	0.17362E-03	-.56655E-01	0.0000	-.16028E-02	0.15029
45.0	0.32067	0.10684	-.12077	-10.172	-.37139	0.17032
	0.32054	0.48619E-01	-.12024	-2.8227	-.25528	0.16951
22.5	0.38077	0.33060	-.18175	-11.683	-.84868	0.11147
	0.38064	0.27552	-.18371	-8.9841	-1.0425	0.10727
0.0	0.45259	0.99563	-.14776	-28.099	-3.6437	-.50961
	0.45224	1.2534	-.14598	-52.605	-5.7135	0.92083E-01
-22.5	0.45004	2.0583	0.76828E-01	0.0000	0.35137	-.11431
	0.44983	2.0566	0.73004E-01	0.0000	0.30127	-.17303E-01
-45.0	0.41594	1.9023	0.85775E-01	0.0000	0.39228	0.53065E-01
	0.41570	1.8997	0.87653E-01	0.0000	0.39493	0.11882
-67.5	0.38857	1.7771	0.49450E-01	0.0000	0.22616	0.11778
	0.38855	1.7772	0.51306E-01	0.0000	0.23270	0.13692
-90.0	0.37872	1.7321	-.56604E-08	0.0000	-.25887E-07	0.12949
	0.37872	1.7321	0.0000	0.0000	0.0000	0.12947

Table 7 (continued)

Z = 0.19127

φ(deg)	r	r_Z	r_ϕ	r_{ZZ}	$r_{Z\phi}$	$r_{\phi\phi}$
90.0	0.27495	0.0000	0.61629E-08	0.0000	0.0000	0.38297
	0.27495	0.19664E-06	0.0000	0.0000	0.0000	0.14072
67.5	0.28600	0.0000	-.57192E-01	0.0000	0.0000	0.38836
	0.28596	0.17362E-03	-.56723E-01	0.0000	-.16028E-02	0.15083
45.0	0.32124	0.0000	-.12467	0.0000	0.0000	0.38431
	0.32124	-.18097E-04	-.12443	0.0000	0.59822E-05	0.19032
22.5	0.38582	0.0000	-.20576	0.0000	0.0000	0.30329
	0.38580	0.41937E-04	-.20496	0.0000	-.64055E-03	0.22599
0.0	0.47763	0.29554	-.23854	-11.338	-1.4703	-.11518
	0.47849	0.20938	-.23985	0.45425E-01	-1.1705	-.97582
-22.5	0.53693	2.0583	0.91660E-01	0.0000	0.35137	-.13638
	0.53772	1.9552	0.30994E-01	-59.209	-2.0932	-2.7008
-45.0	0.49624	1.9023	0.10233	0.0000	0.39228	0.63310E-01
	0.49587	1.8997	0.10452	0.0000	0.39493	0.16401
-67.5	0.46359	1.7771	0.58997E-01	0.0000	0.22616	0.14052
	0.46357	1.7772	0.61114E-01	0.0000	0.23270	0.15589
-90.0	0.45183	1.7321	-.67531E-08	0.0000	-.25887E-07	0.15449
	0.45183	1.7321	0.0000	0.0000	0.0000	0.15452

Table 7 (continued)

Z = 0.23402

ϕ(deg)	r	r_Z	r_ϕ	r_{ZZ}	$r_{Z\phi}$	$r_{\phi\phi}$
90.0	0.27495	0.0000	0.61629E-08	0.0000	0.0000	0.38297
	0.27495	0.19664E-06	0.0000	0.0000	0.0000	0.14083
67.5	0.28600	0.0000	-.57192E-01	0.0000	0.0000	0.38836
	0.28596	0.17362E-03	-.56792E-01	0.0000	-.16028E-02	0.15137
45.0	0.32124	0.0000	-.12467	0.0000	0.0000	0.38431
	0.32124	-.18097E-04	-.12443	0.0000	0.59822E-05	0.19039
22.5	0.38582	0.0000	-.20576	0.0000	0.0000	0.30329
	0.38580	0.41937E-04	-.20493	0.0000	-.64055E-03	0.22555
0.0	0.48173	0.0000	-.27687	0.0000	0.0000	0.12301
	0.48182	-.20133E-03	-.27817	0.0000	0.63530E-02	0.80193E-01
-22.5	0.58260	0.54689	-.18505	-14.807	-2.7137	-.63255
	0.58278	0.58213	-.16600	-14.329	-4.6267	-.45954
-45.0	0.57758	1.9023	0.11911	0.0000	0.39228	0.73686E-01
	0.57708	1.8986	0.12158	-2.8382	0.34374	0.21094
-67.5	0.53958	1.7771	0.68667E-01	0.0000	0.22616	0.16355
	0.53956	1.7772	0.71058E-01	0.0000	0.23270	0.17531
-90.0	0.52589	1.7321	-.78600E-08	0.0000	-.25887E-07	0.17982
	0.52589	1.7321	0.0000	0.0000	0.0000	0.17986

Table 7 (continued)

Z = 0.27705

ϕ(deg)	r	r_Z	r_ϕ	r_{ZZ}	$r_{Z\phi}$	$r_{\phi\phi}$
90.0	0.27495	0.0000	0.61629E-08	0.0000	0.0000	0.25000
	0.27495	0.19664E-06	0.0000	0.0000	0.0000	0.14089
67.5	0.28600	0.0000	-.57192E-01	0.0000	0.0000	0.25193
	0.28597	0.17362E-03	-.56861E-01	0.0000	-.16028E-02	0.15191
45.0	0.32124	0.0000	-.12467	0.0000	0.0000	0.23828
	0.32124	-.18097E-04	-.12443	0.0000	0.59822E-05	0.19044
22.5	0.38582	0.0000	-.20576	0.0000	0.0000	0.14529
	0.38580	0.41937E-04	-.20491	0.0000	-.64055E-03	0.22510
0.0	0.48173	0.0000	-.27687	0.0000	0.0000	-.40892E-01
	0.48181	-.20133E-03	-.27813	0.0000	0.63530E-02	0.81945E-01
-22.5	0.59474	0.49592E-01	-.27620	-10.037	-1.8395	-.42909
	0.59464	0.64388E-03	-.27338	0.0000	-.12508E-01	-.32953
-45.0	0.65627	1.3002	0.22099E-01	-44.130	-8.0812	-1.6003
	0.65540	1.8467	0.78294E-02	-30.732	-.97031	-1.1319
-67.5	0.61604	1.7771	0.78399E-01	0.0000	0.22616	0.18673
	0.61603	1.7772	0.81057E-01	0.0000	0.23270	0.19491
-90.0	0.60042	1.7321	-.89739E-08	0.0000	-.25887E-07	0.20530
	0.60042	1.7321	0.0000	0.0000	0.0000	0.20535

Table 7 (continued)

Z = 0.32022

ϕ(deg)	r	r_Z	r_ϕ	r_{ZZ}	$r_{Z\phi}$	$r_{\phi\phi}$
90.0	0.27495	0.0000	0.61629E-08	0.0000	0.0000	-.75433E-01
	0.27495	0.19664E-06	0.0000	0.0000	0.0000	0.14095
67.5	0.28600	0.0000	-.57192E-01	0.0000	0.0000	-.81971E-01
	0.28598	0.17362E-03	-.56931E-01	0.0000	-.16028E-02	0.15246
45.0	0.32124	0.0000	-.12467	0.0000	0.0000	-.11914
	0.32124	-.18097E-04	-.12442	0.0000	0.59822E-05	0.19049
22.5	0.38582	0.0000	-.20576	0.0000	0.0000	-.24144
	0.38580	0.41937E-04	-.20488	0.0000	-.64055E-03	0.22466
0.0	0.48173	0.0000	-.27687	0.0000	0.0000	-.44206
	0.48180	-.20133E-03	-.27809	0.0000	0.63530E-02	0.83687E-01
-22.5	0.59486	0.0000	-.28528	0.0000	0.0000	-.47438
	0.59441	0.18328E-02	-.28241	0.0000	-.85144E-01	0.21244E-01
-45.0	0.68856	0.38712	-.14510	-12.330	-2.2579	-.62050
	0.69053	0.32595	-.13846	-.75976E-03	-3.6951	-1.8983
-67.5	0.69275	1.7771	0.88161E-01	0.0000	0.22616	0.20998
	0.69274	1.7746	0.91101E-01	-17.736	0.13554	0.21448
-90.0	0.67519	1.7321	-.10091E-07	0.0000	-.25887E-07	0.23086
	0.67519	1.7317	0.0000	-2.4968	0.0000	0.23129

Table 7 (continued)

Z = 0.36345

ϕ(deg)	r	r_Z	r_ϕ	r_{ZZ}	$r_{Z\phi}$	$r_{\phi\phi}$
90.0	0.27495	0.0000	0.61629E-08	0.0000	0.0000	-.75433E-01
	0.27495	0.19664E-06	0.0000	0.0000	0.0000	0.14100
67.5	0.28600	0.0000	-.57192E-01	0.0000	0.0000	-.81971E-01
	0.28599	0.17362E-03	-.57001E-01	0.0000	-.16028E-02	0.15300
45.0	0.32124	0.0000	-.12467	0.0000	0.0000	-.11914
	0.32124	-.18097E-04	-.12442	0.0000	0.59822E-05	0.19055
22.5	0.38582	0.0000	-.20576	0.0000	0.0000	-.24144
	0.38580	0.41937E-04	-.20486	0.0000	-.64055E-03	0.22421
0.0	0.48173	0.0000	-.27687	0.0000	0.0000	-.44206
	0.48179	-.20133E-03	-.27805	0.0000	0.63530E-02	0.85406E-01
-22.5	0.59486	0.0000	-.28528	0.0000	0.0000	-.47438
	0.59456	0.18328E-02	-.28344	0.0000	-.85144E-01	-.15735E-01
-45.0	0.69531	0.0000	-.21599	0.0000	0.0000	-.24374
	0.69540	0.46091E-03	-.21483	0.0000	-.12147E-02	-.43688
-67.5	0.74461	0.62437	-.39695E-01	-16.385	-1.8464	-.33325
	0.74534	0.65451	-.48150E-01	-16.063	-2.1128	-.45132
-90.0	0.74658	1.1620	-.33222E-08	-36.032	0.48095E-06	0.76003E-01
	0.74491	1.3722	0.0000	-20.652	0.0000	.13714

Table 7 (continued)

Z = 0.40672

ϕ(deg)	r	r_Z	r_ϕ	r_{ZZ}	$r_{Z\phi}$	$r_{\phi\phi}$
90.0	0.27495	0.0000	0.61629E-08	0.0000	0.0000	-.45199
	0.27495	0.19664E-06	0.0000	0.0000	0.0000	0.14107
67.5	0.28600	0.0000	-.57192E-01	0.0000	0.0000	-.46832
	0.28599	0.17362E-03	-.57070E-01	0.0000	-.16028E-02	0.15355
45.0	0.32124	0.0000	-.12467	0.0000	0.0000	-.53270
	0.32124	-.18097E-04	-.12442	0.0000	0.59822E-05	0.19061
22.5	0.38582	0.0000	-.20576	0.0000	0.0000	-.68891
	0.38580	0.41937E-04	-.20484	0.0000	-.64055E-03	0.22378
0.0	0.48173	0.0000	-.27687	0.0000	0.0000	-.90625
	0.48178	-.20133E-03	-.27801	0.0000	0.63530E-02	0.87170E-01
-22.5	0.59486	0.0000	-.28528	0.0000	0.0000	-.92185
	0.59471	0.18328E-02	-.28445	0.0000	-.85144E-01	-.52557E-01
-45.0	0.69531	0.0000	-.21599	0.0000	0.0000	-.65730
	0.69535	0.46091E-03	-.21395	0.0000	-.12147E-02	-.33982
-67.5	0.75932	0.97402E-01	-.99079E-01	-10.143	-1.1430	-.38584
	0.75848	0.15197E-02	-.87498E-01	-4.6333	0.88919E-02	-.15776
-90.0	0.77591	0.34401	0.75965E-08	-11.827	0.15786E-06	-.17379
	0.77791	0.23519	0.0000	-13.383	0.0000	-.23735

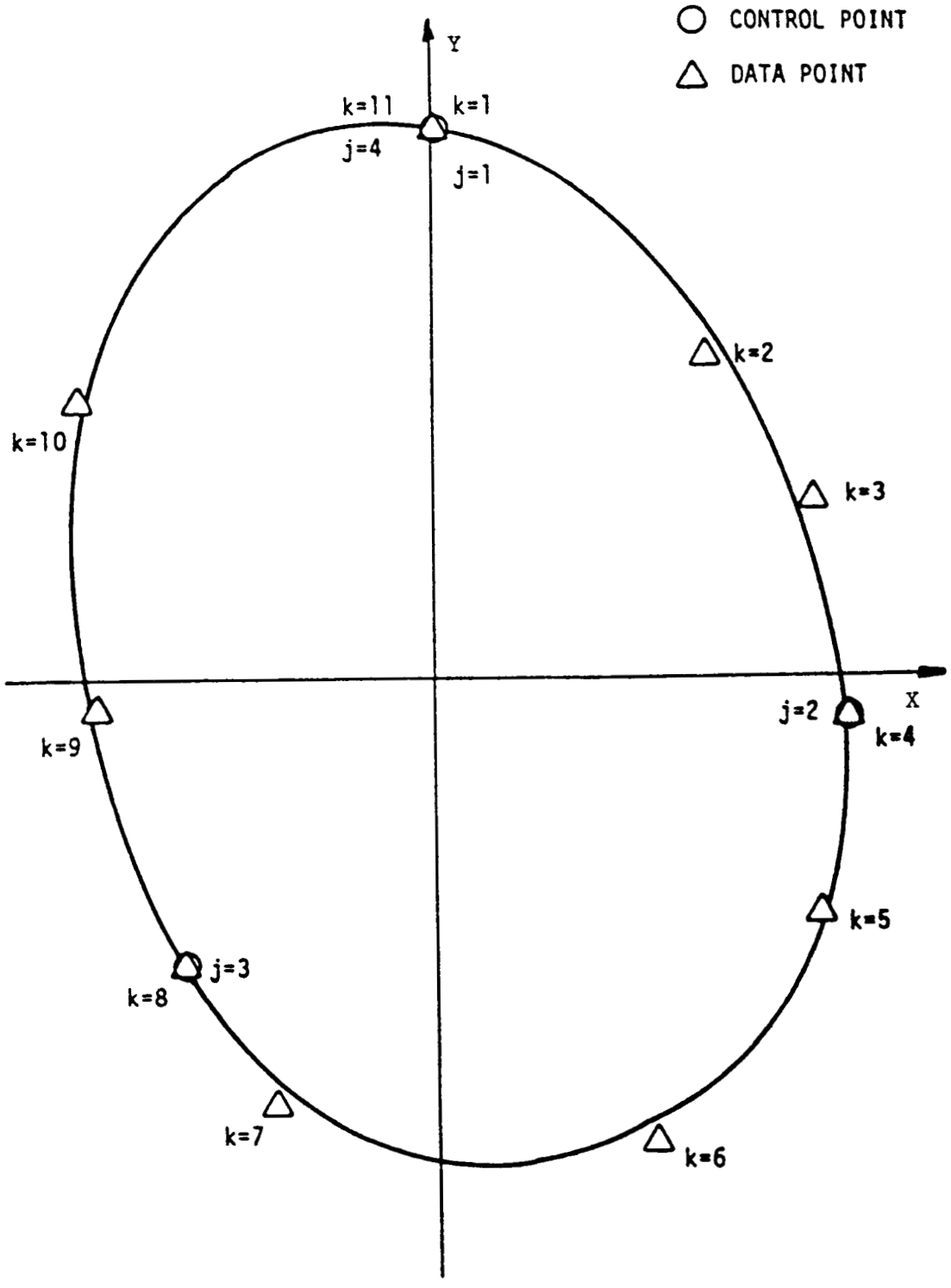

Figure 2.1. Data points and control points in a cross section.

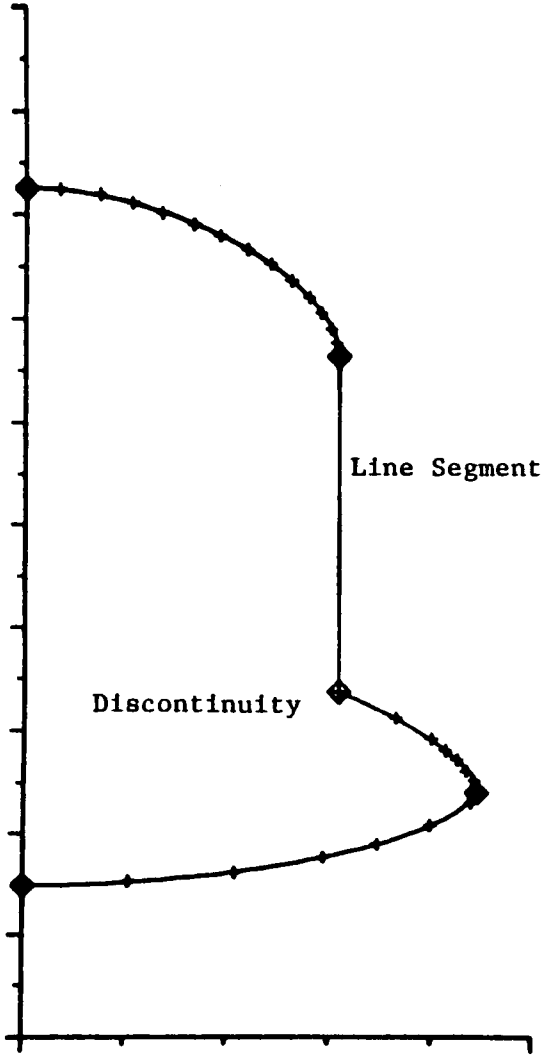

Figure 2.2. Slope specifications in a cross section.

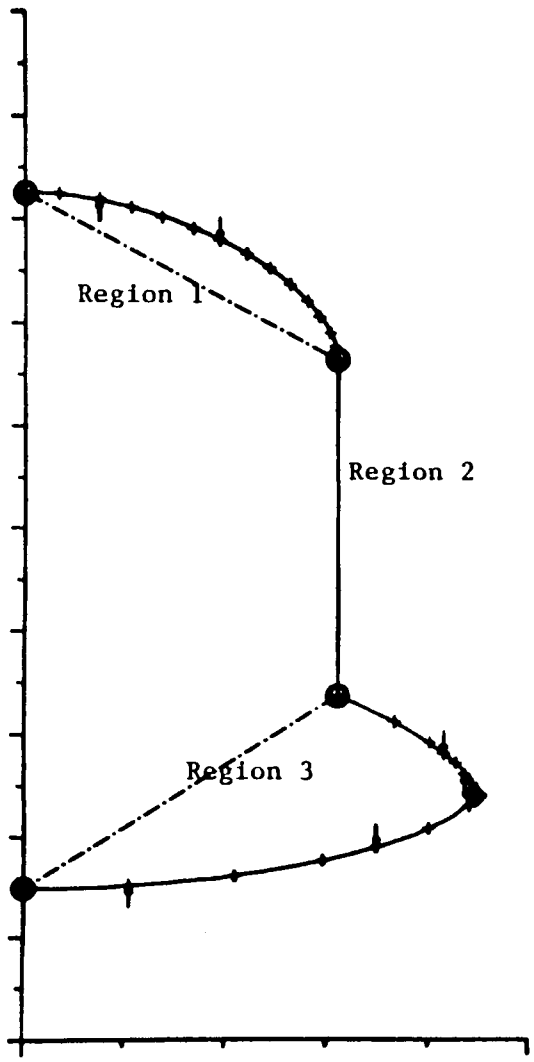

Figure 2.3. Fitting regions in a cross section.

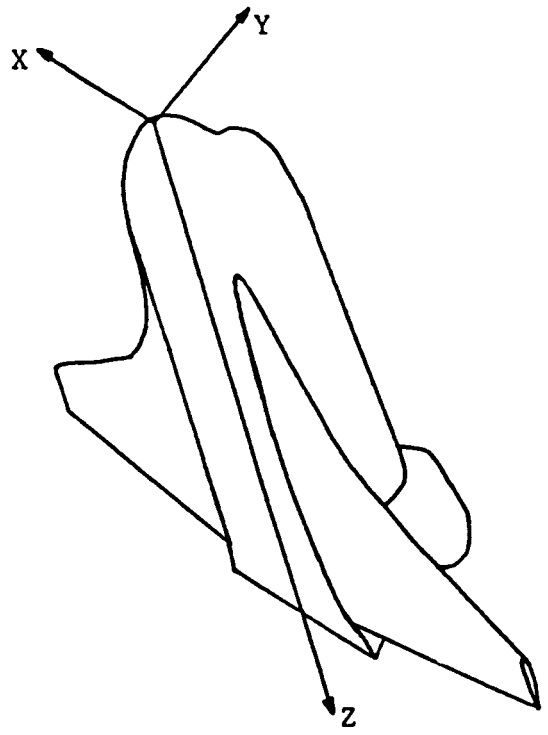

Figure 2.4. Fuselage global coordinate system.

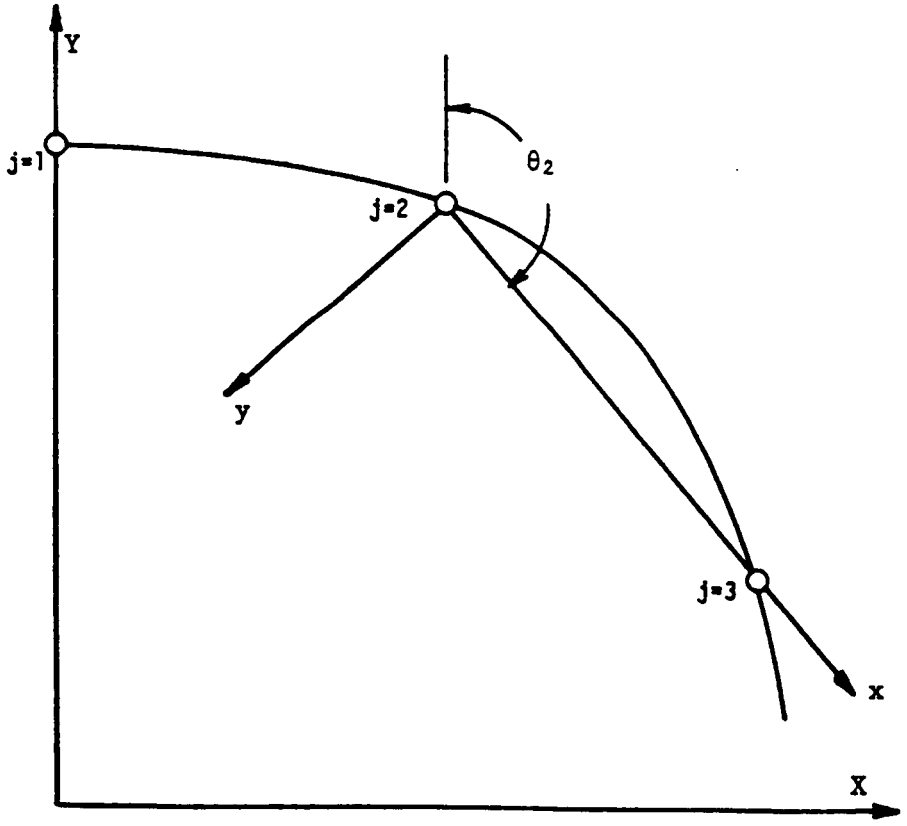

Figure 2.5. Local coordinate system, illustrated for arc j = 2.

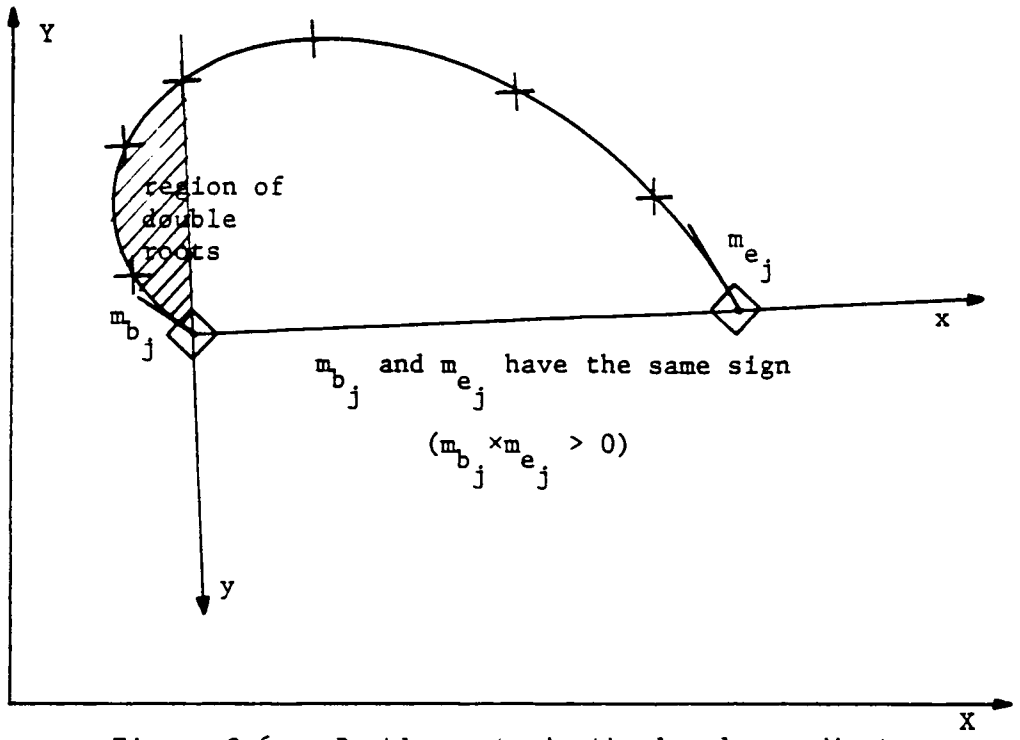

Figure 2.6a. Double roots in the local coordinate system of arc j.

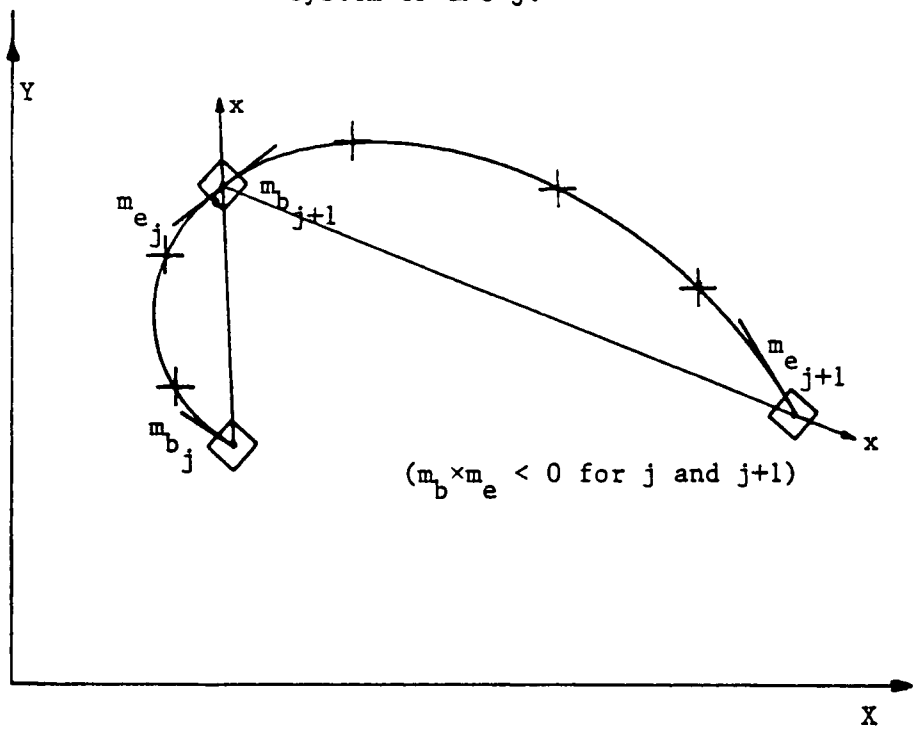

Figure 2.6b. Double root situation avoided with the addition of a control point.

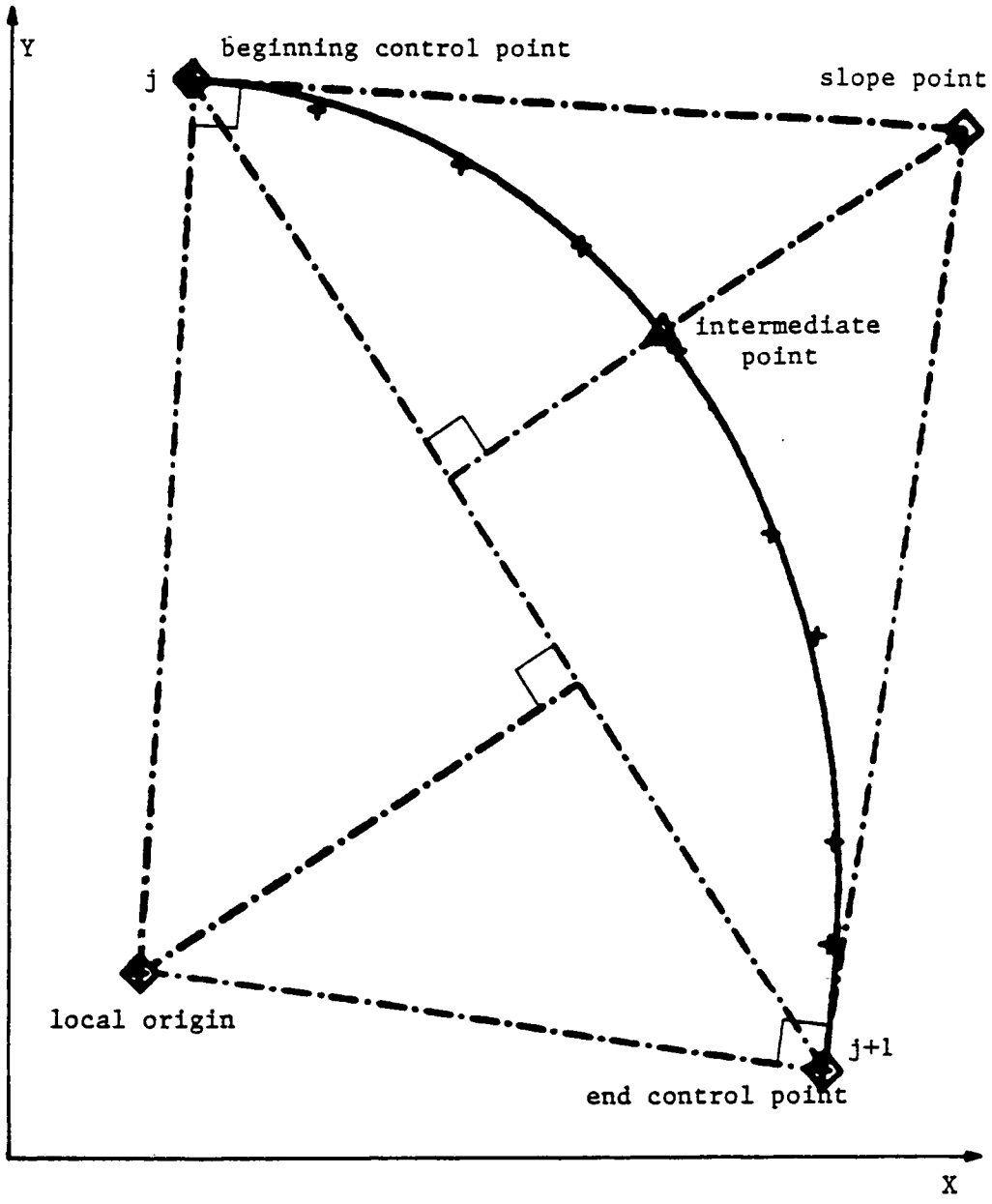

Figure 2.7. Defining points (and local origin) for arc j.

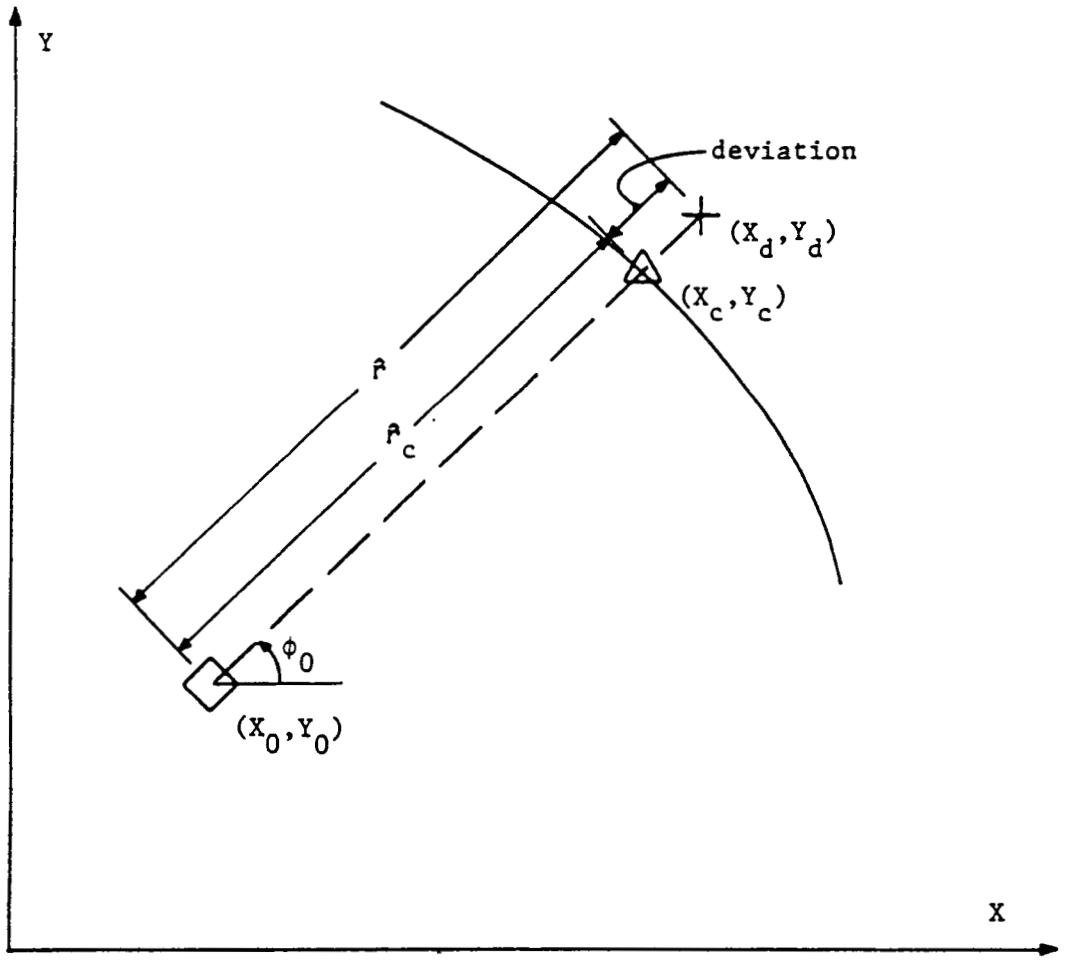

Figure 2.8. Comparison between input and calculated values of the original data points.

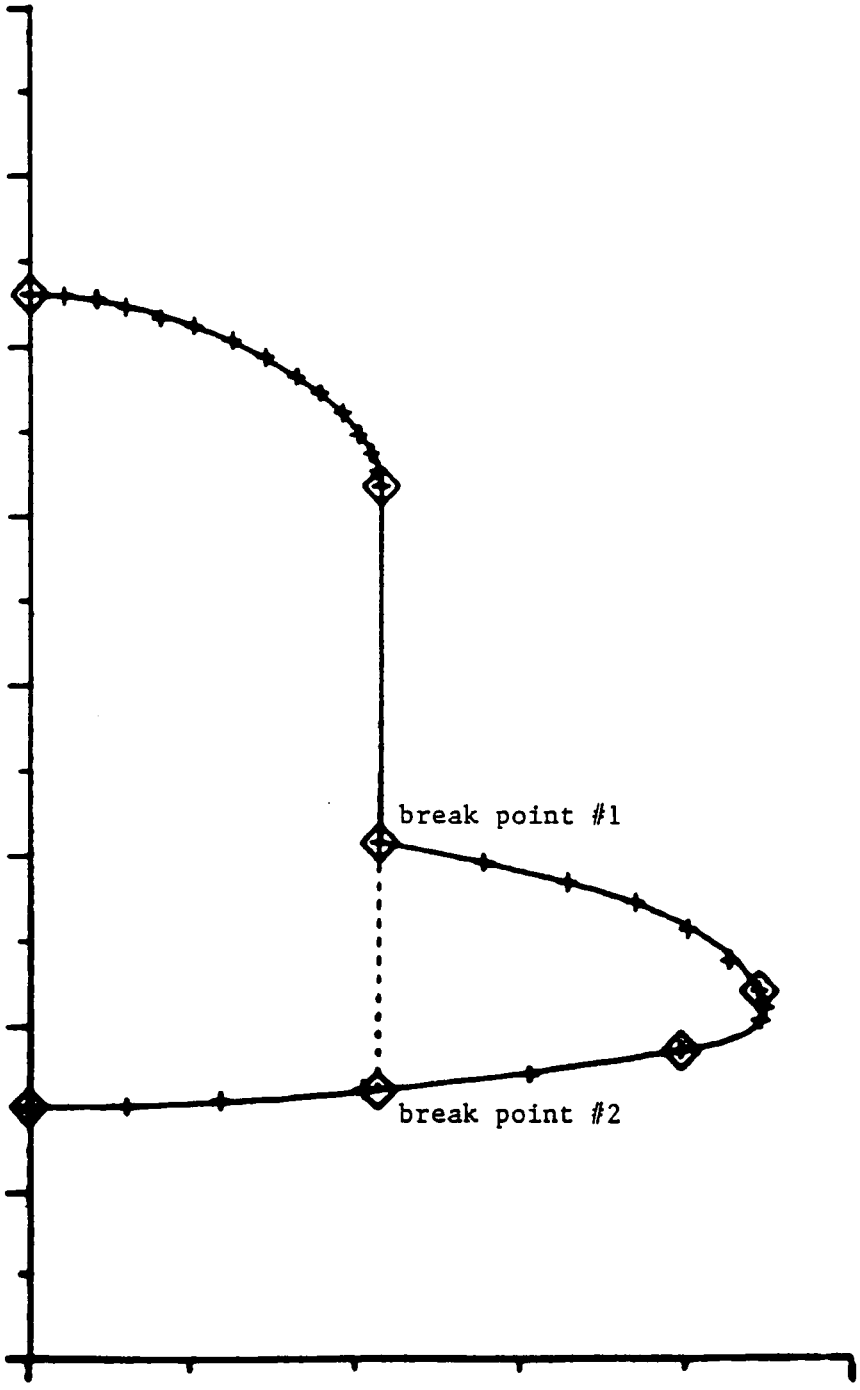

Figure 2.9. Break points for a given cross section.

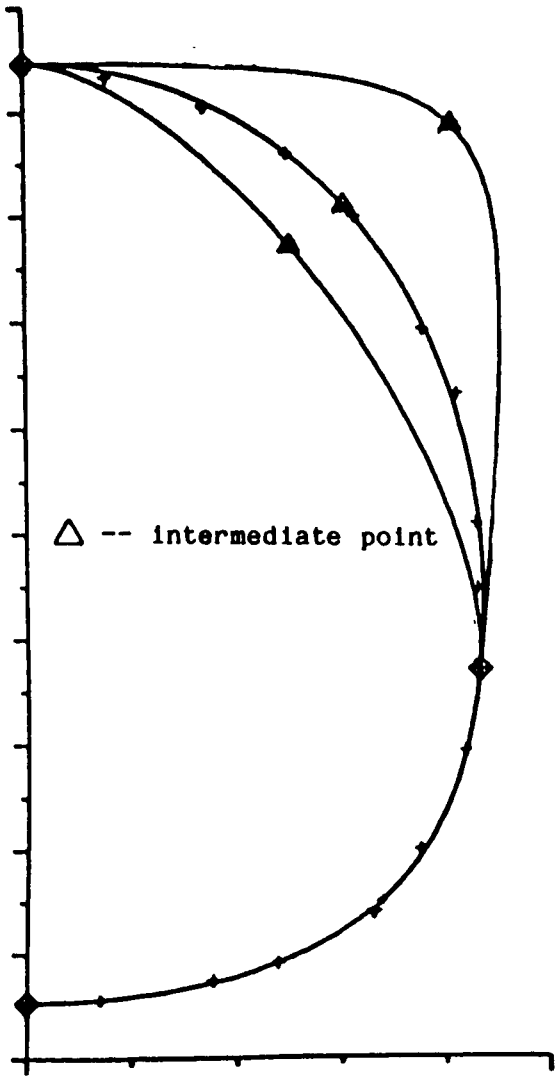

Figure 3.1. Variation of arc intermediate point.

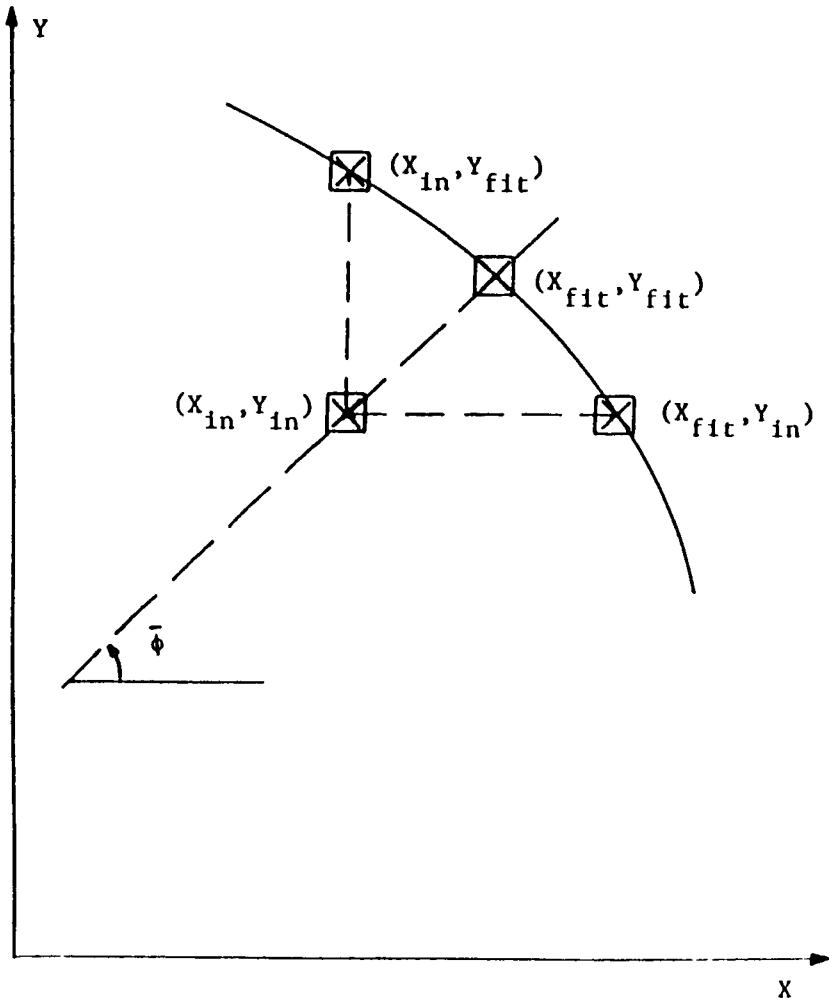

Figure 3.2. Interpretation of user input of coordinates via the cross-hair.

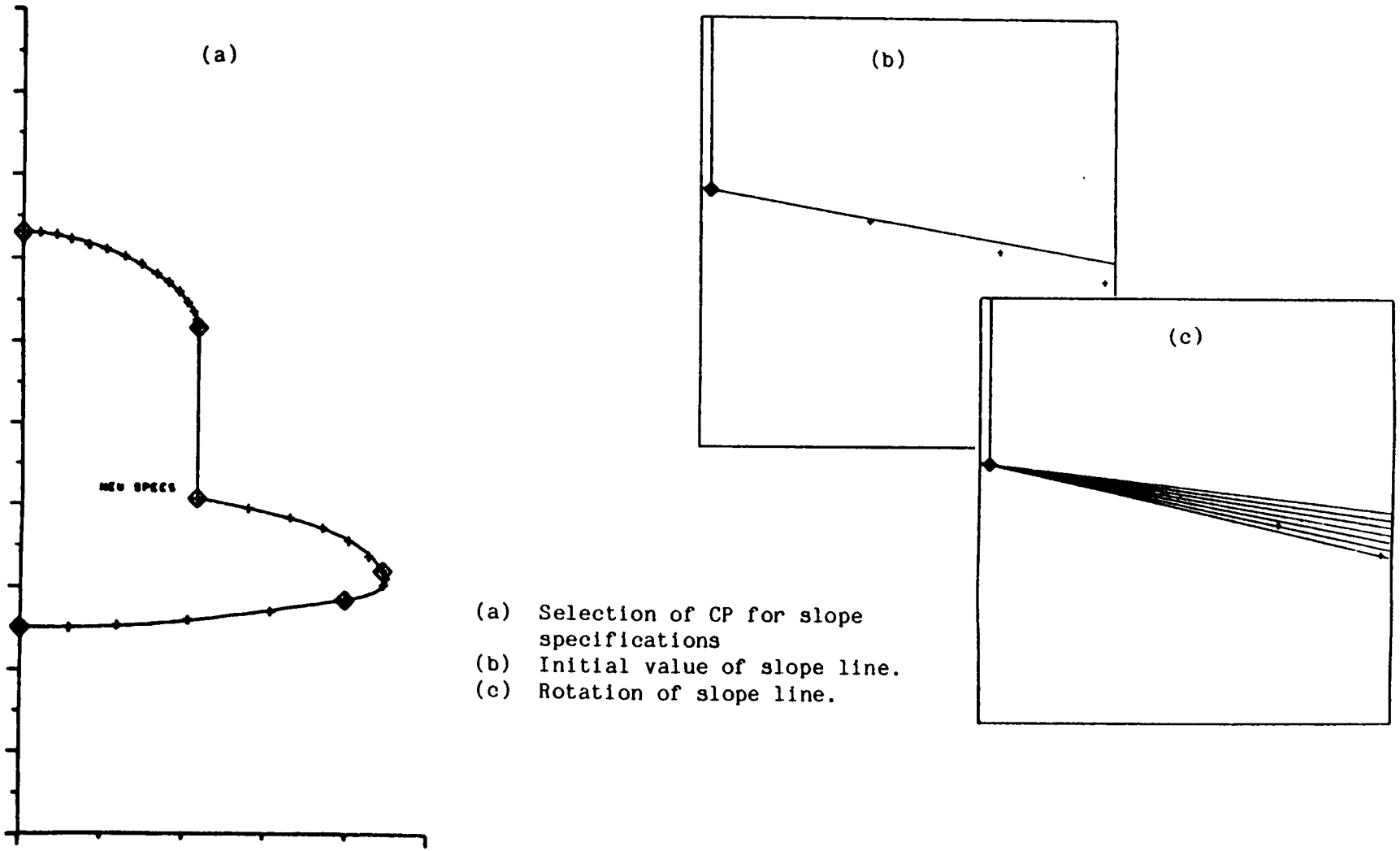

(a) Selection of CP for slope specifications
(b) Initial value of slope line.
(c) Rotation of slope line.

Figure 3.3. Slope specification at a given control point via the "slope-line".

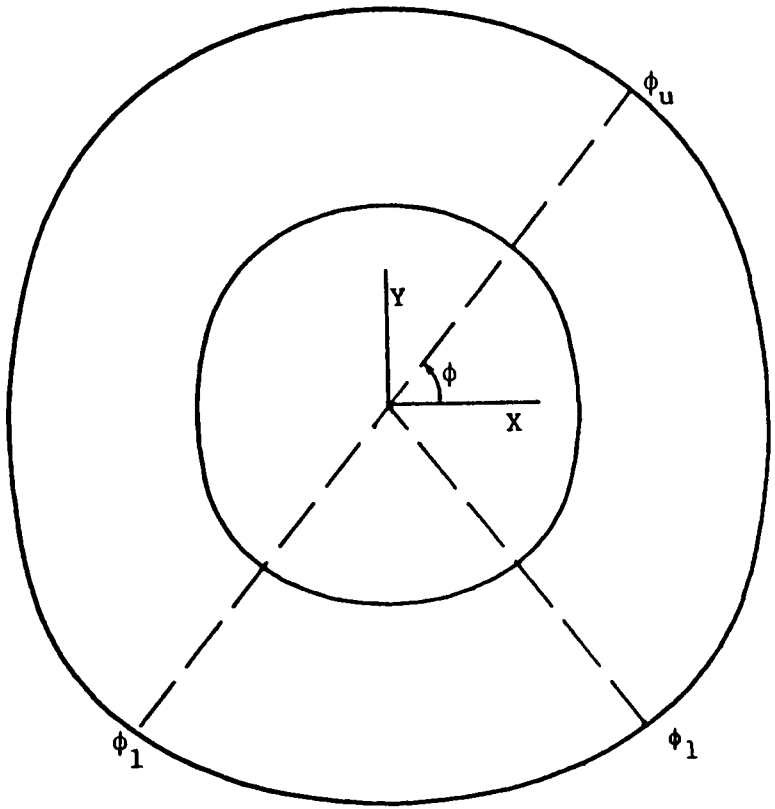

Figure 4.1. Intersections between meridional cut and the two defining cross sections of the nose region.

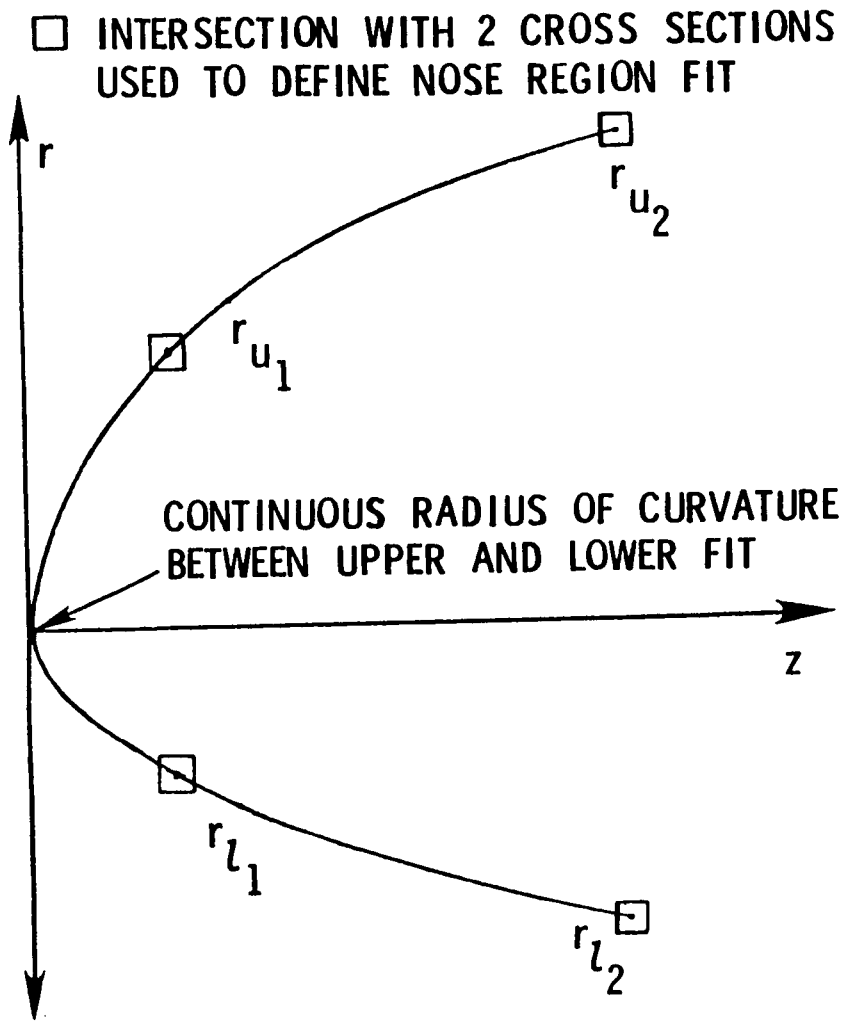

Figure 4.2. Constraints on a given meridional cut of the nose region.

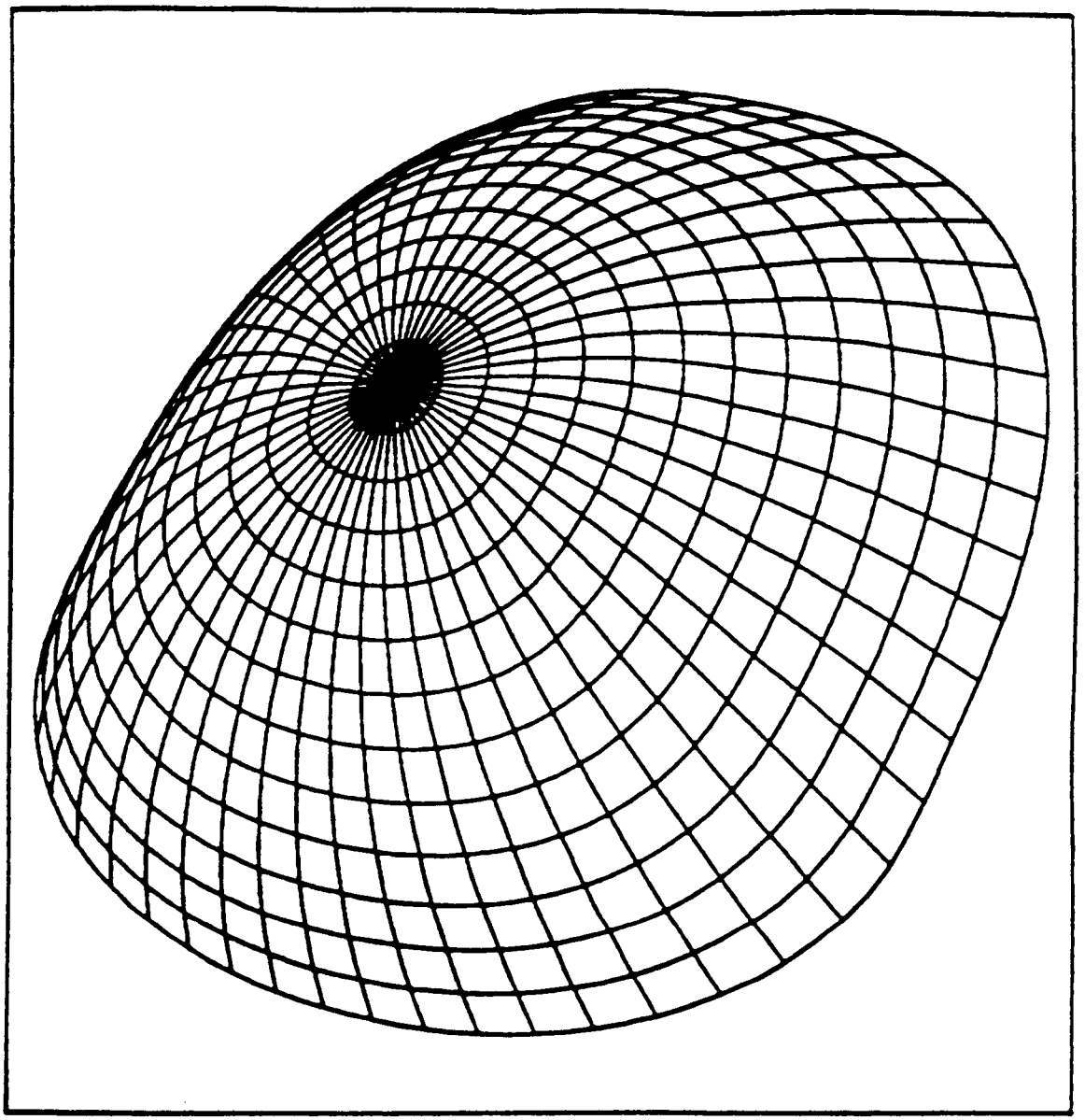

Figure 4.3. Orthographic view of nose region fit.

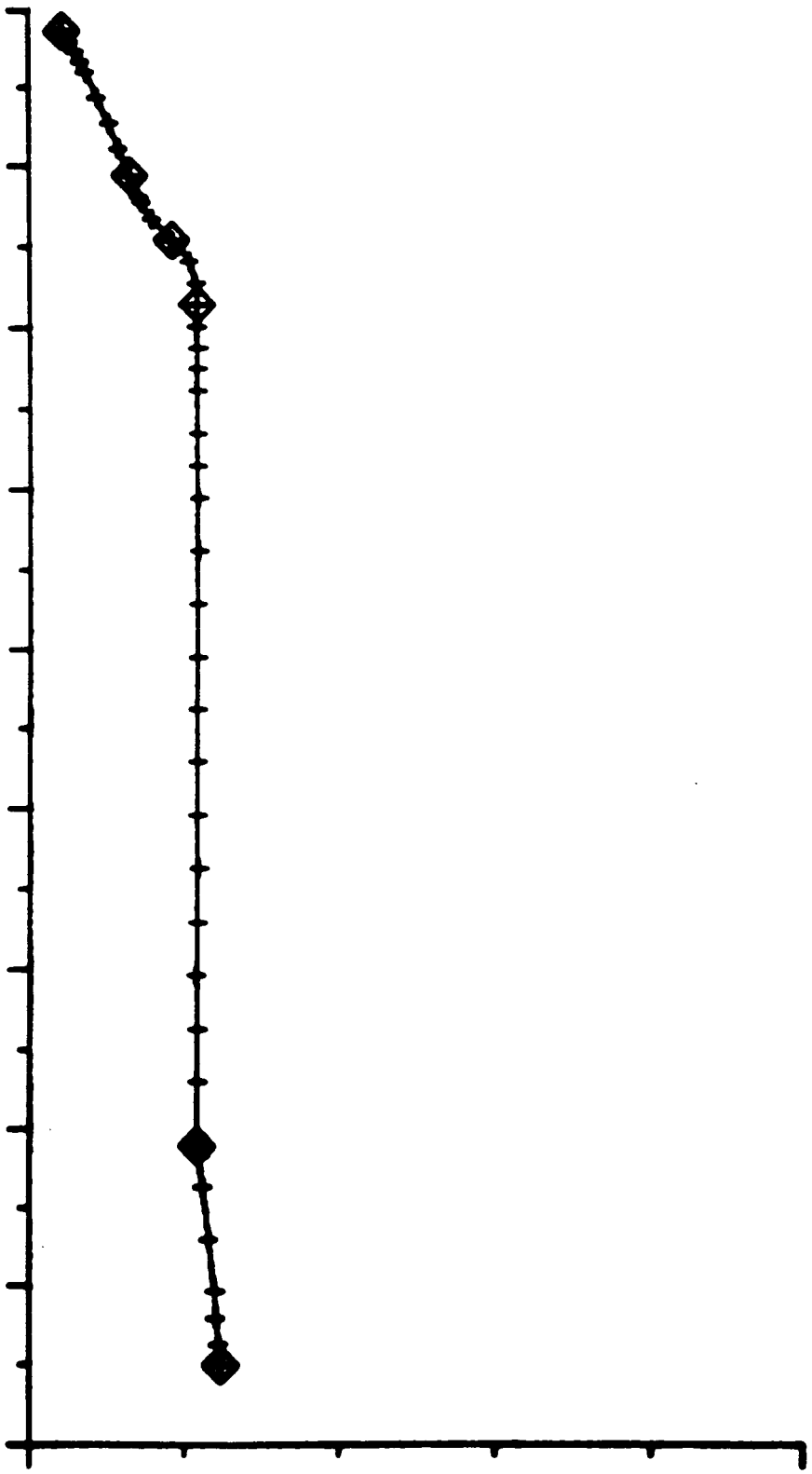

Figure 5.1. Curve-fit for a given meridional cut of the fuselage.

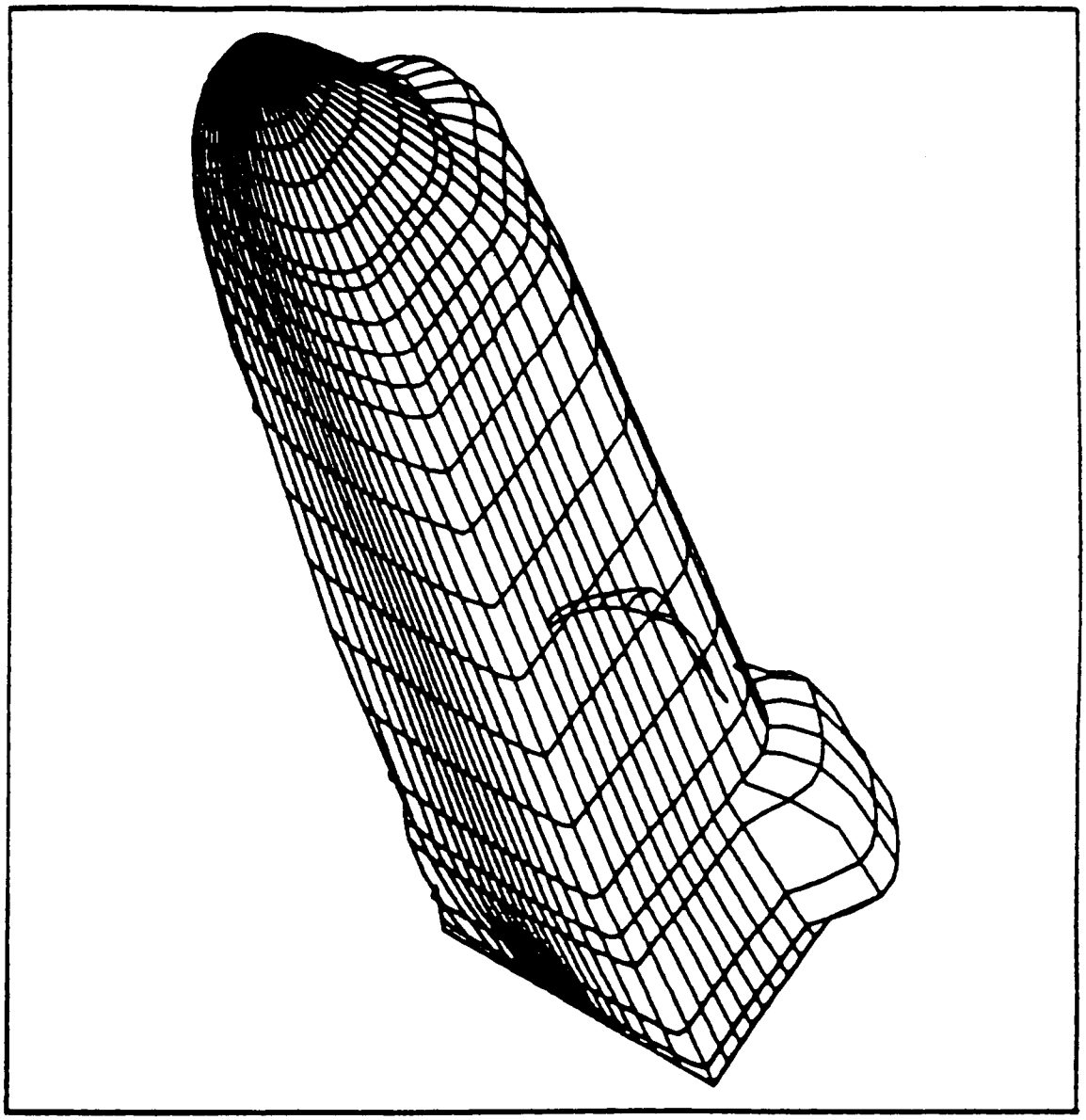

Figure 5.2. Orthographic view of fuselage surface-fit.

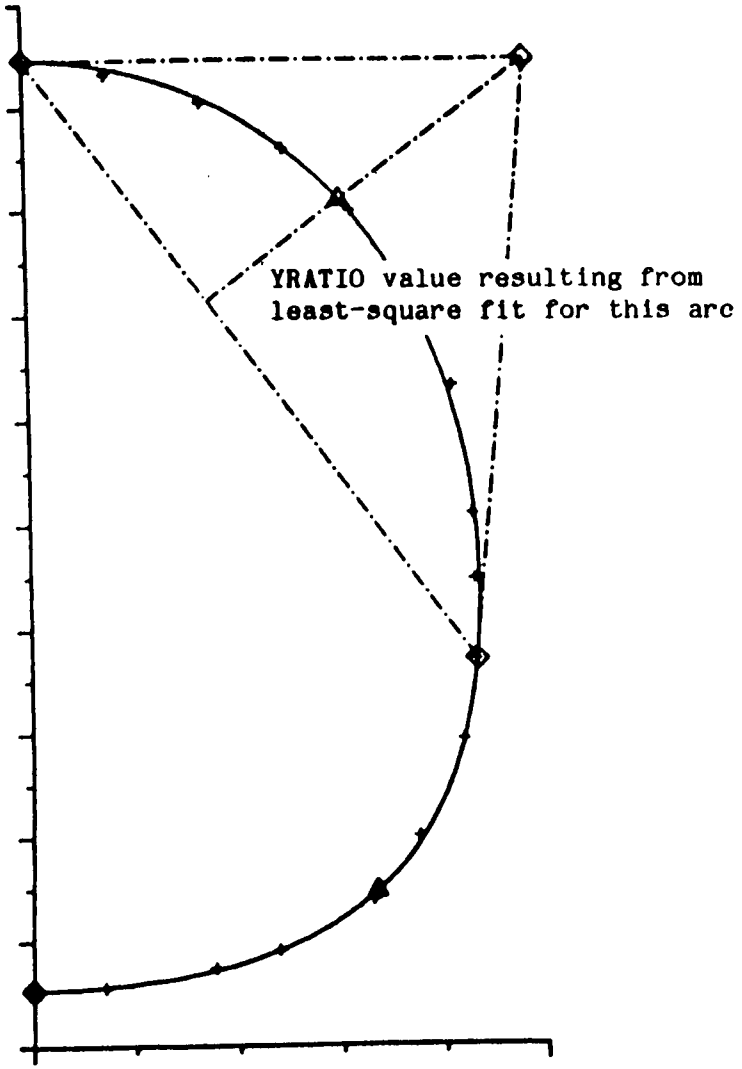

Figure 6.1. Arc defining triangle.

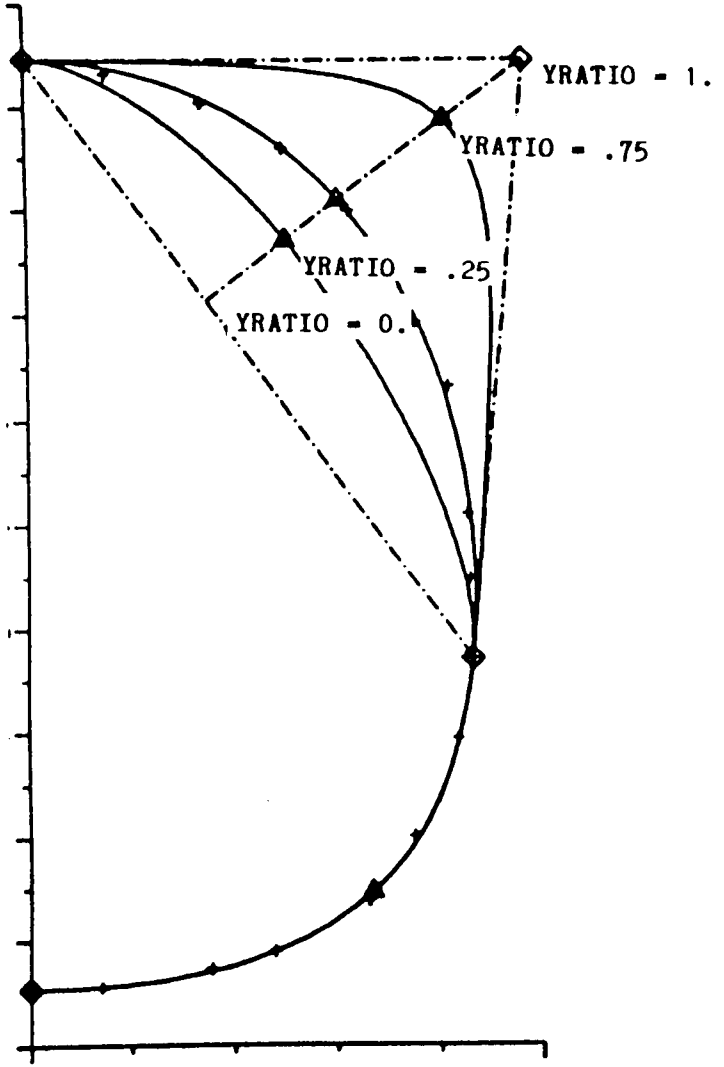

Figure 6.2. Variation of arc intermediate point with the defining triangle as a guide.

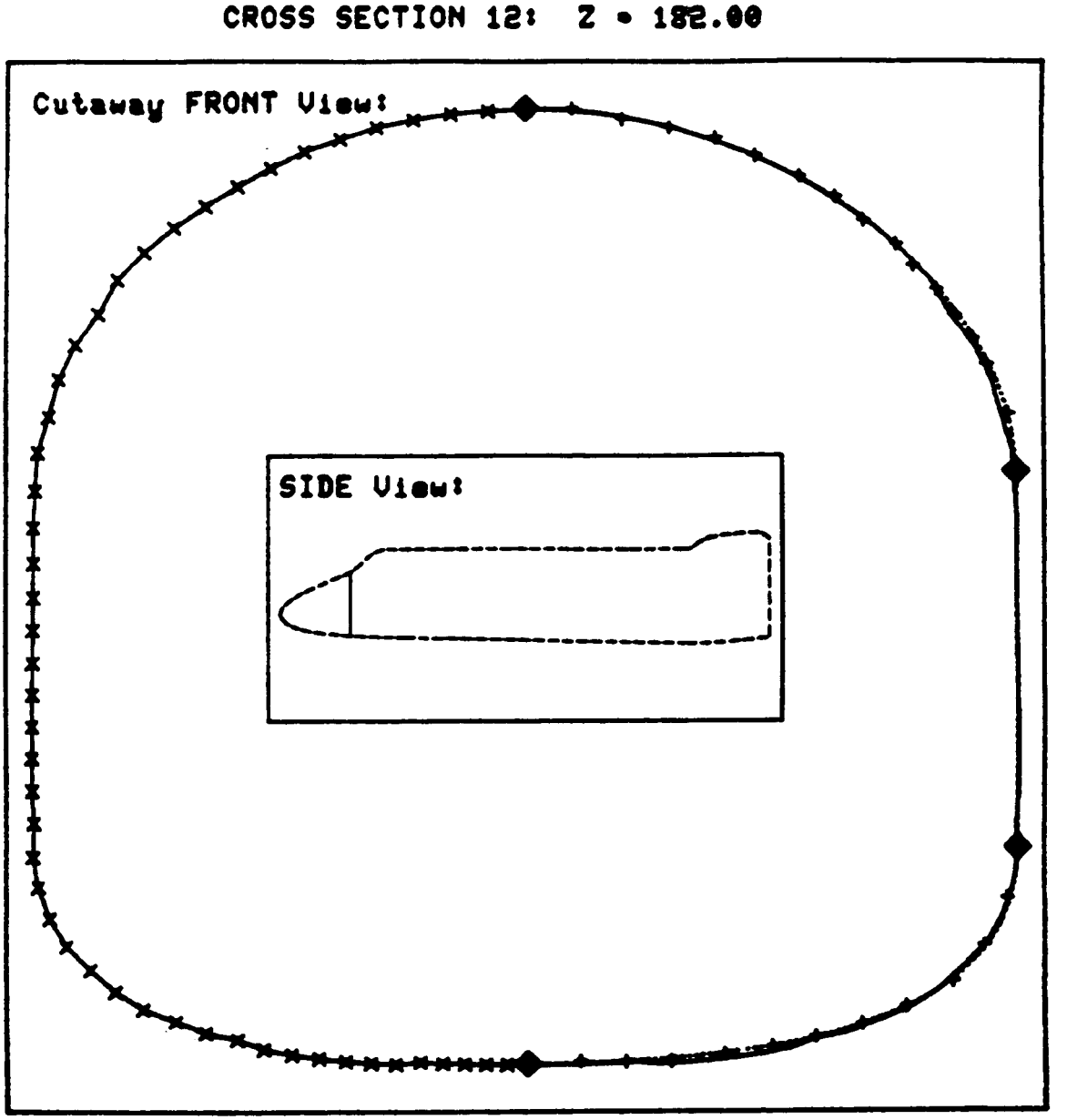

Figure 6.3. Comparison between original cross section curve-fit and the resulting surface-fit.

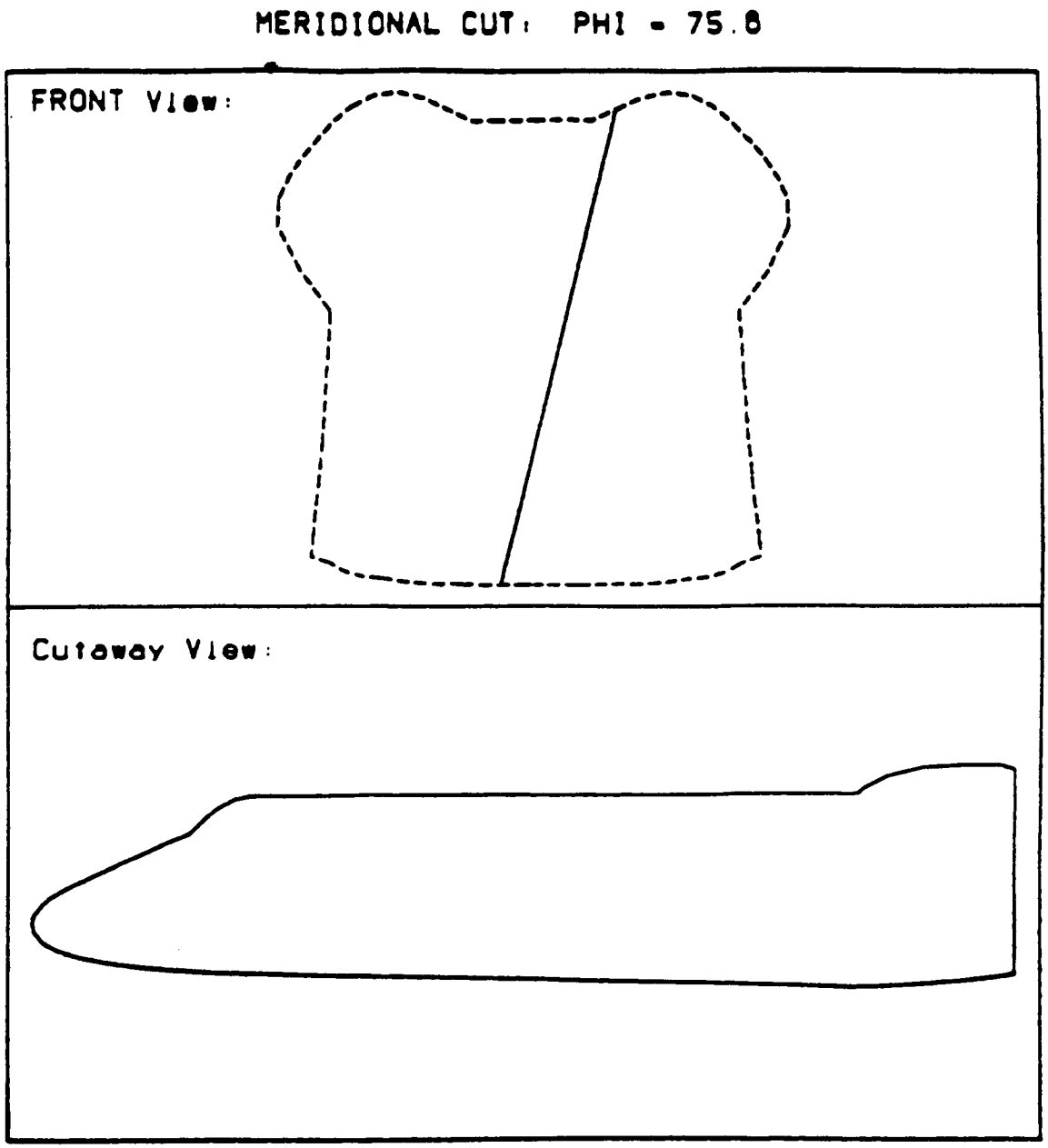

Figure 6.4. Viewing a meridional pair from the fuselage surface-fit.

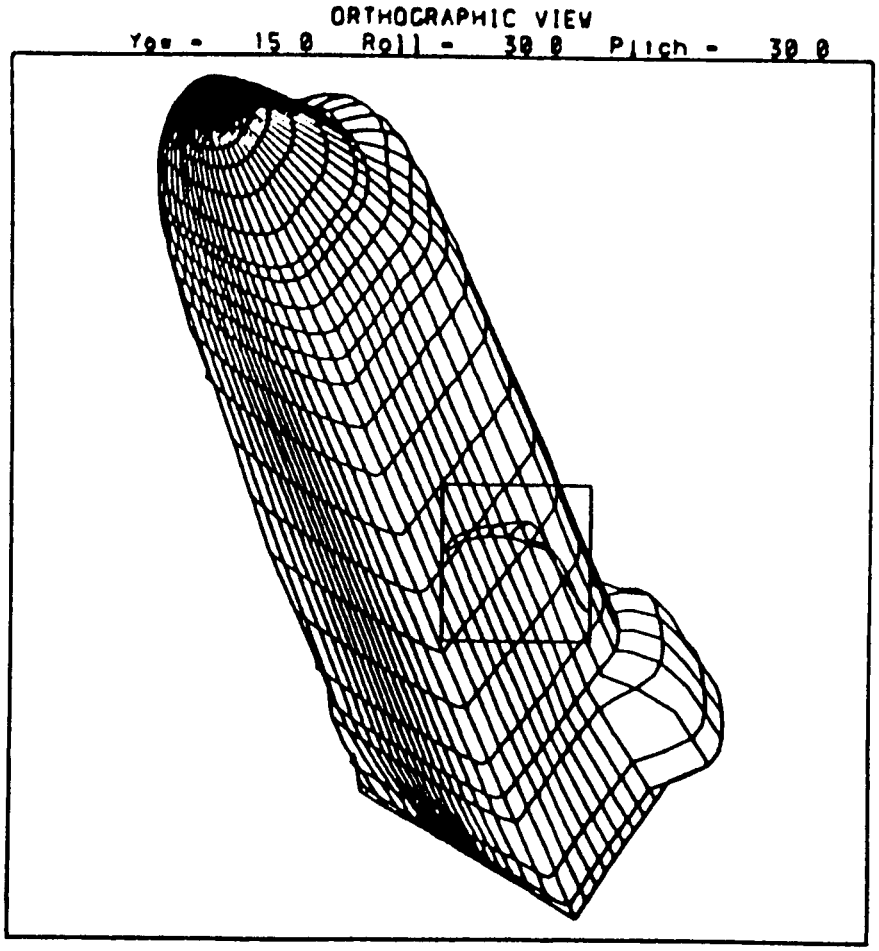

Figure 6.5a. Activation of zoom feature for a given view.

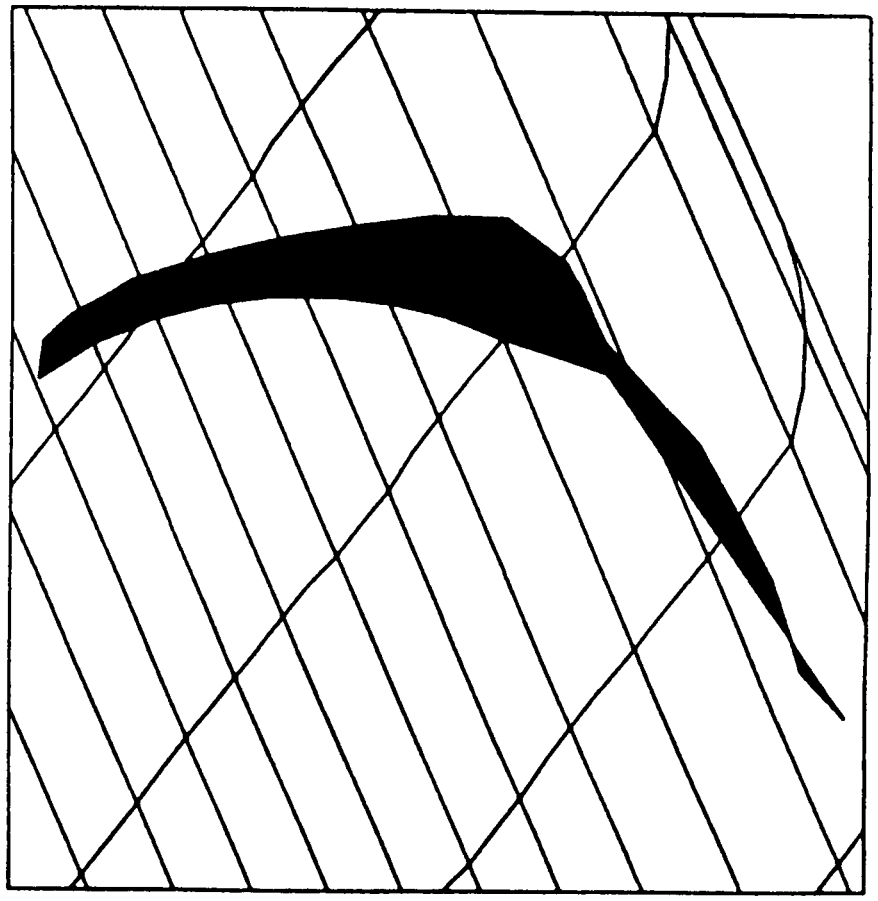

Figure 6.5b. Zoomed portion of the original view (darkened portion would not be drawn if a universal hidden-line-removal technique was employed).

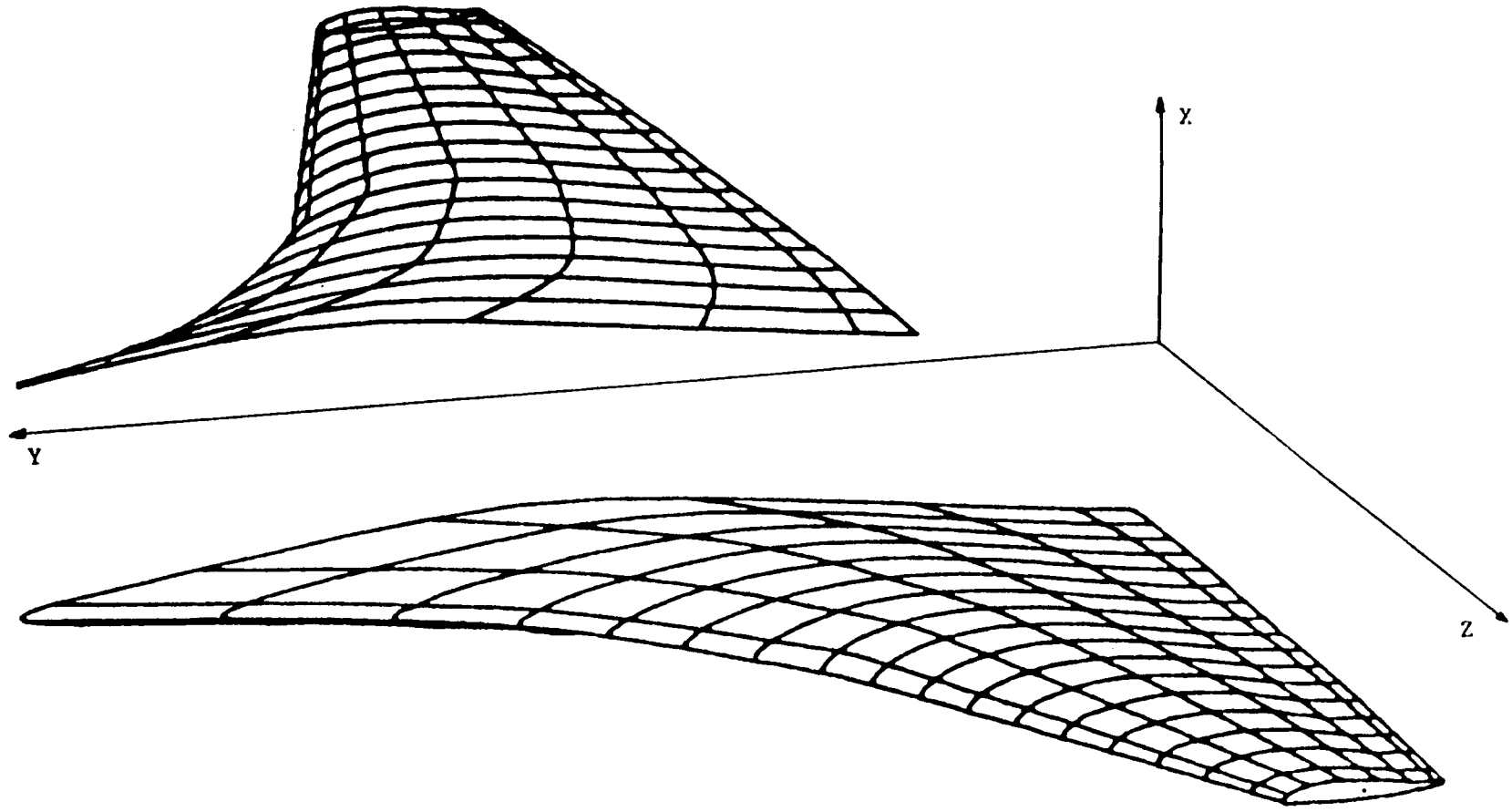

Figure 7.1. Wing global coordinate system.

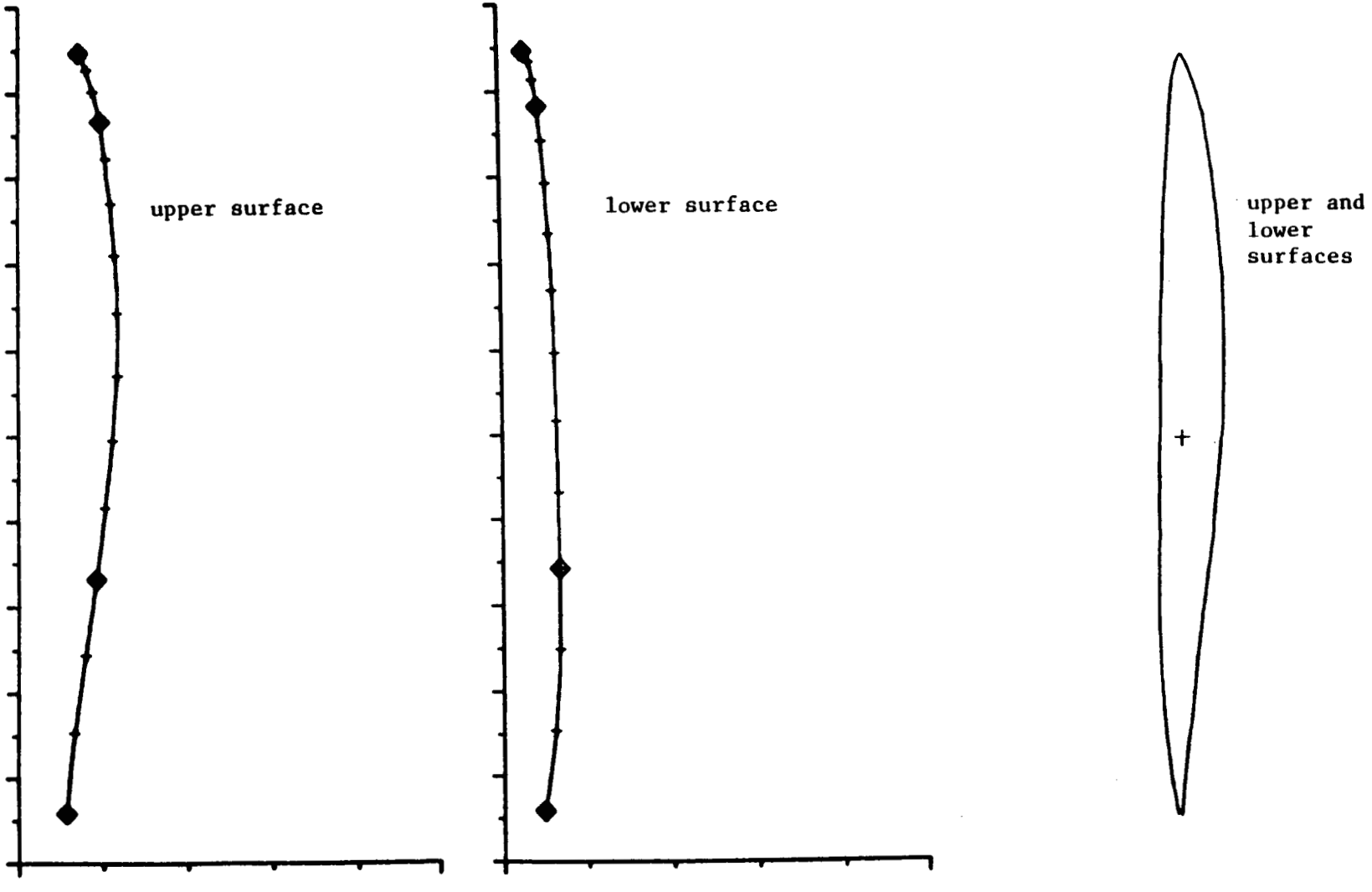

Figure 7.2. Curve-fit for wing cross section.

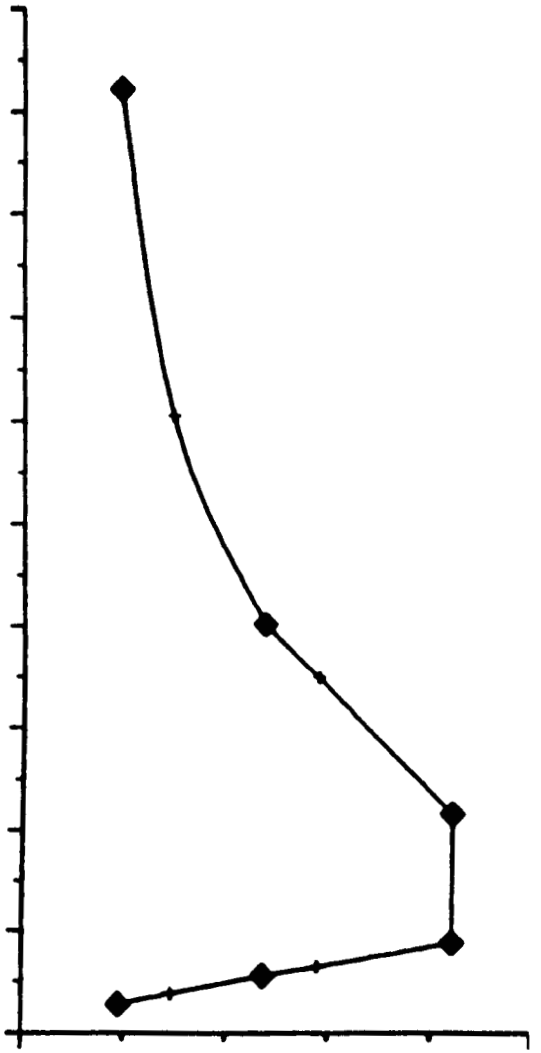

Figure 8.1. Curve-fit of wing planform.

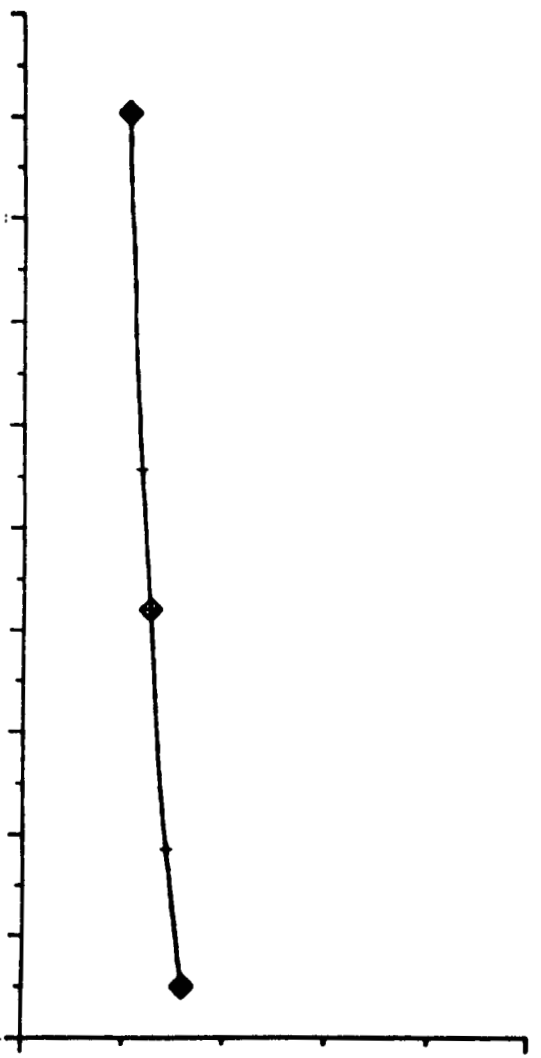

Figure 9.1. Typical curve-fit of spanwise variation of wing cross sections.

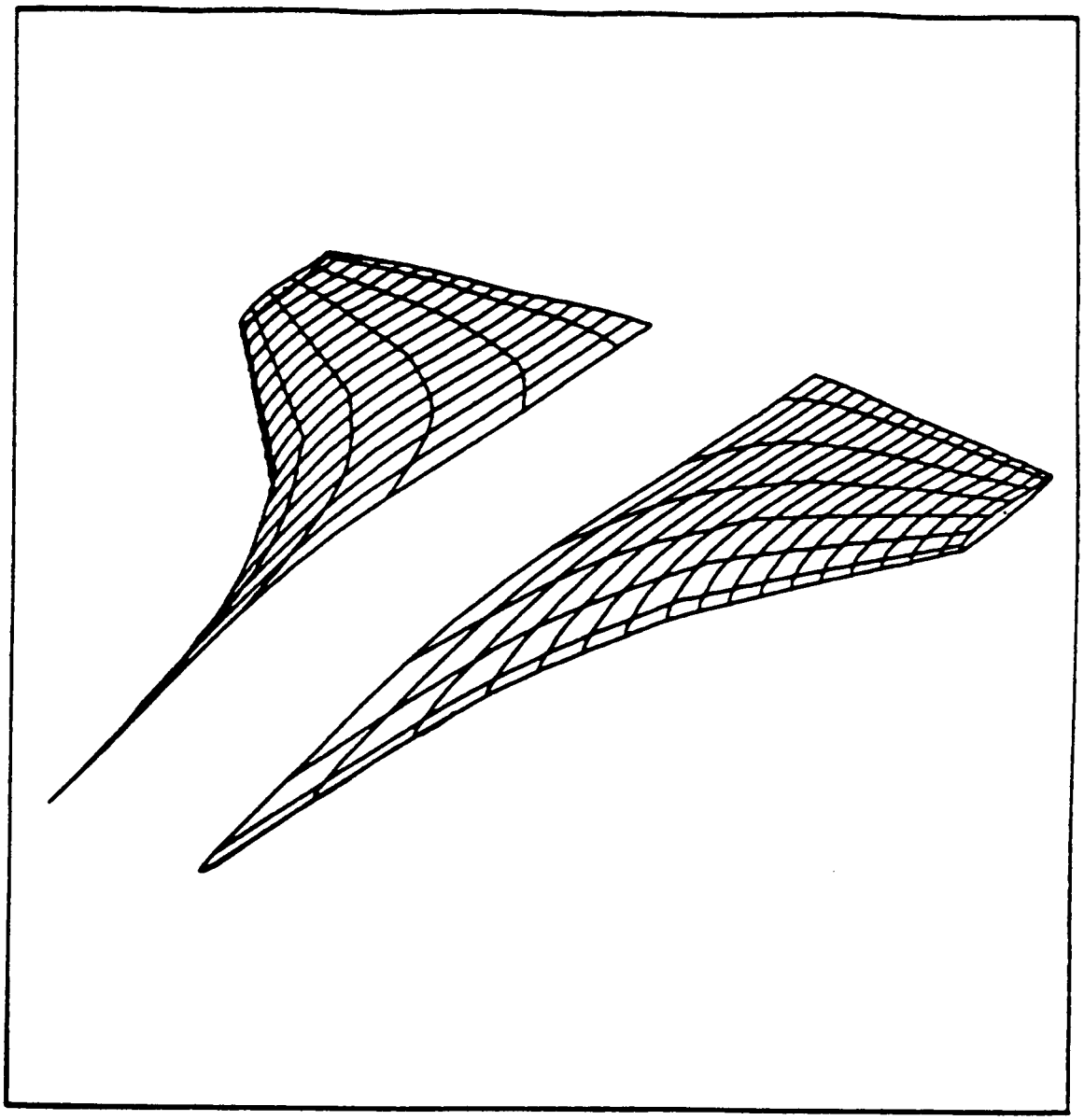

Figure 9.2. Orthographic view of wing surface fit.

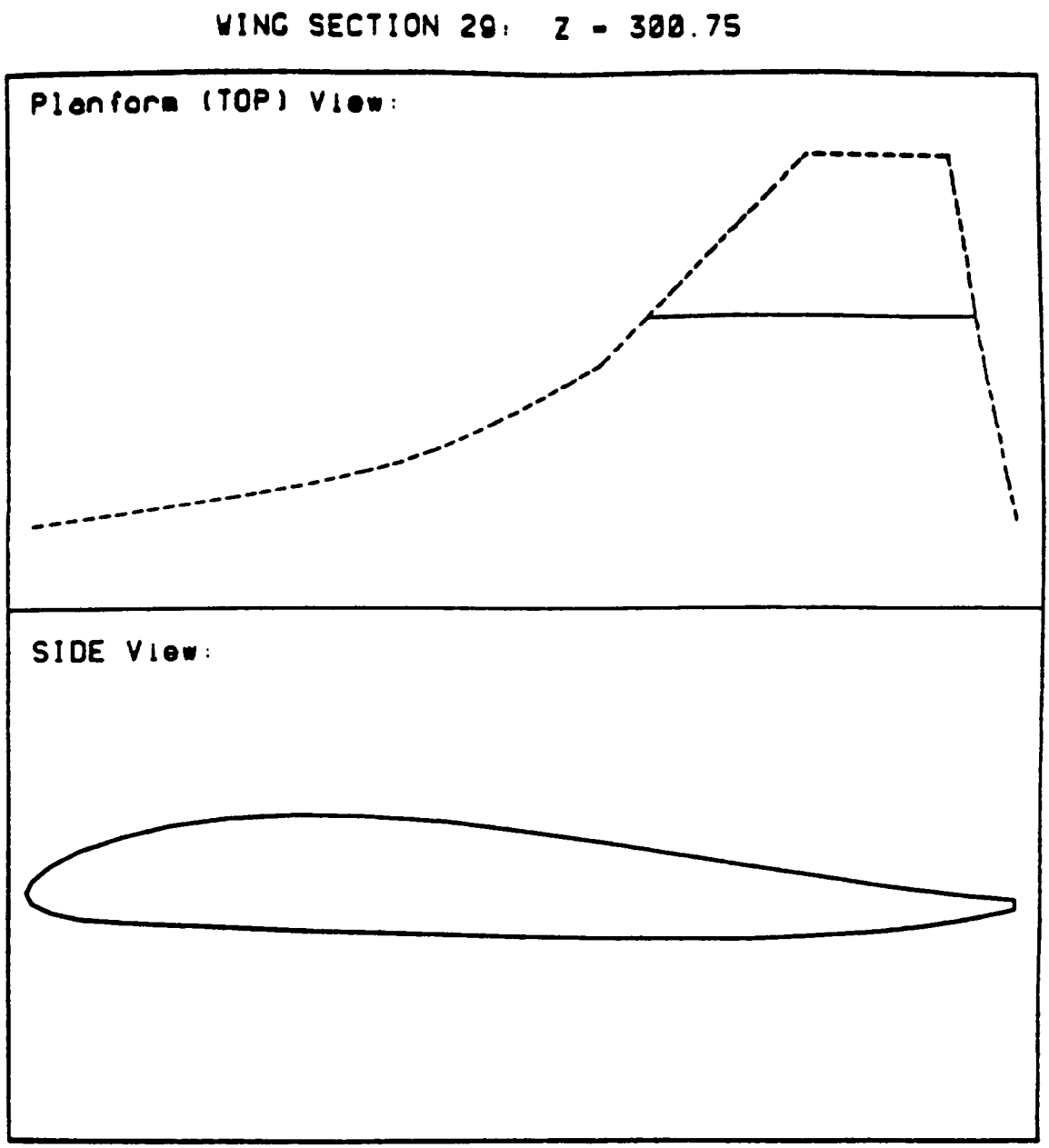

Figure 10.1. Viewing of a wing section as generated from the wing surface-fit.

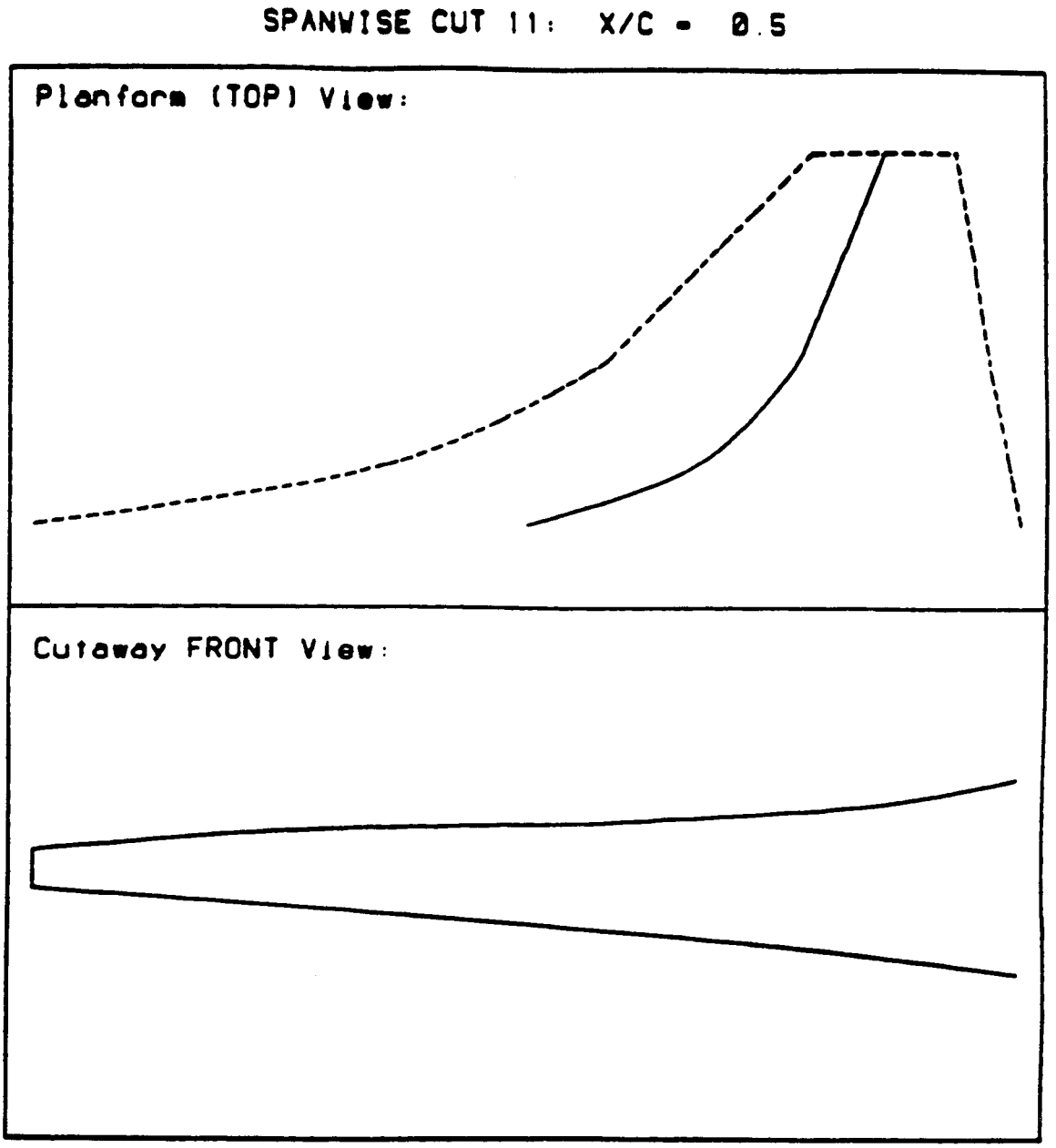

Figure 10.2. Viewing a spanwise pair from the wing surface-fit.

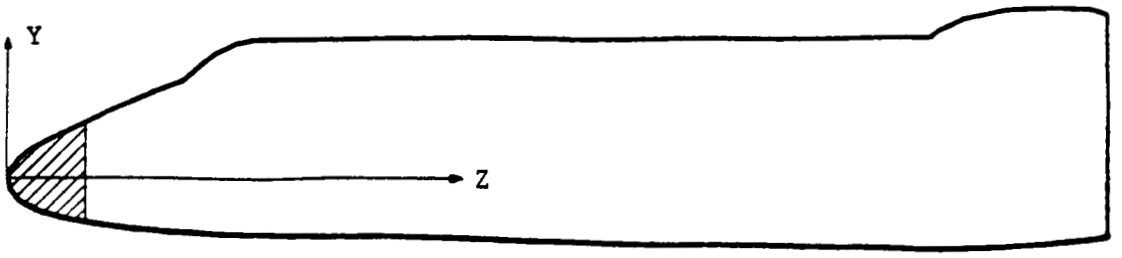

Figure 12.1. Side view of fuselage surface-fit with nose region highlighted.

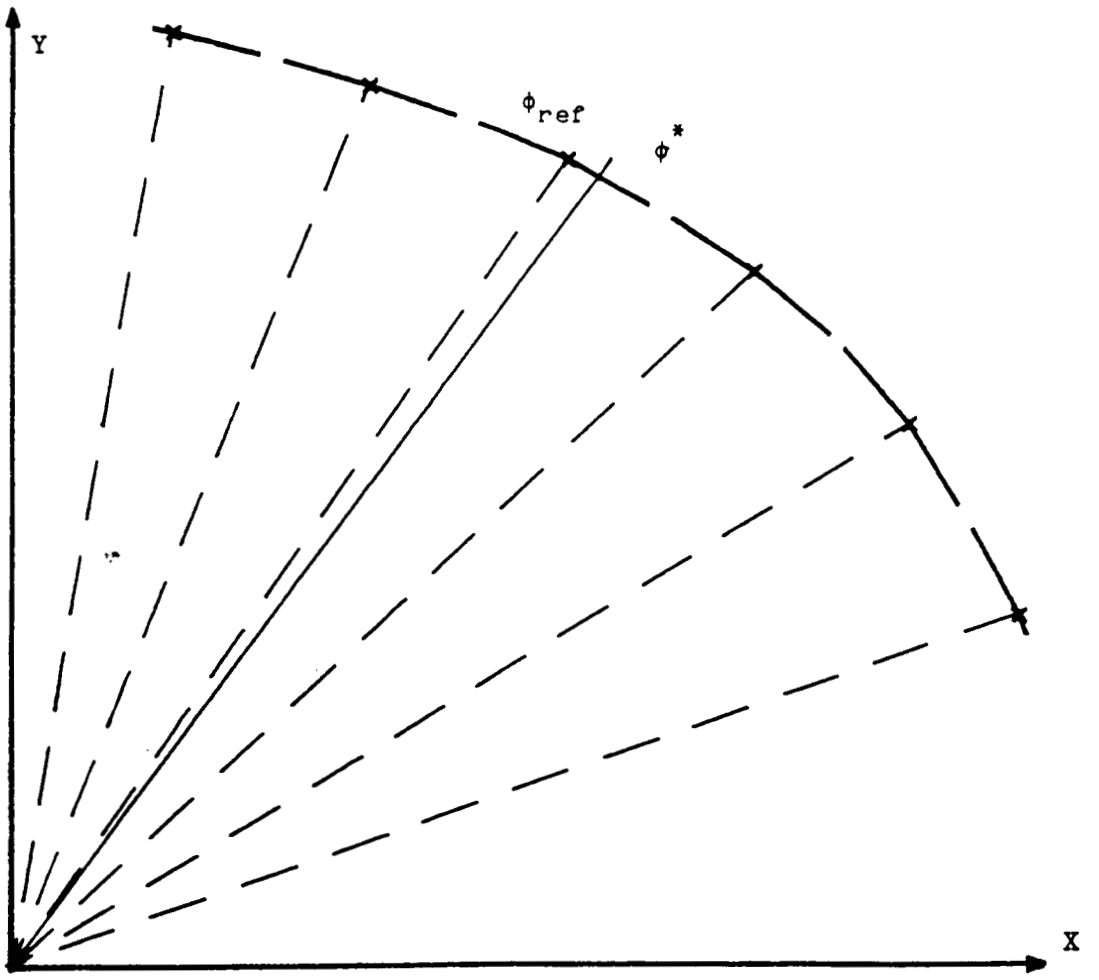

Figure 12.2. Meridional cut neighborhood of ϕ^*.

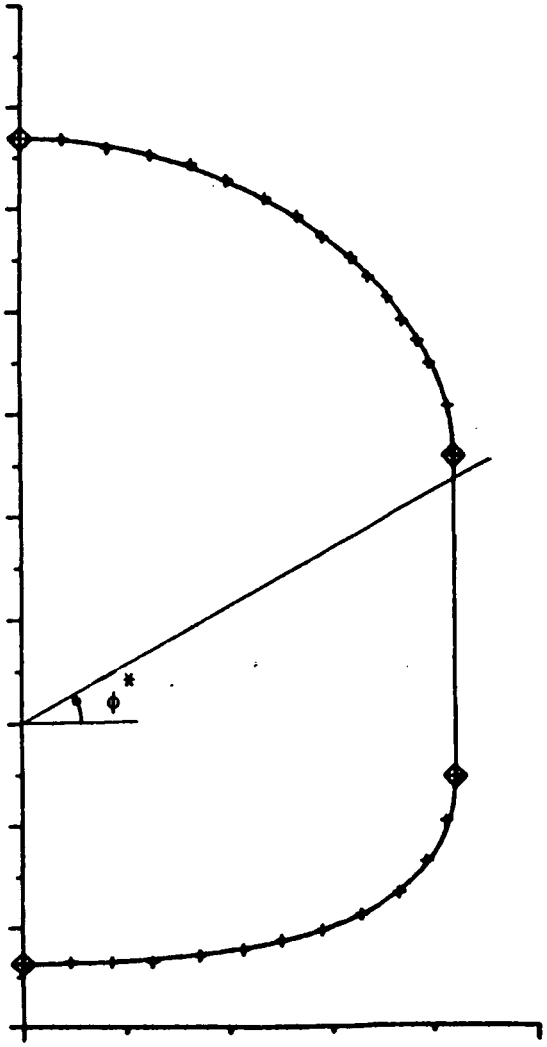

Figure 12.3. Location of ϕ^* in original curve-fit of cross section at $Z = Z_{ref}$.

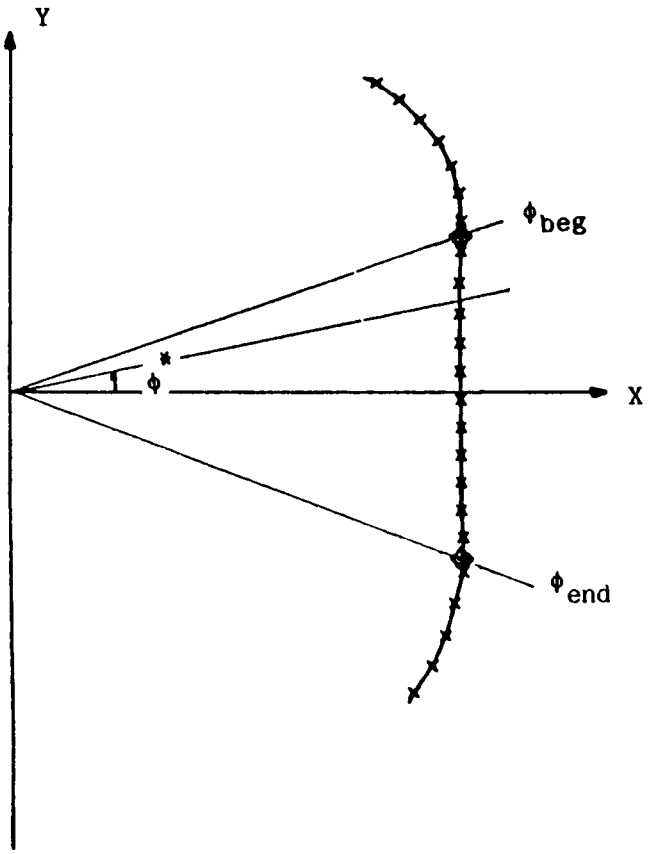

Figure 12.4. Meridional cut neighborhood of ϕ^* for line segment fit.

$$\xi^* = \frac{Z - Z_{LE}}{Z_{TE} - Z_{LE}}$$

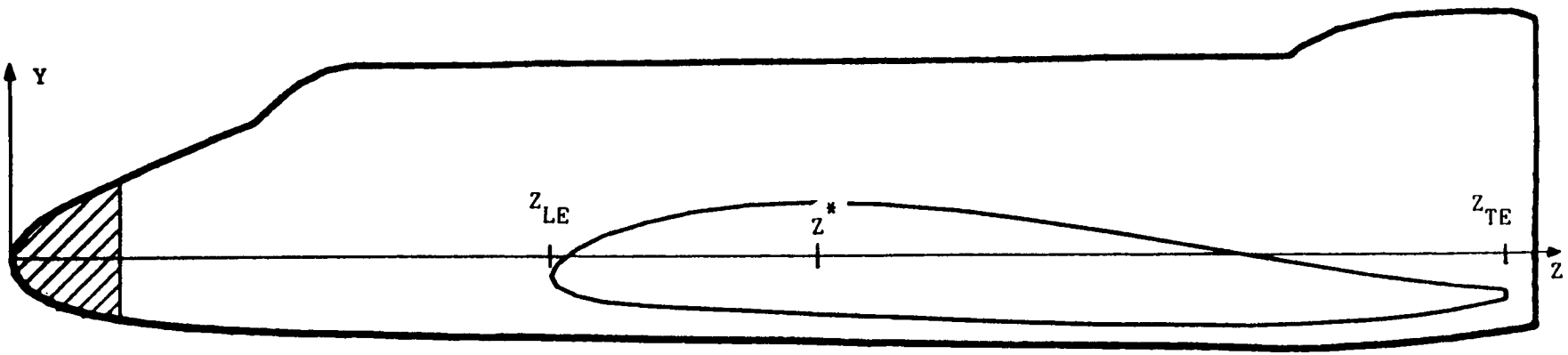

Figure 12.5. Percent chord location of $Z = Z^*$ at a given spanwise station.

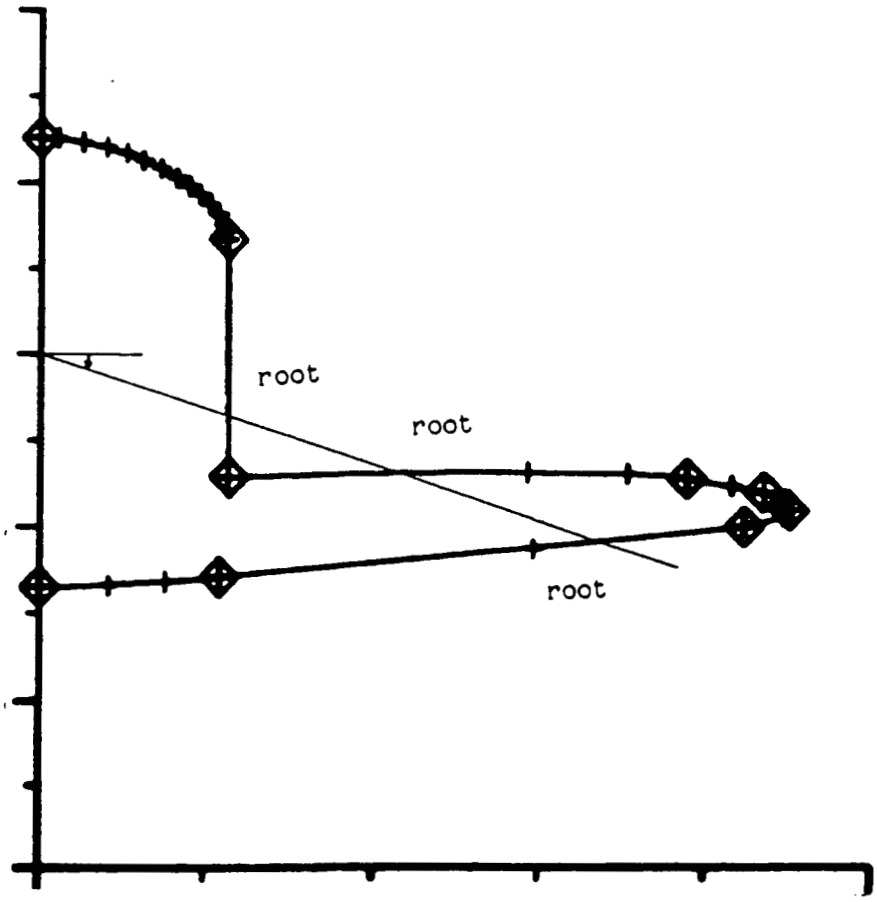

Figure 12.6. Multiple roots at a given axial location for the wing-body combination.

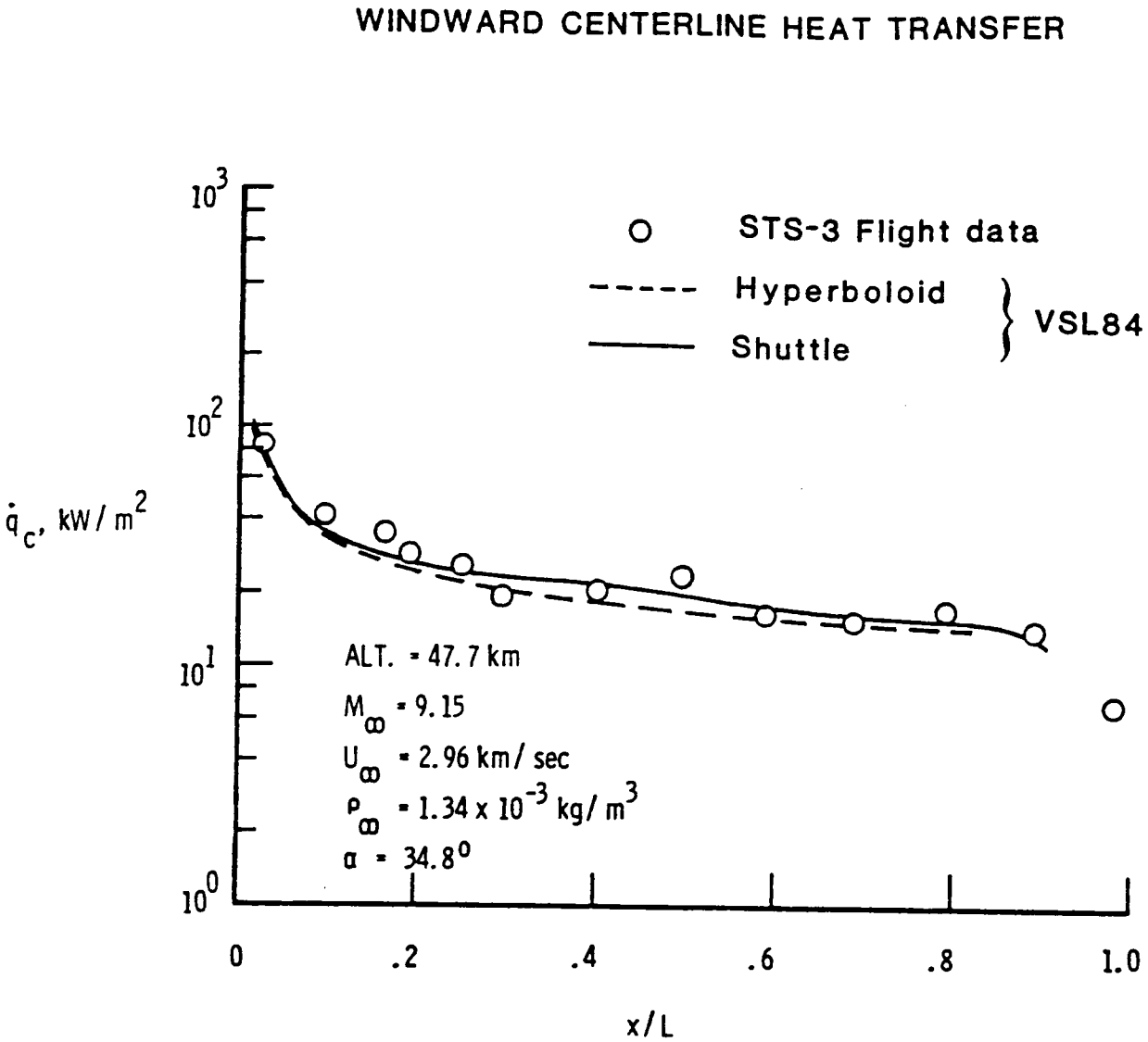

Figure 14.1. Effect of accuracy of geometry model on viscous flowfield calculations.

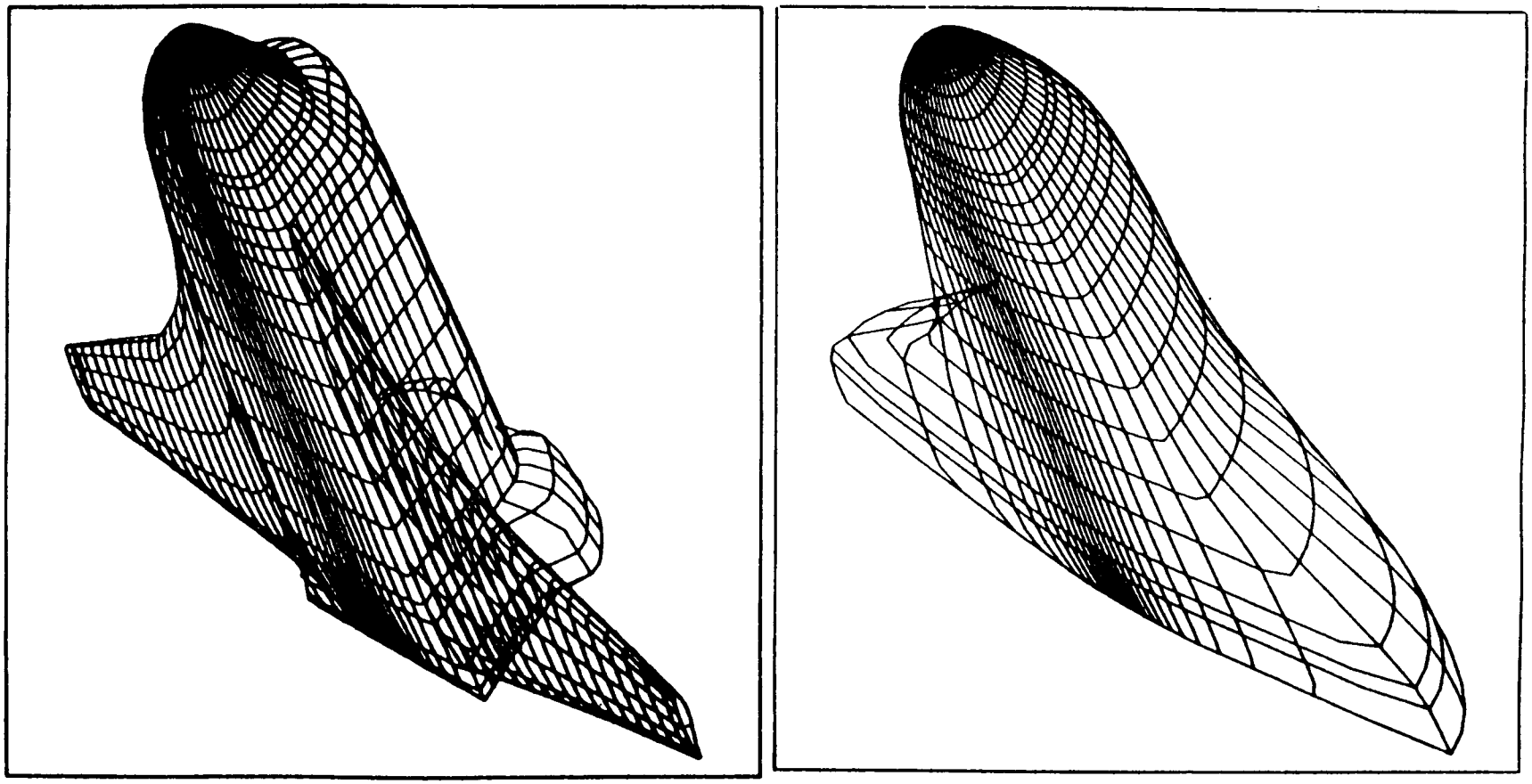

ASTUD QUICK

Figure 14.2. Orthographic view of the two geometry models.

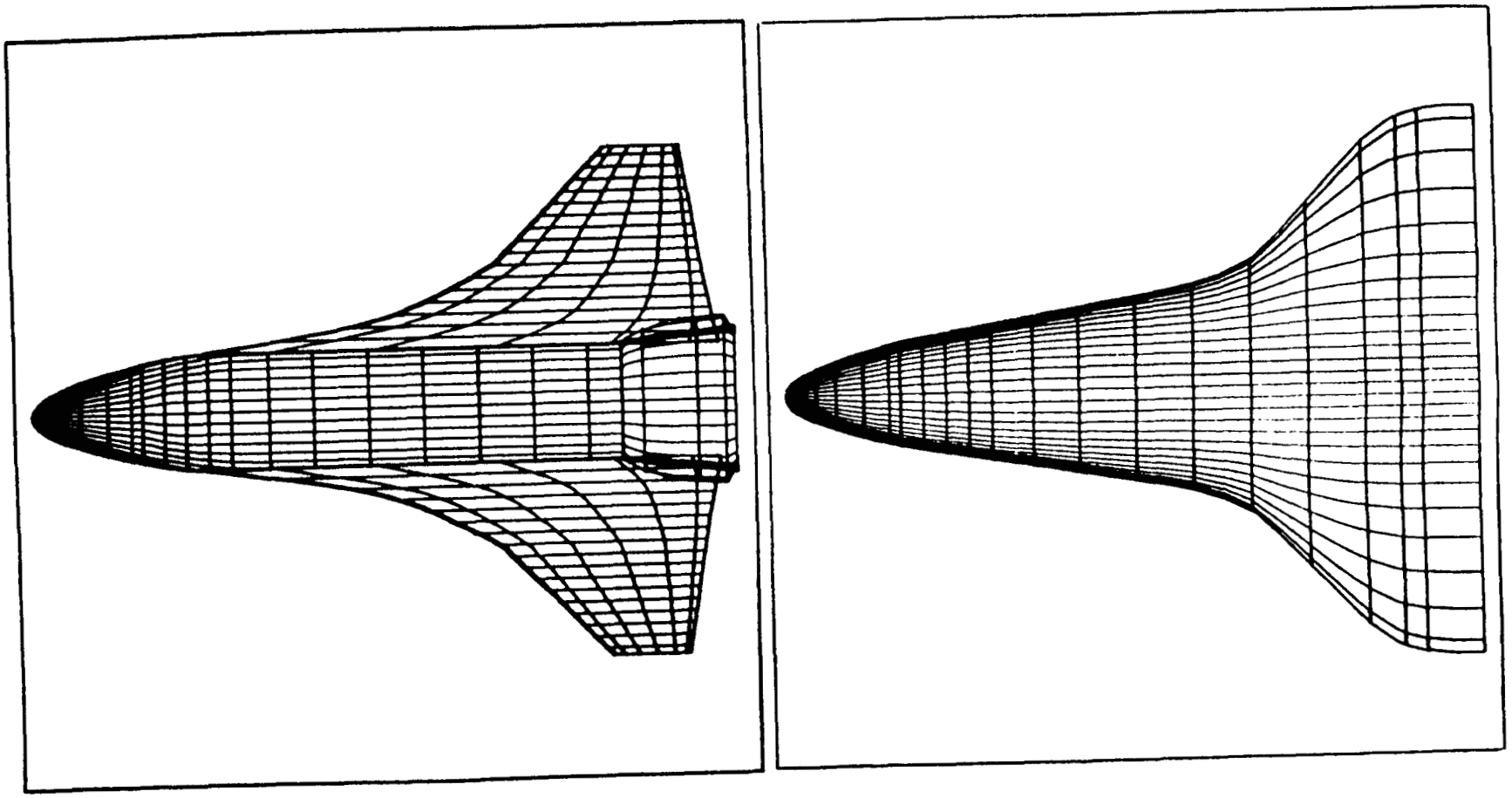

ASTUD

QUICK

Figure 14.3. Top view of the two geometry models.

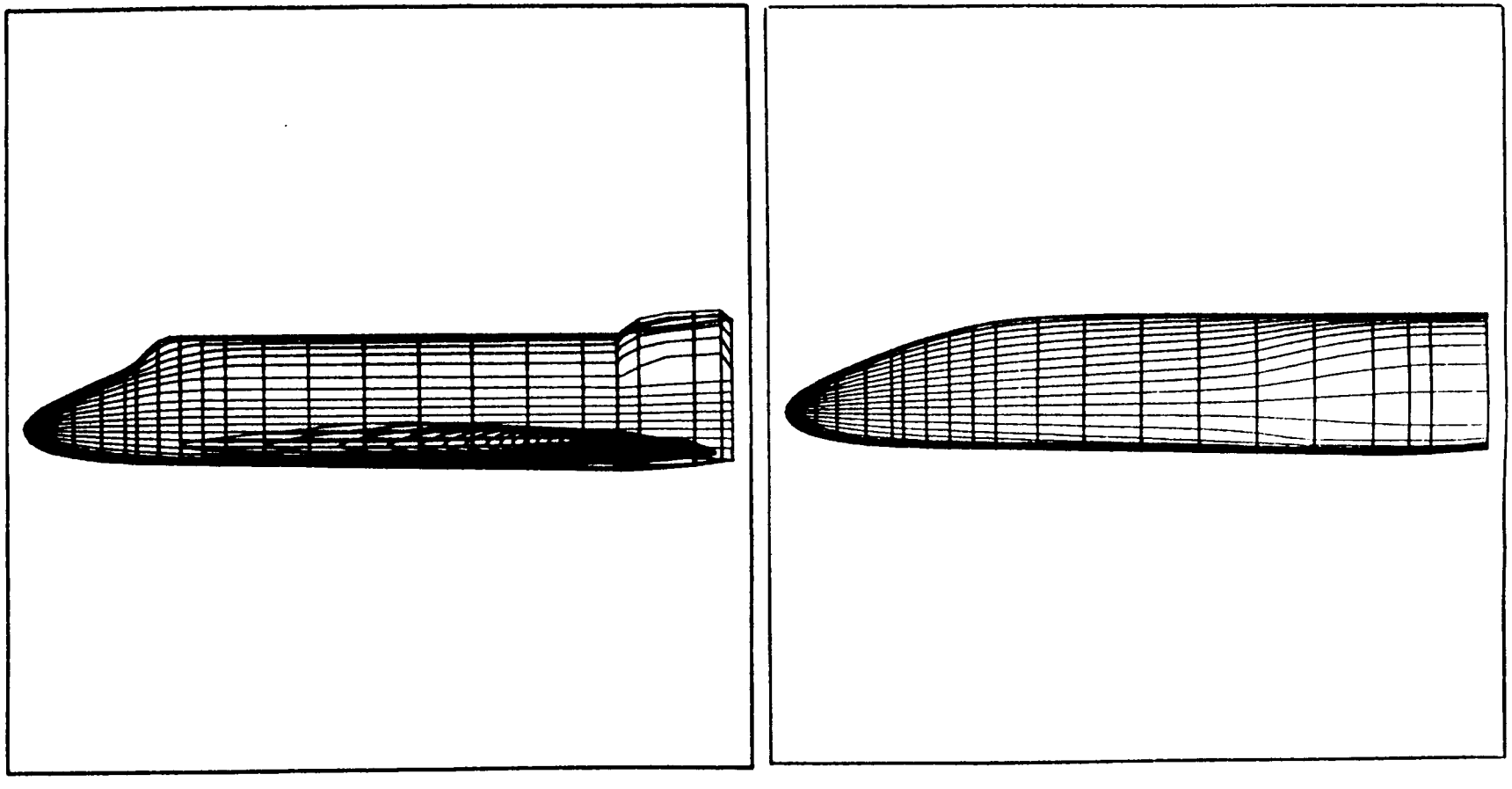

ASTUD

QUICK

Figure 14.4. Side view of the two geometry models.

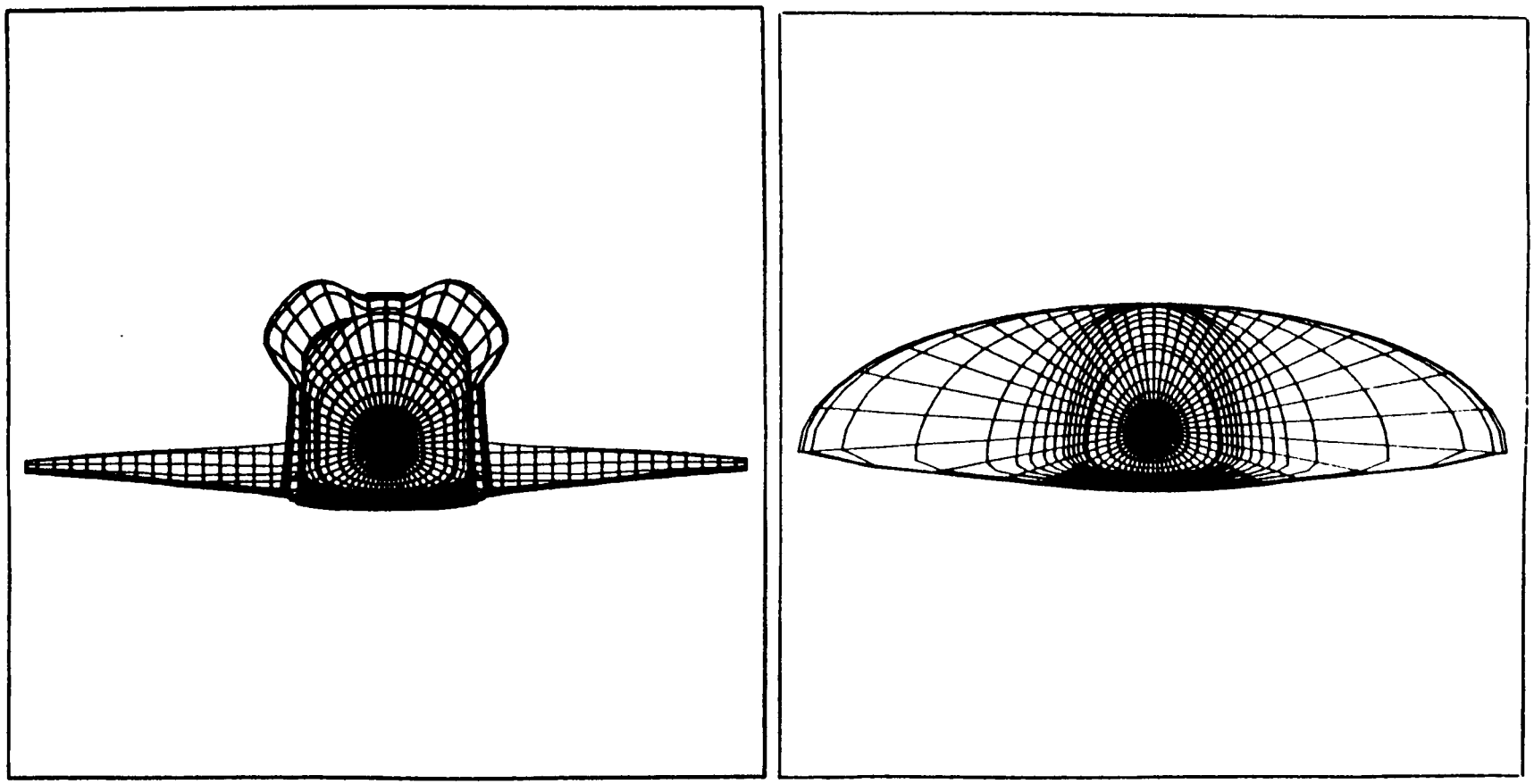

ASTUD QUICK

Figure 14.5. Front view of the two geometry models.

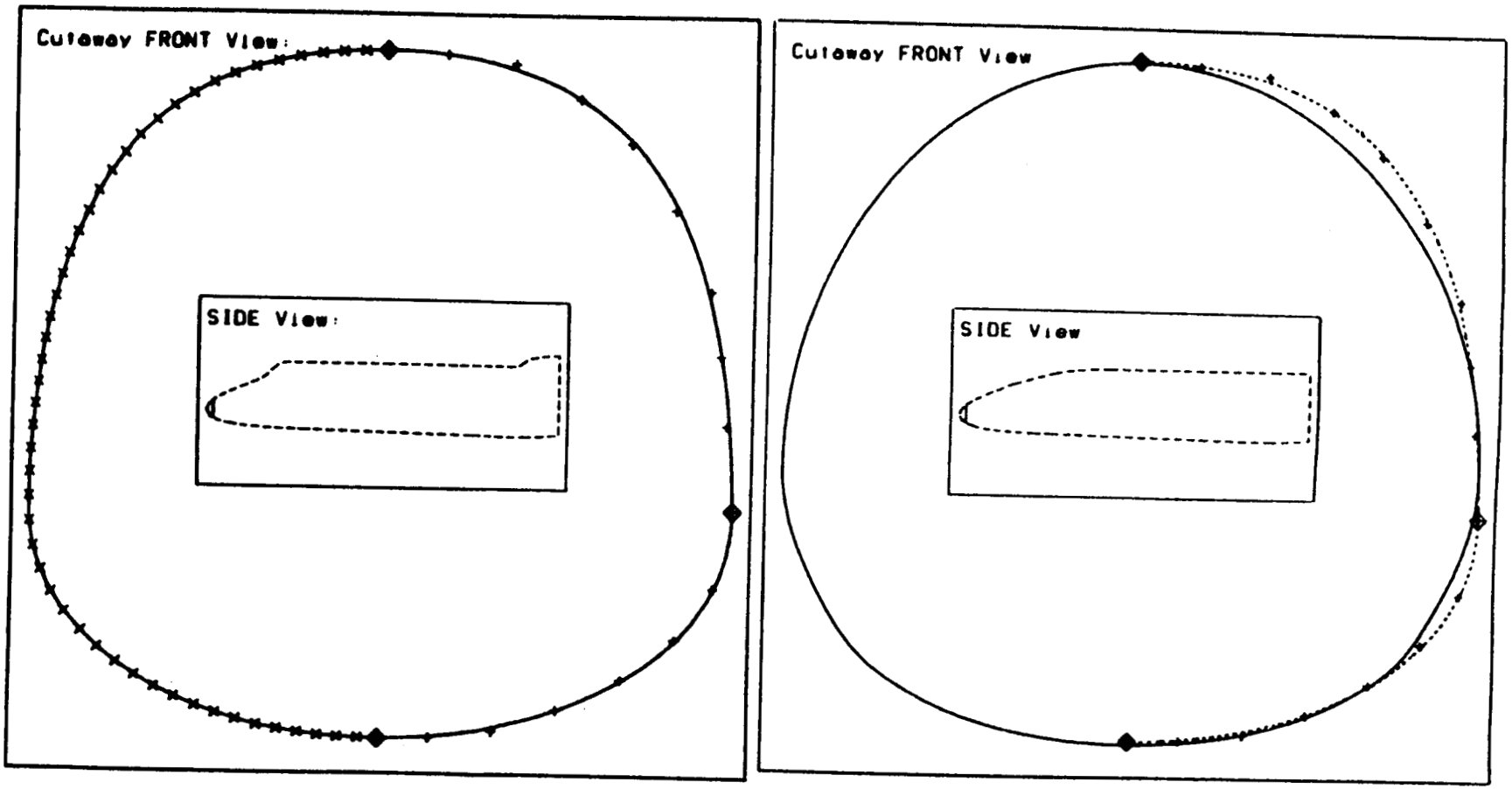

ASTUD

QUICK

Figure 14.6. Cross section #3 (Z = 22.) of the two geometry models.

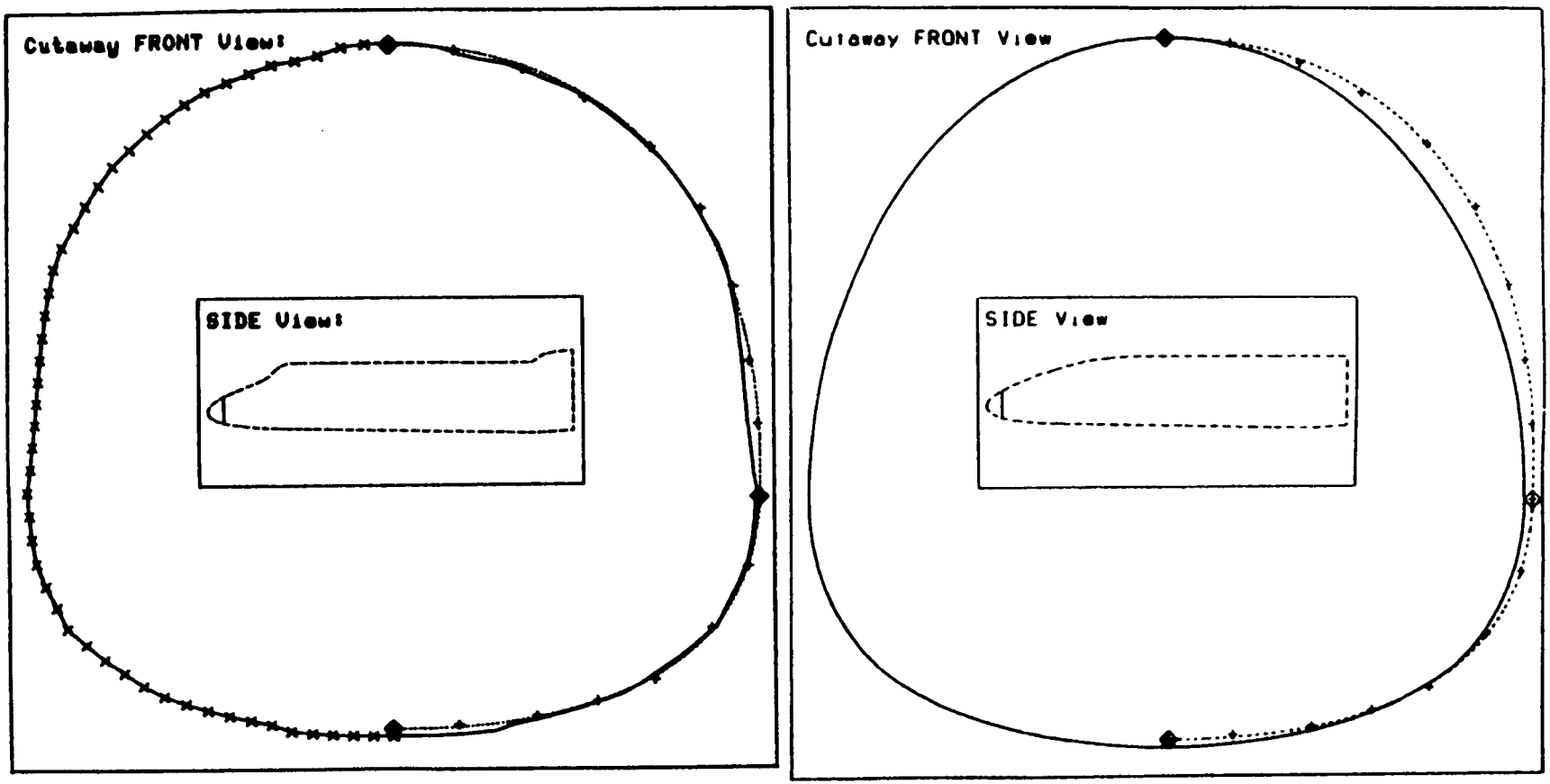

ASTUD QUICK

Figure 14.7. Cross section #6 (Z = 52.) of the two geometry models.

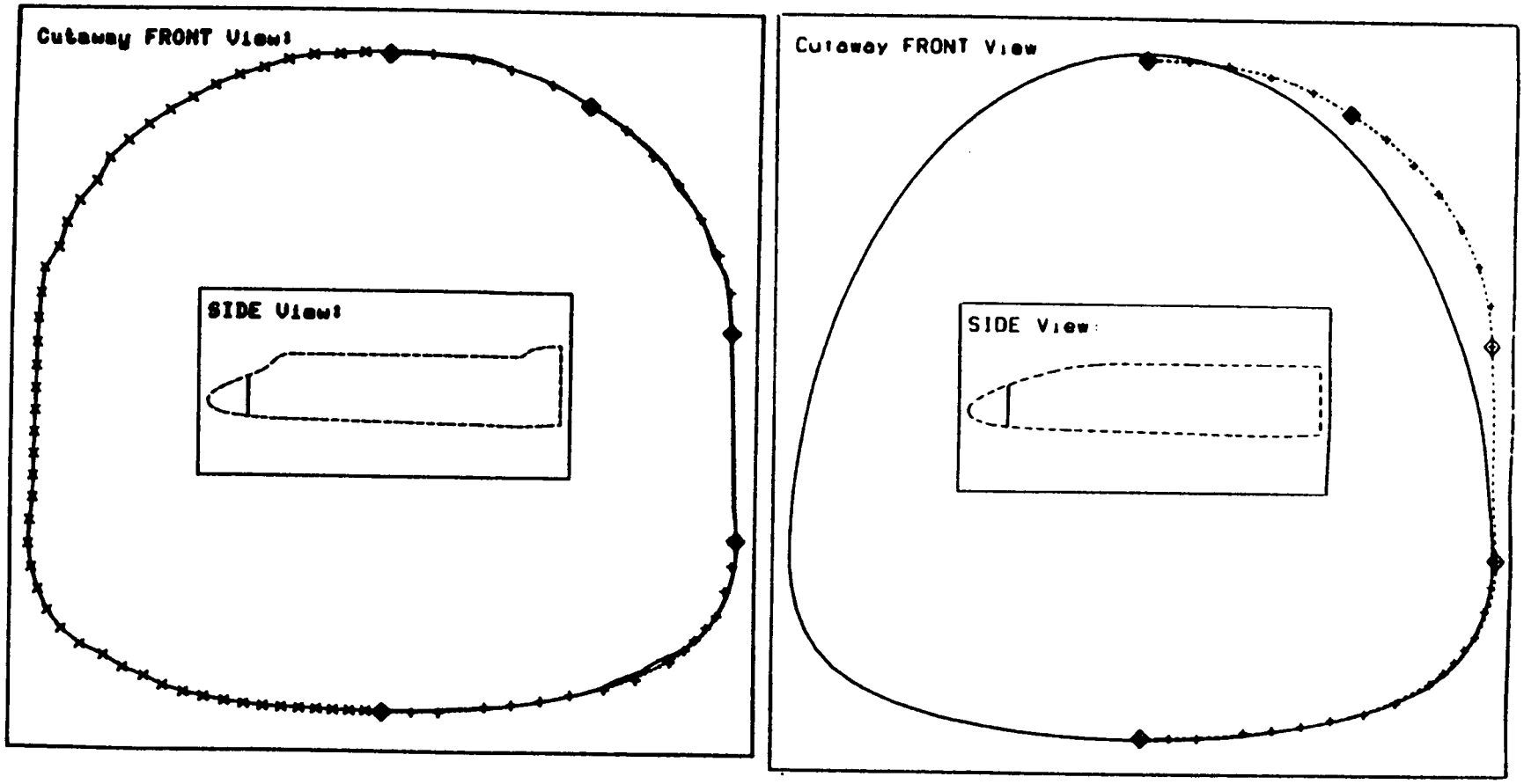

ASTUD

QUICK

Figure 14.8. Cross section #10 (Z = 137.) of the two geometry models.

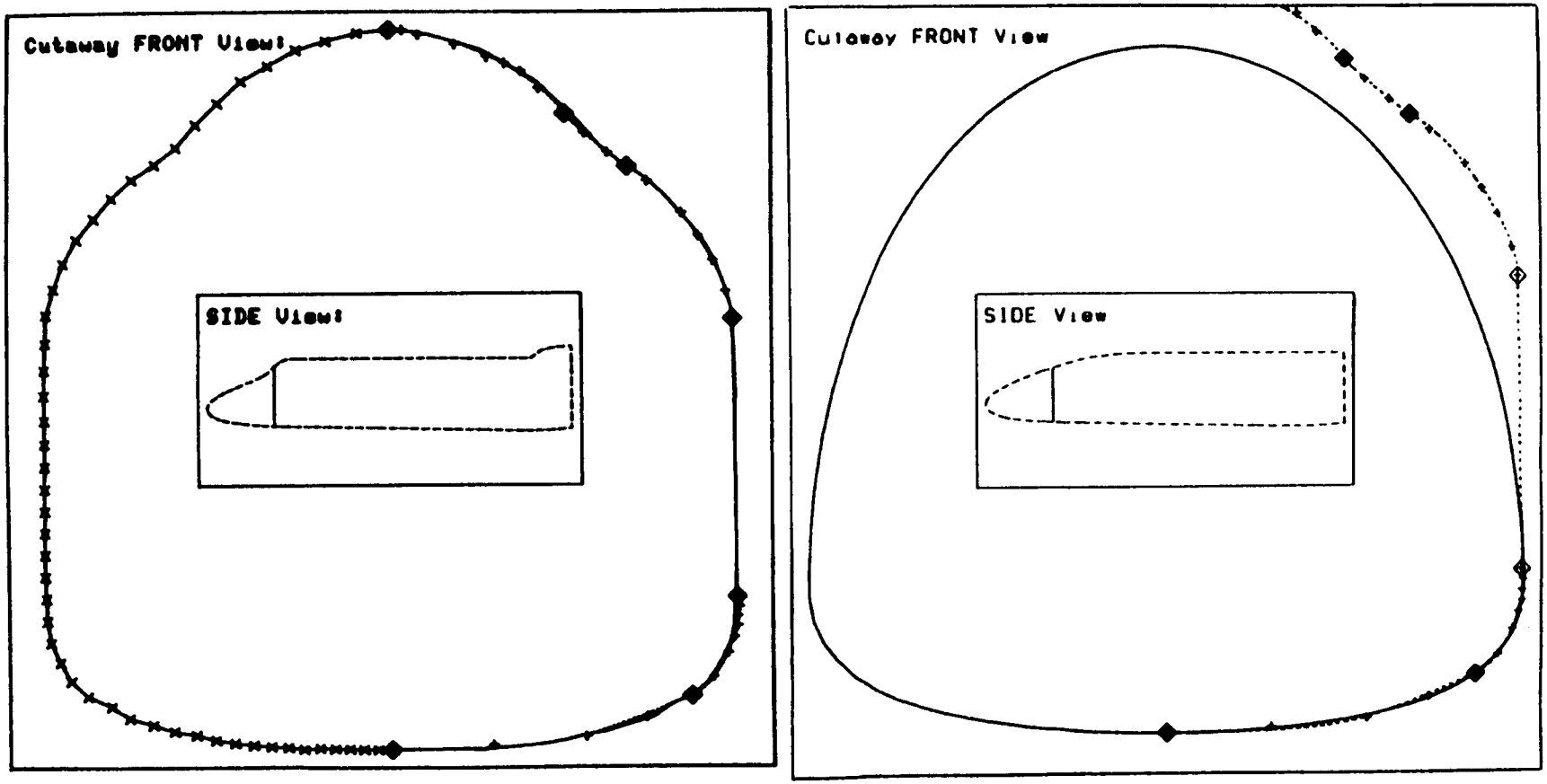

ASTUD

QUICK

Figure 14.9. Cross section #15 (Z = 222.) of the two geometry models.

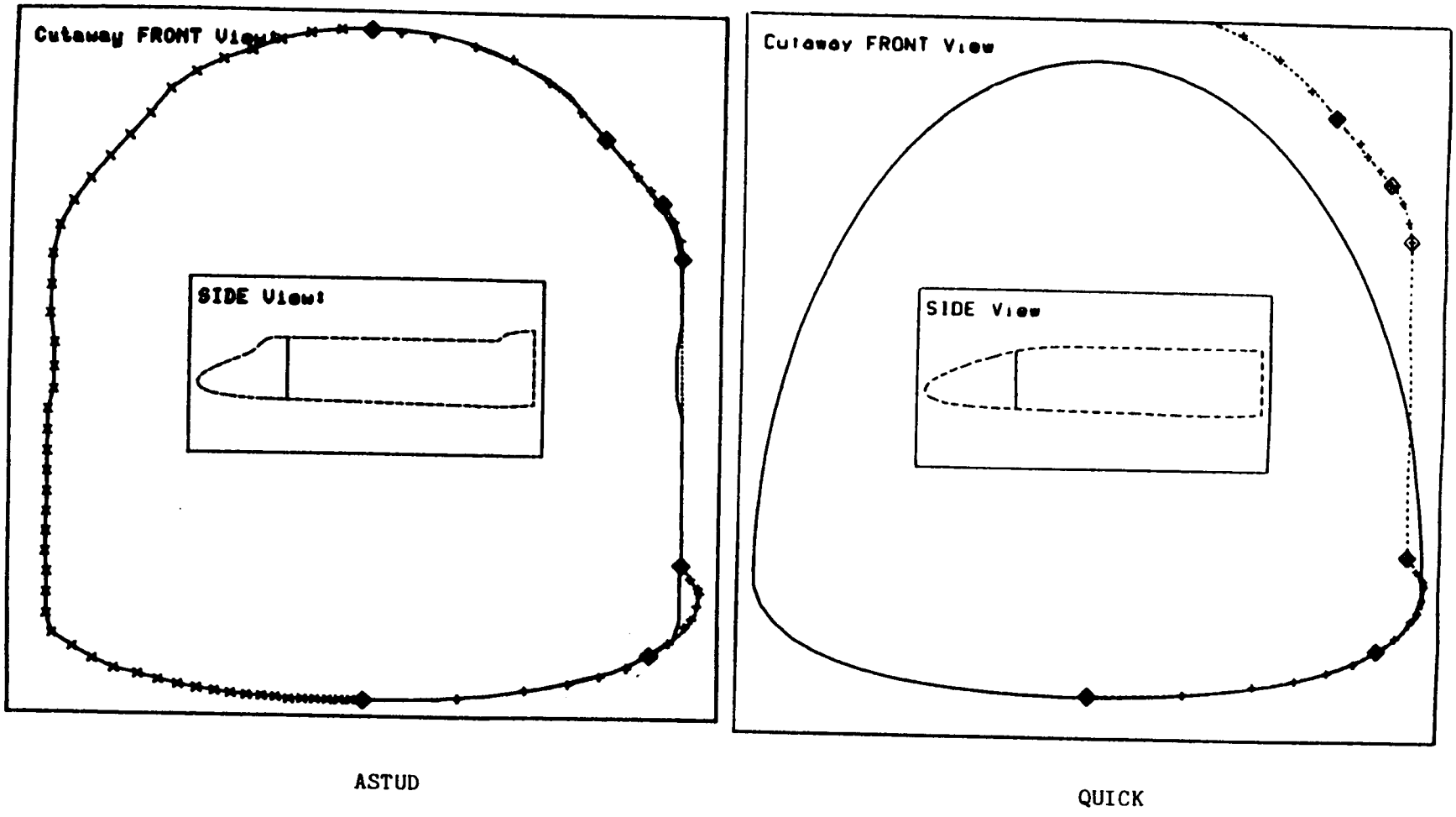

ASTUD

QUICK

Figure 14.10. Cross section #20 (Z = 322.) of the two geometry models.

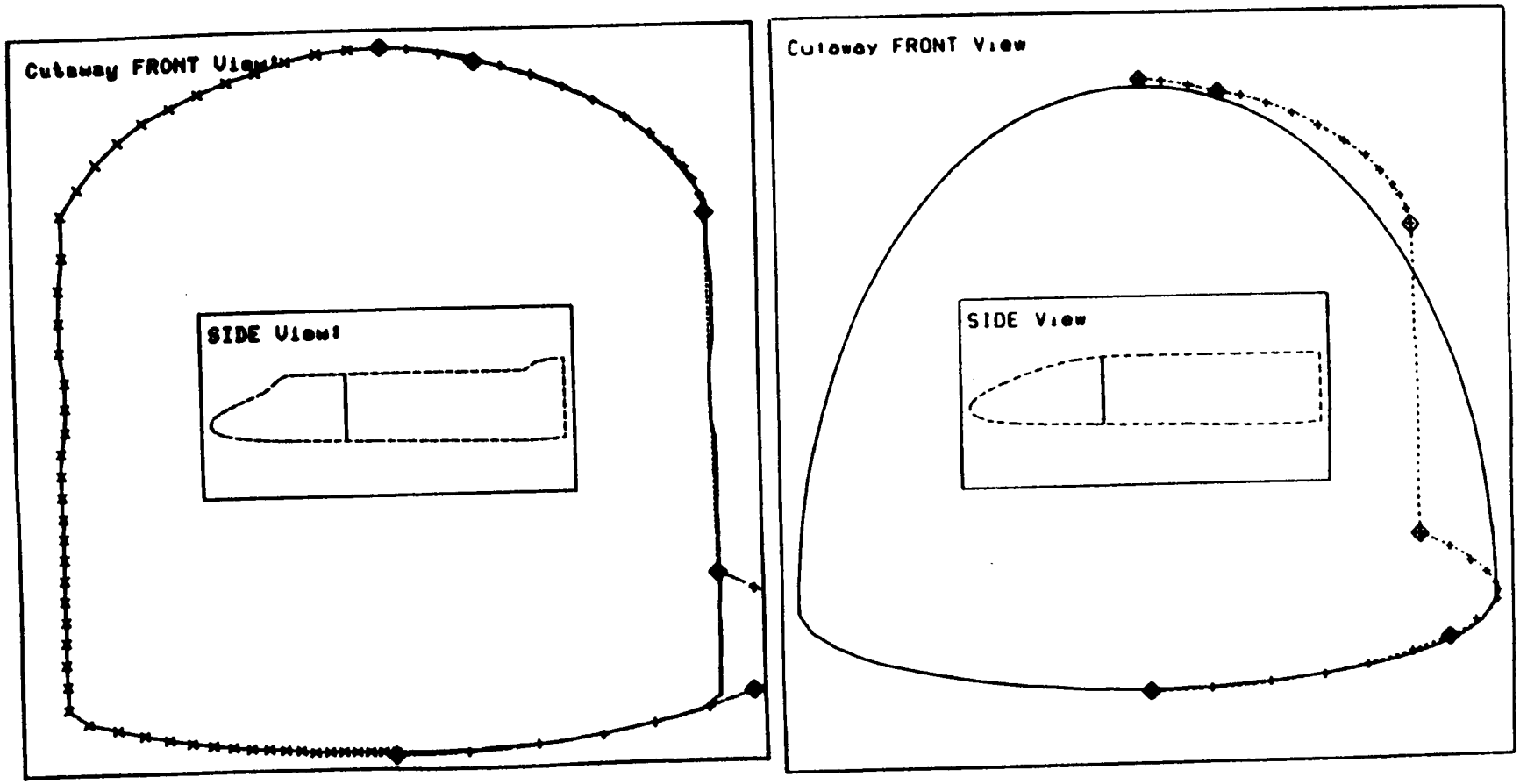

ASTUD

QUICK

Figure 14.11. Cross section #25 (Z = 462.) of the two geometry models.

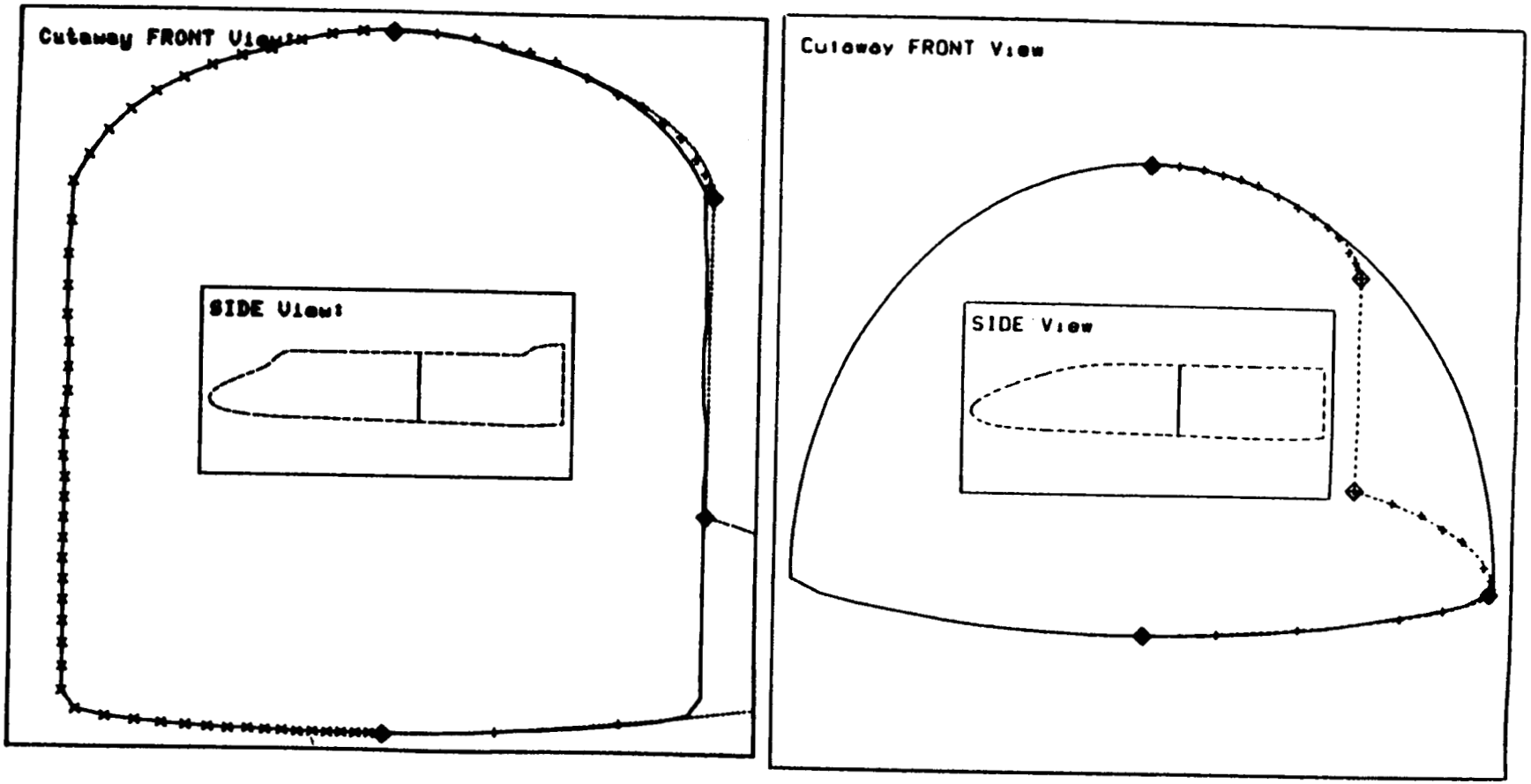

ASTUD

QUICK

Figure 14.12. Cross section #30 (Z = 712.) of the two geometry models.

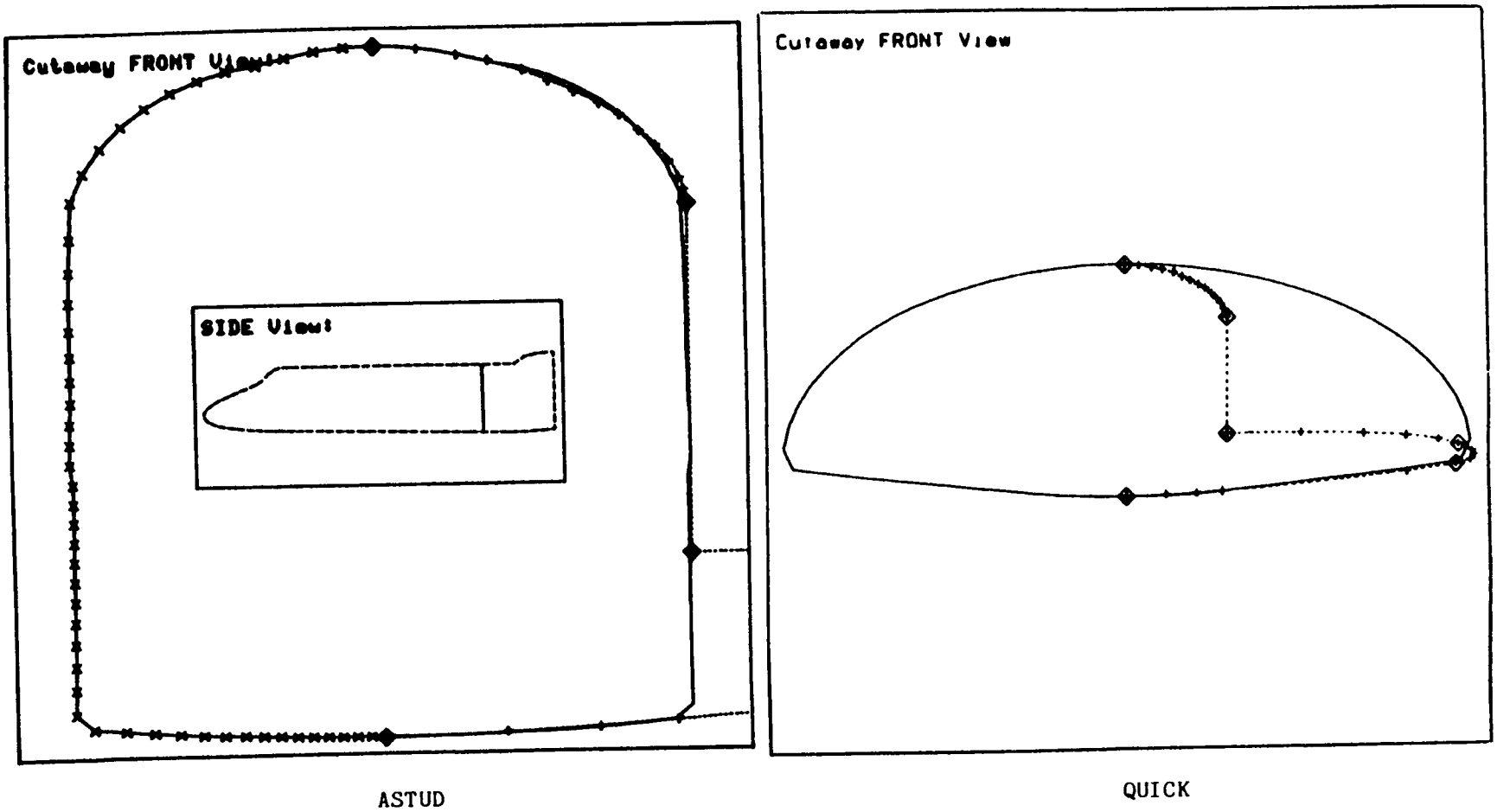

Figure 14.13. Cross section #35 (Z = 962.) of the two geometry models.

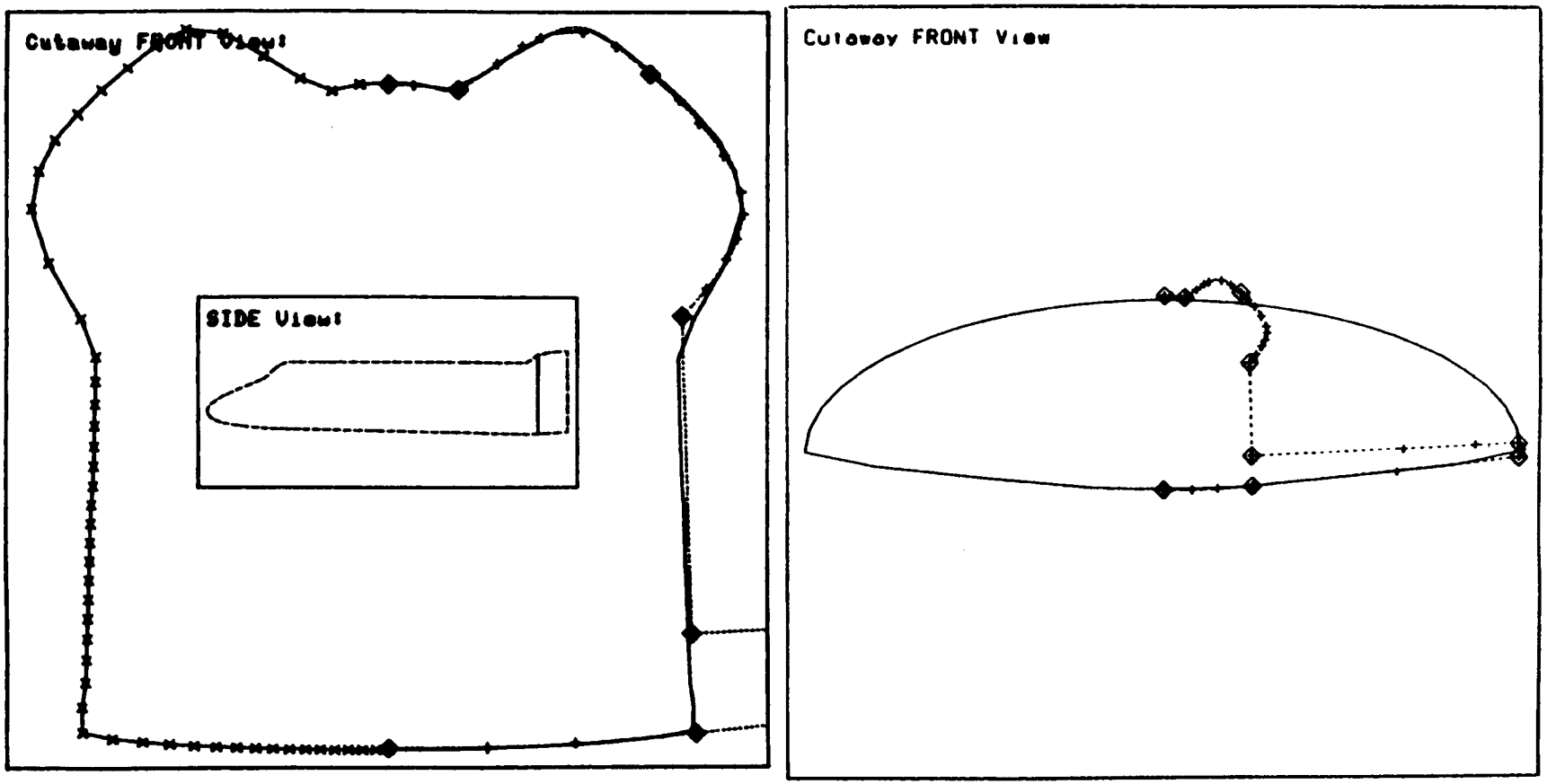

ASTUD QUICK

Figure 14.14. Cross section #40 (Z = 1112.) of the two geometry models.

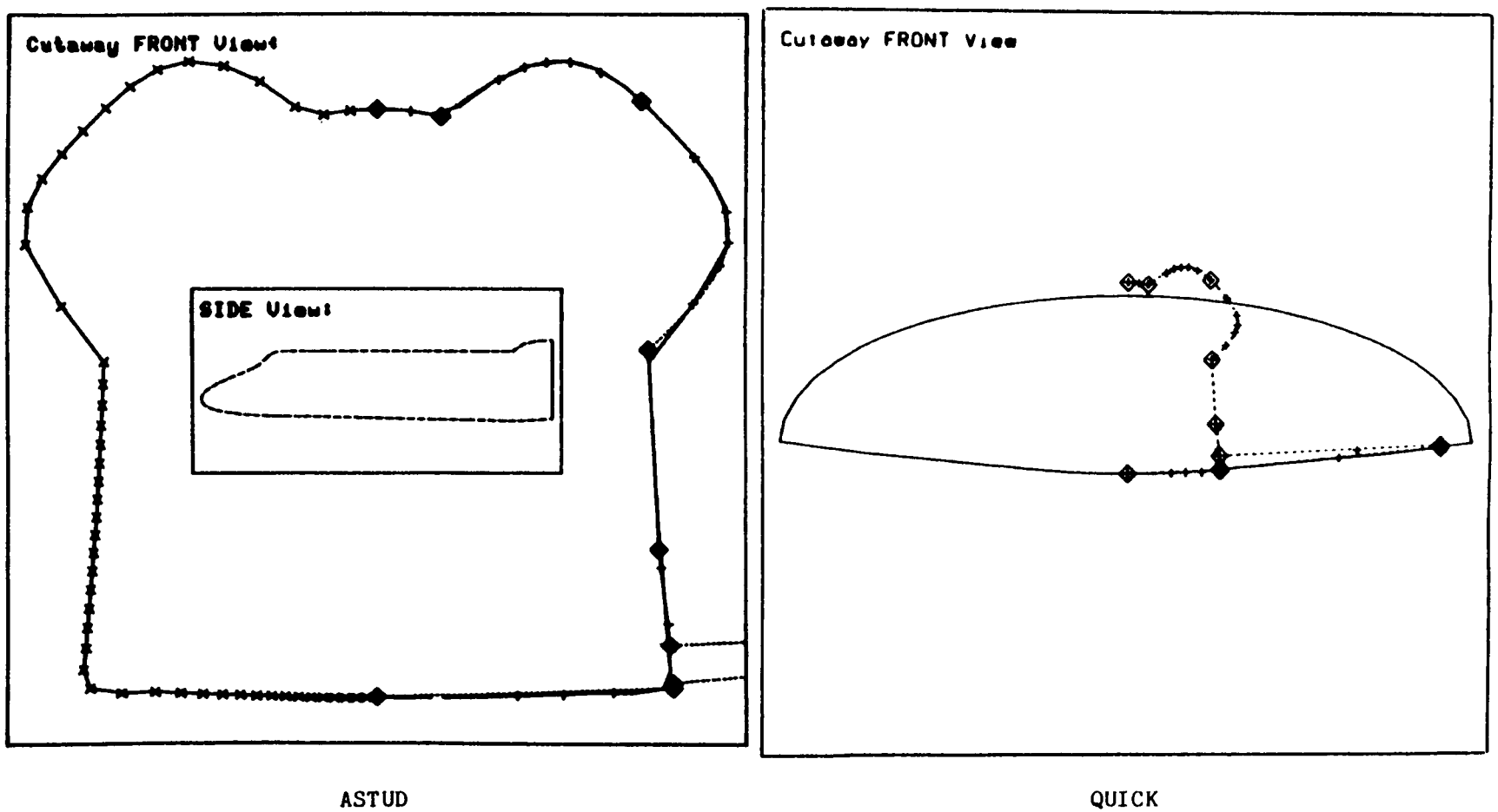

Figure 14.15. Cross section #42 (Z = 1212.) of the two geometry models.

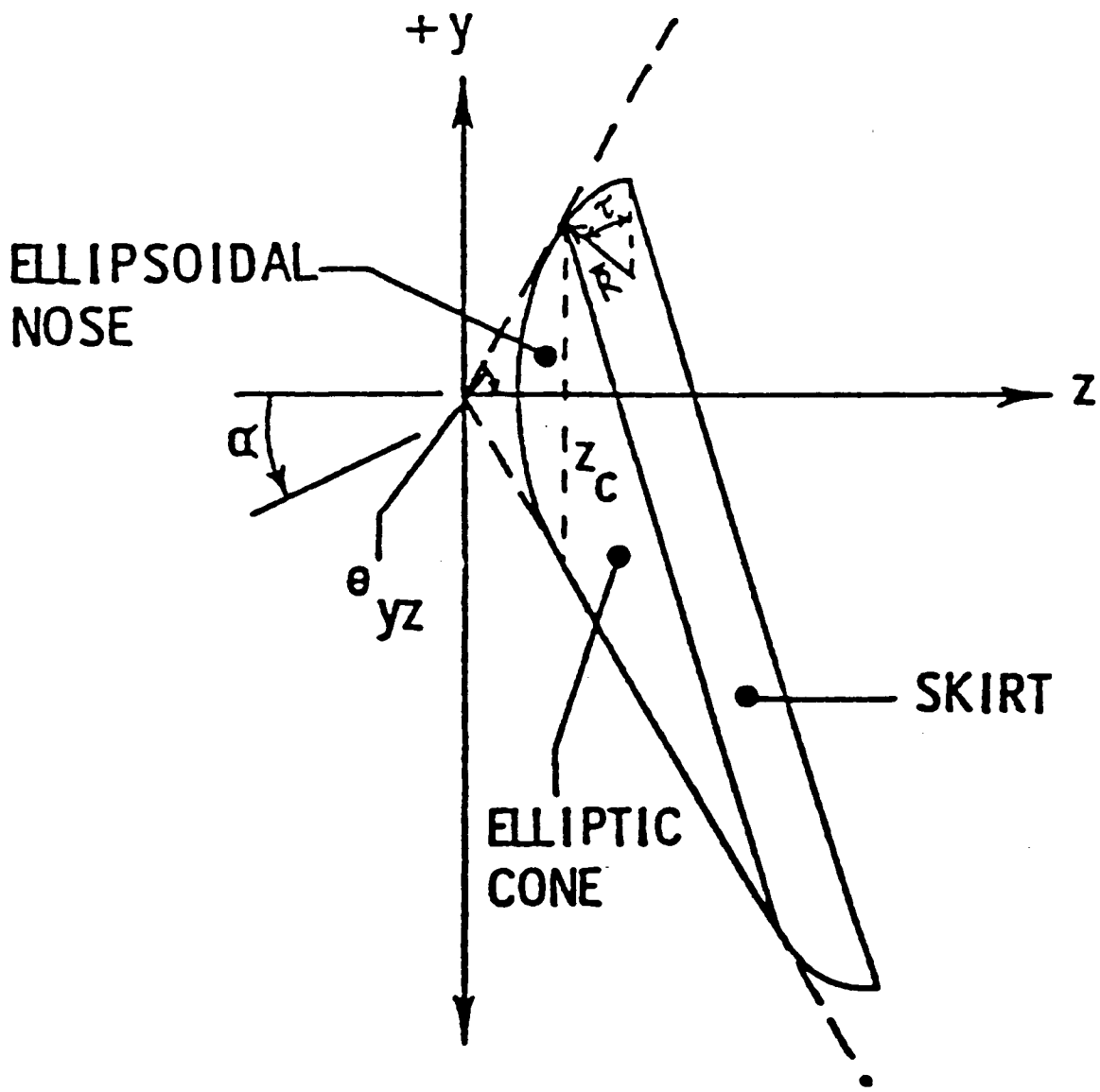

Figure 14.16. Defining parameters of AFE geometry.

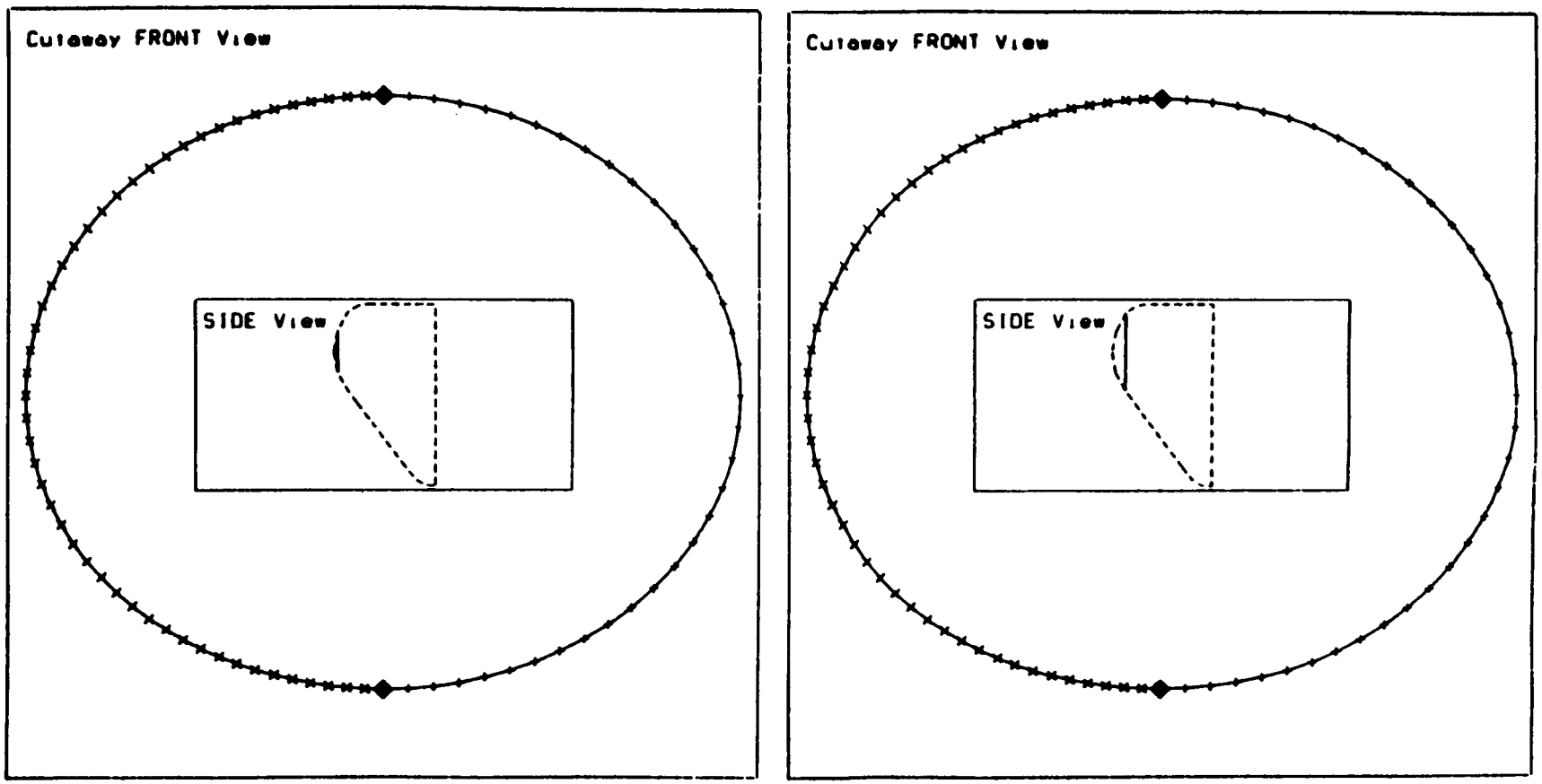

Figure 14.17. The two defining cross sections of AFE nose region are symmetric about the XZ-plane.

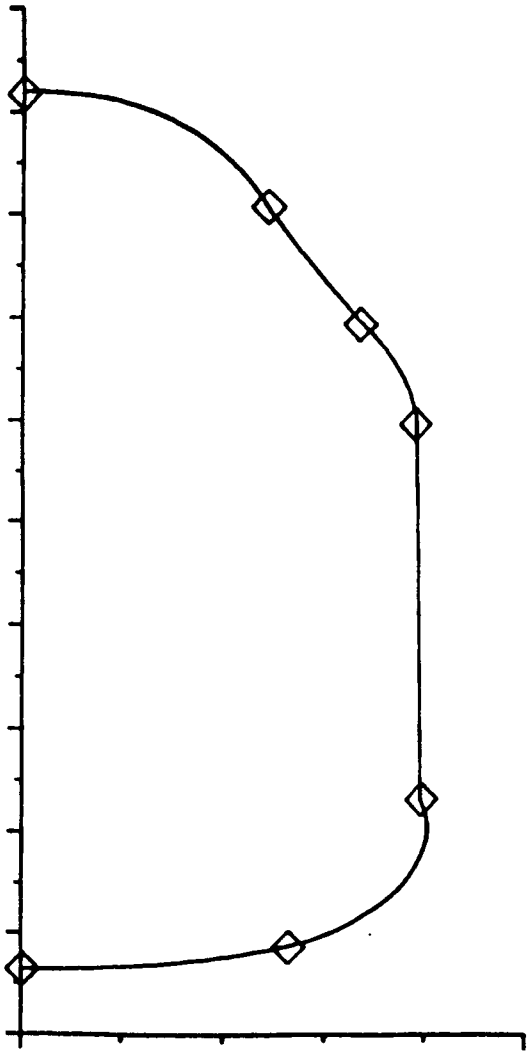

Figure 14.19. Location of control points in a cross-sectional curve-fit.

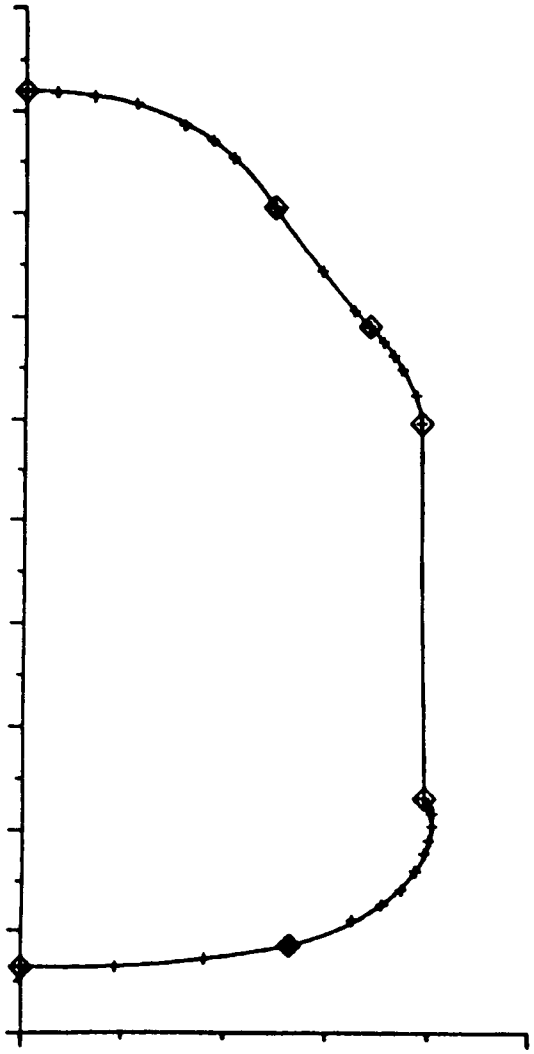

Figure 14.20. Additional data points in a cross section.

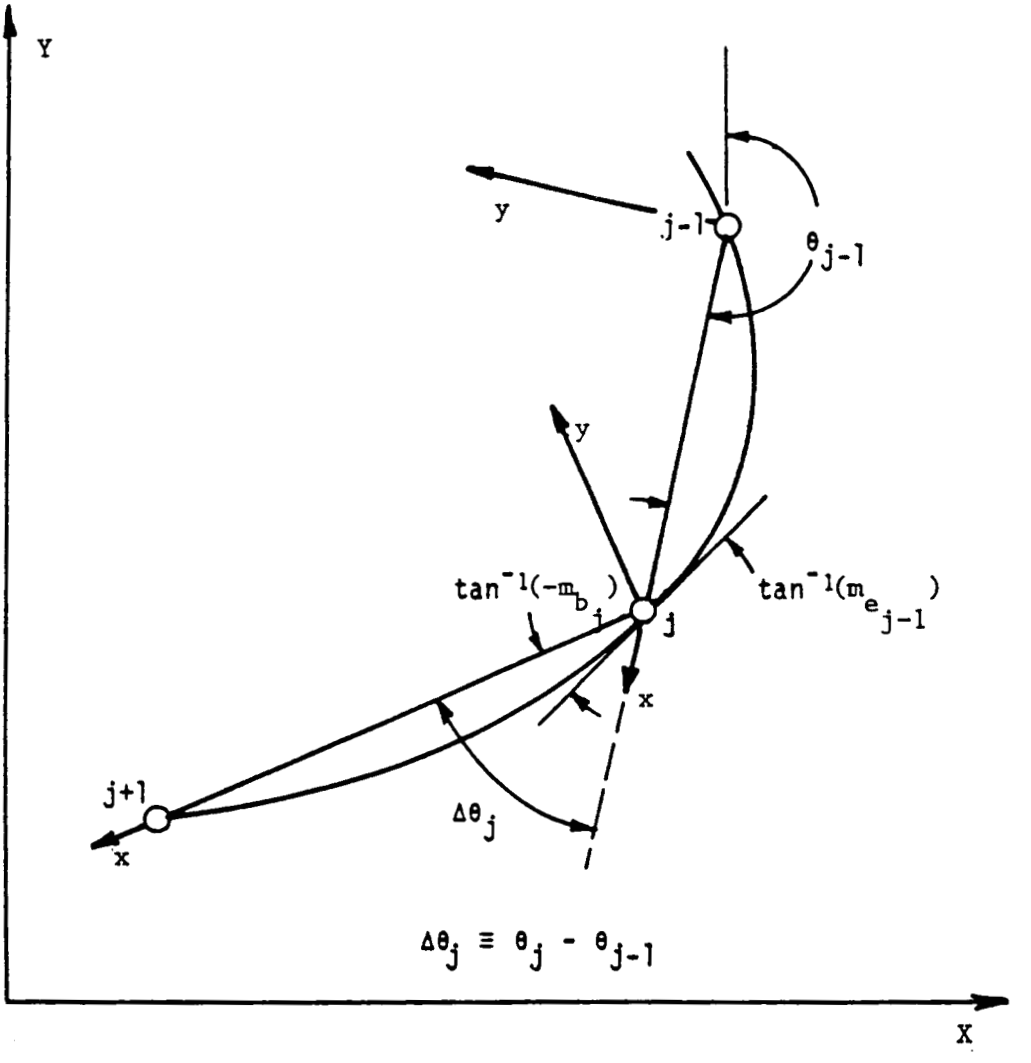

Figure A.1. Continuity of slope at control point where slope is left arbitrary.

NASA
National Aeronautics and Space Administration

Report Documentation Page

1. Report No.	2. Government Accession No.	3. Recipient's Catalog No.
NASA CR-4126		

4. Title and Subtitle

An Interactive User-Friendly Approach to Surface-Fitting Three-Dimensional Geometries

5. Report Date

March 1988

6. Performing Organization Code

7. Author(s)

F. McNeil Cheatwood and Fred R. DeJarnette

8. Performing Organization Report No.

10. Work Unit No.

506-40-11-01

9. Performing Organization Name and Address

North Carolina State University
Dept. of Mechanical and Aerospace Engineering
Raleigh, NC 27695-7910

11. Contract or Grant No.

NCC1-100 and NCC1-22

13. Type of Report and Period Covered

Contractor Report
1-1-84 thru 12-31-86

12. Sponsoring Agency Name and Address

NASA Langley Research Center
Hampton, VA 23665-5225

14. Sponsoring Agency Code

15. Supplementary Notes

Langley Technical Monitor: H. Harris Hamilton II
Final Report

16. Abstract

A surface-fitting technique has been developed which addresses two problems with existing geometry packages: computer storage requirements and the time required of the user for the initial setup of the geometry model. Coordinates of cross sections are fit using segments of general conic sections. The next step is to blend the cross-sectional curve-fits in the longitudinal direction using general conics to fit specific meridional half-planes. Provisions are made to allow the fitting of fuselages and wings so that entire wing-body combinations may be modeled. This report includes the development of the technique along with a User's Guide for the various menus within the program. Results for the modeling of the Space Shuttle and a proposed Aeroassist Flight Experiment geometry are presented.

17. Key Words (Suggested by Author(s))	18. Distribution Statement
Geometry model Surface fit Analytic Description Space Shuttle	Unclassified - Unlimited Subject Category 02

19. Security Classif. (of this report)	20. Security Classif. (of this page)	21. No. of pages	22. Price
Unclassified	Unclassified	148	A07

NASA FORM 1626 OCT 86

NASA-Langley, 1988

For sale by the National Technical Information Service, Springfield, Virginia 22161-2171